AEDC-TR-73-5

HANDBOOK
UNCERTAINTY IN GAS TURBINE MEASUREMENTS

Dr. R. B. Abernethy et al.
Pratt & Whitney Aircraft
and
J. W. Thompson, Jr.
ARO, Inc.

February 1973

ENGINE TEST FACILITY
ARNOLD ENGINEERING DEVELOPMENT CENTER
AIR FORCE SYSTEMS COMMAND
ARNOLD AIR FORCE STATION, TENNESSEE

NOTICES

When U. S. Government drawings specifications, or other data are used for any purpose other than a definitely related Government procurement operation, the Government thereby incurs no responsibility nor any obligation whatsoever, and the fact that the Government may have formulated, furnished, or in any way supplied the said drawings, specifications, or other data, is not to be regarded by implication or otherwise, or in any manner licensing the holder or any other person or corporation, or conveying any rights or permission to manufacture, use, or sell any patented invention that may in any way be related thereto.

Qualified users may obtain copies of this report from the Defense Documentation Center.

References to named commercial products in this report are not to be considered in any sense as an endorsement of the product by the United States Air Force or the Government.

HANDBOOK
UNCERTAINTY IN GAS TURBINE MEASUREMENTS

Dr. R. B. Abernethy et al.
Pratt & Whitney Aircraft

and

J. W. Thompson, Jr.
ARO, Inc.

FOREWORD

The work reported herein was sponsored by the Arnold Engineering Development Center, Air Force Systems Command, United States Air Force, under Program Element 65802F.

The results presented were compiled by ARO, Inc. (a subsidiary of Sverdrup & Parcel and Associates, Inc.), contract operator of the Arnold Engineering Development Center (AEDC), Air Force Systems Command (AFSC), Arnold Air Force Station, Tennessee, under Contract F40600-73-C-0004. The preparation of the text was accomplished by Dr. R. B. Abernethy, Senior Project Engineer, Billy D. Powell, David L. Colbert, and Daniel G. Sanders, Pratt & Whitney Aircraft, under subcontract to ARO, Inc. The contracted work consisted of a revision to the material in the "Interagency Chemical Rocket Propulsion Group (ICRPG) Handbook for Estimating the Uncertainty in Measurements made with Liquid Propellant Rocket Engine Systems," CPIA Publication No. 180 (same authors as above), substituting treatment of gas turbine measurement errors for rocket engine treatment and writing additional material applicable to gas turbine measurement errors. The report was prepared under ARO Project No. RW5245, and the manuscript was submitted for publication on May 8, 1972.

The authors are indebted to the many engineers and statisticians who have contributed to the work. A few must be noted for their particular contributions, Dr. Joan Rosenblatt, Dr. H. H. Ku, and J. M. Cameron of the National Bureau of Standards for their helpful discussions and comments on both this handbook and CPIA 180, and similarly, R. E. Smith, Jr., Chief of T-Cells Division, as well as T. C. Austin, C. R. Bartlett, W. O. Boals, Jr., and T. J. Gillard of ARO, Inc., at the Arnold Engineering Development Center. Engineers at Pratt & Whitney Aircraft, Florida and Connecticut facilities, provided the authors with constructive and spirited criticism in every section. Various technical committees under the American Society of Mechanical Engineers (ASME), the American Institute of Aeronautics and Astronautics, and the International Standards Organizations expressed interest and comments.

This technical report has been reviewed and is approved.

EULES L. HIVELY
Research and Development Division
Directorate of Technology

ROBERT O. DIETZ
Director of Technology

ABSTRACT

The lack of a standard method for estimating the errors associated with gas turbine performance data has made it impossible to compare measurement systems between facilities, and there has been confusion over the interpretation of error analysis. Therefore, a standard uncertainty methodology is proposed in this Handbook. The mathematical uncertainty model presented is based on two components of measurement error: the fixed (bias) error and the random (precision) error. The result of applying the model is an estimate of the error in the measured performance parameter. The uncertainty estimate is the interval about the measurement which is expected to encompass the true value. The propagation of error from basic measurements through calculated performance parameters is presented. Traceability of measurement back to the National Bureau of Standards and associated error sources is reviewed.

CONTENTS

Page

ILLUSTRATIONS

TABLES

SECTION I
INTRODUCTION

1.1 OBJECTIVE

The objective of this Handbook is to present a standard method of treating measurement error[1] or uncertainty for gas turbine engine performance parameters, such as thrust, airflow, and thrust specific fuel consumption. The need for a standard is obvious to those who have reviewed the numerous methods currently used. The subject is complex and involves both engineering and statistics. Only one method is presented herein without alternative paths. A single standard method is required to make comparisons between engine manufacturers and between facilities. However, it must be recognized that no single method will give a rigorous, scientifically correct answer for all situations. Further, even for a single set of data, the task of finding and proving one method to be correct is usually impossible. The method selected is believed to be most universally applicable. It is identical with the measurement uncertainty model used in the rocket engine industry which has been well received ("ICRPG Handbook for Estimating the Uncertainty in Measurements made with Liquid Propellant Rocket Engine Systems," CPIA No. 180, AD855130, April 30, 1969).

There are numerous examples for illustration. An effort has been made to use simple prose with a minimum of jargon.

1.2 SCOPE

This Handbook presents a working outline detailing and illustrating the techniques for estimating measurement uncertainty. Section II describes the mathematical model for a typical performance parameter (thrust specific fuel consumption). Sections III, IV, V, and VI treat errors associated with the measurement of force, fuel flow, pressure and temperature, and airflow. Each section includes a discussion of the methods of calibration and lists of the elemental errors and examples of the statistical techniques. Section VII describes the calculations of the uncertainty in net thrust and thrust specific fuel consumption at altitude conditions. Section VIII describes and illustrates several special methods. Section IX is the Glossary. Appendixes with tables, derivations, and proofs are found at the end of the Handbook.

1.3 MEASUREMENT ERROR

All measurements have measurement errors. These errors are the differences between the measurements and the true value defined by the National Bureau of Standards (NBS). Uncertainty is the maximum error which might reasonably be expected and is a measure of accuracy, i.e., the closeness of the measurement to the true value. Measurement error has two components: a fixed error and a random error.

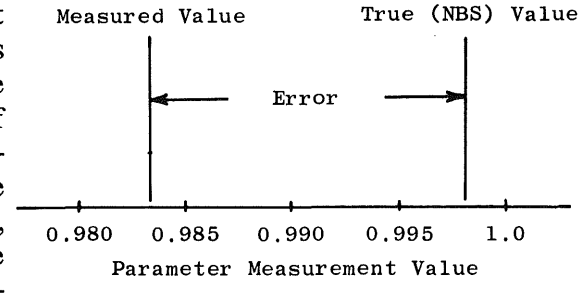

Fig. I-1 Measurement Error

[1]For a definition of terms used in this Handbook, see the Glossary in Section IX.

1.3.1 Precision (Random Error)

Random error is seen in repeated measurements. Measurements do not and are not expected to agree exactly. There are always numerous small effects which cause disagreements. The variation between repeated measurements is called precision error. The standard deviation (σ) is used as a measure of the precision error. A large standard deviation means large scatter in the measurements. The statistic (s) is calculated to estimate the standard deviation and is called the precision index

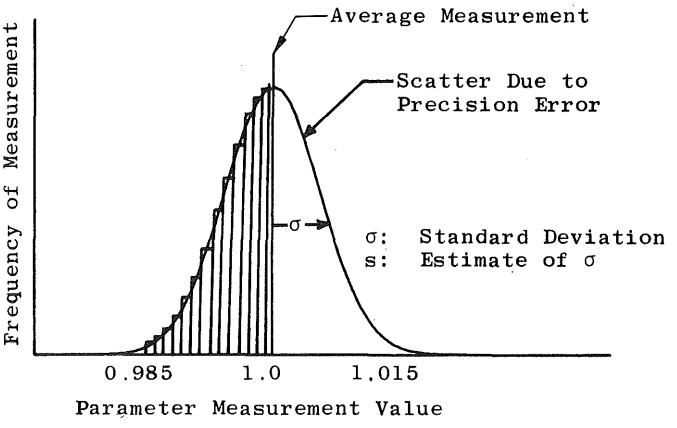

Fig. I-2 Precision Error

$$s = \sqrt{\frac{\sum_{i=1}^{N} (X_i - \bar{X})^2}{N - 1}}$$

where N is the number of measurements made and $\bar{X}$ is the average value of individual measurements X_i.

1.3.2 Bias (Fixed Error)

The second component, bias, is the constant or systematic error. In repeated measurements, each measurement has the same bias. The bias cannot be determined unless the measurements are compared with the true value of the quantity measured.

Bias is categorized into five classes: (1) large known biases, (2) small known biases, (3) large unknown biases, and small unknown biases which may have (4) unknown sign (±) or (5) known sign.

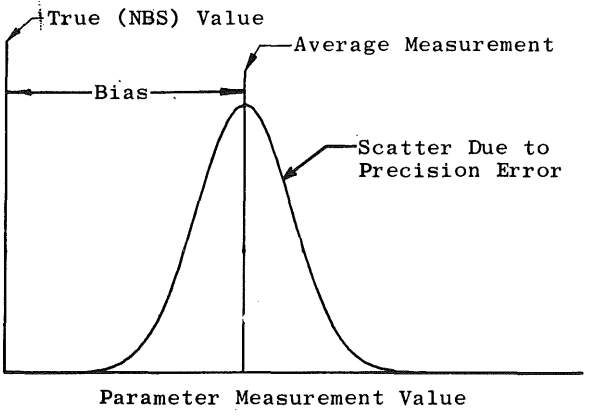

Fig. I-3 Bias Error

	Known Sign and Magnitude	Unknown Magnitude	
Large	(1) Calibrated Out	(3) Assumed to be Eliminated	
Small	(2) Negligible, Contributes to Bias Limit	(4) Unknown Sign	(5) Known Sign
		Contributes to Bias Limit	

Fig. I-4 Five Types of Bias Errors

1.3.2.1 Large Known Biases

The large known biases are eliminated by comparing the instrument with a standard instrument and obtaining a correction. This process is called calibration.

1.3.2.2 Small Known Biases

Small known biases may or may not be corrected depending on the difficulty of the correction and the magnitude of the bias.

1.3.2.3 Large Unknown Biases

Unknown biases are not correctable. That is, they may exist, but the magnitude of the bias is not known, and perhaps even the sign is not known.

Every effort must be made to eliminate all large unknown biases. The introduction of such errors converts the controlled measurement process into an uncontrolled worthless effort. Large unknown biases usually come from human errors in data processing, incorrect handling and installation of instrumentation, and unexpected environmental disturbances such as shock and bad flow profiles. In a well-controlled measurement process, the assumption is that there are no large unknown biases. To ensure that a controlled measurement process exists, all measurements should be monitored with statistical quality control charts. A list of references describing the use of statistical quality control charts is included at the end of this section. Drifts, trends, and movements leading to out-of-control situations should be identified and investigated. Histories of data from calibrations are required for effective control. It is assumed throughout this Handbook that these precautions are observed and that the measurement process is in control; if not, the methods contained herein are invalid.

1.3.2.4 Small Biases, Unknown Sign, and Unknown Magnitude

In most cases, the bias error is equally likely to be plus or minus about the measurement. That is, it is not known if the limit is positive or negative, and the estimate reflects this. The bias limit is estimated as an upper limit on the maximum fixed error. For example, ±5 pounds is a typical bias limit.

It is both difficult and frustrating to estimate the limit of an unknown bias. To determine the exact bias in a measurement, it would be necessary to compare the true value and the measurements. This is almost always impossible. An effort must be made to obtain special tests or data that will provide bias information. The following are examples of such data:

1. Interlab, interfacility, intercompany tests on measurement devices, test rigs, and full-scale engines.

2. Flight test data versus altitude test chamber data versus ground test data.

3. Special comparisons of standards with instruments in the actual test environment.

4. Ancillary or concomitant functions that provide the same performance parameter; i.e., in an altitude engine test, airflow may be measured with (1) an orifice and (2) a bellmouth, (3) estimated from compressor speed-flow rig data, (4) estimated from turbine flow parameter, and (5) jet nozzle calibrations.

5. When it is known that a bias results from a particular cause, special calibrations may be performed allowing the cause to perturbate through its complete range to determine the range of bias.

If there is no source of data for bias, the judgment of the most knowledgeable instrumentation expert on the measurement must be used. However, without data, the upper limit on the largest possible bias error must reflect the lack of knowledge.

1.3.2.5 Small Biases, Known Sign, and Unknown Magnitude

Sometimes the physics of the measurement system provide knowledge of the sign but not the magnitude of the bias. For example, thermocouples radiate and conduct energy to indicate lower temperatures. The bias limits which result are nonsymmetrical, i.e., not of the form ±b. They are of the form $^{+b}_{-c}$ where both limits may be positive or negative or the limits may be of mixed sign as indicated. Table I below lists several nonsymmetrical bias limits for illustration.

Table I Nonsymmetrical Bias Limits

Bias Limits	Explanation
0, +10 deg	The bias will range from zero to plus 10 deg.
-5, +15 lb	The bias will range from minus 5 to plus 15 lb.
+3, +7 psia	The bias will range from plus 3 to plus 7 psia.
-8, -3 deg	The bias will range from minus 8 to minus 3 deg.

In summary, measurement systems are subject to two types of errors, bias and precision error (Fig. I-5). One sample standard deviation is used as the precision index. The bias limit is estimated as an upper limit on the maximum fixed error.

1.4 MEASUREMENT UNCERTAINTY

For simplicity of presentation a single number (some combination of bias and precision) is needed to express a reasonable limit for error. The single number must have a simple interpretation (the largest error reasonably expected) and be useful without complex explanation. It is impossible to define a single rigorous statistic because the bias is an upper limit based on judgment which has unknown characteristics. Any function of these two numbers must be a hybrid combination of an unknown quantity (bias) and a statistic (precision). However, the need for a single number to measure error is so great that the adoption of an arbitrary standard is warranted. The standard most widely used is

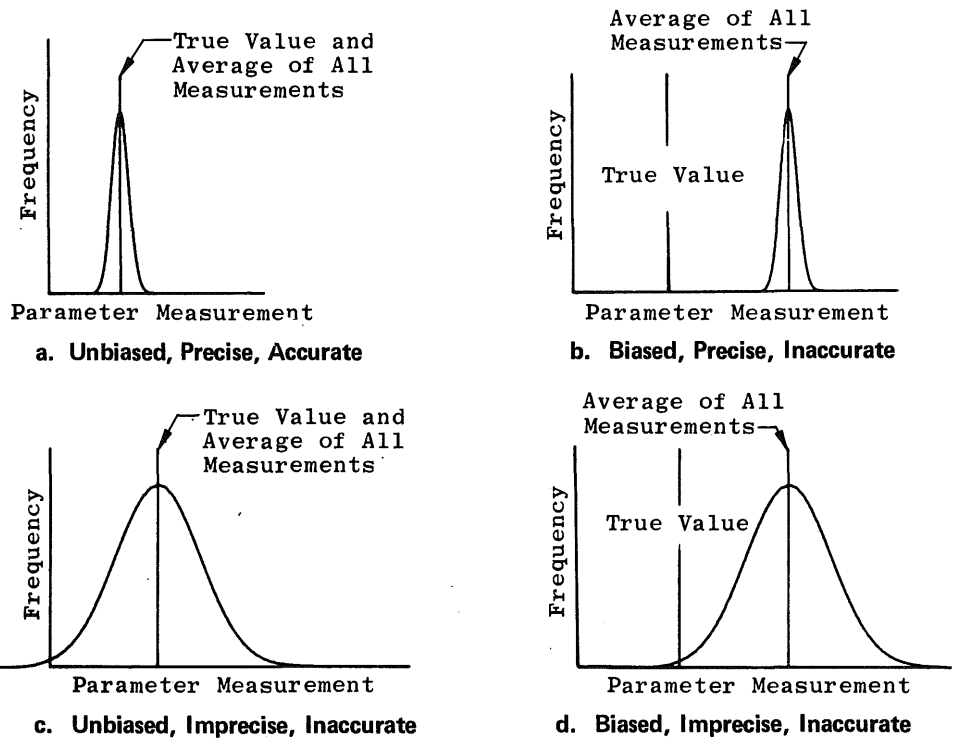

Fig. I-5 Measurement Error (Bias, Precision, and Accuracy)

the bias limit plus a multiple of the precision index. This method is recognized and recommended by the NBS[2] and has been widely used in industry.

Uncertainty (Fig. I-6) may be centered about the measurement and is defined herein as:

$$U = \pm(B + t_{95}S) \tag{I-1}$$

where B is the bias limit, S is the precision index, and t_{95} is the 95th percentile point for the two-tailed Students "t" distribution (Table E-1, Appendix E). The t value is a function of the number of degrees of freedom (df) used in calculating S. For small samples, t will be large, and for larger samples t will be smaller, approaching 1.96 as a lower limit. The use of the t arbitrarily inflates the limit U to reduce the risk of underestimating S when a small sample is used to calculate S. Since 30 degrees of freedom yield a t of 2.04 and infinite degrees of freedom yield a t of 1.96, an arbitrary selection of t = 2 for values of df from 30 to infinity was made, i.e., $U = \pm(B + 2S)$, when $df \geqslant 30$.

In a sample, the number of degrees of freedom is the size of the sample. When a statistic is calculated from the sample, the degrees of freedom associated with the statistic

[2]Eisenhart, C. "Expression of Uncertainties of Final Results, Precision Measurement and Calibration," NBS Handbook 91, Vol I, February 1969, pp. 69-72.

Ku, H. H. "Expressions of Imprecision, Systematic Error, and Uncertainty Associated with a Reported Value, Precision Measurement and Calibration," NBS Handbook 91, Vol I, February 1969, pp. 73-78.

are reduced by one for every estimated parameter used in calculating the statistic. For example, from a sample of size N, $\overline{X}$ is calculated:

$$\overline{X} = \sum_{i=1}^{N} X_i / N \tag{I-2}$$

which has N degrees of freedom and

$$S = \sqrt{\frac{\sum_{i=1}^{N} (X_i - \overline{X})^2}{N-1}} \tag{I-3}$$

which has N-1 degrees of freedom because $\overline{X}$ (based on the same sample of data) is used to calculate S. In calculating other statistics, more than one degree of freedom may be lost. For example, in calculating the standard error of a curve fit, the number of degrees of freedom which are lost is equal to the number of estimated coefficients for the curve.

It is recommended that the uncertainty parameter (U) be used for simplicity of presentation; however, the components (bias, precision, and degrees of freedom) should be available in an appendix or in supporting documentation. These three components may be required (1) to substantiate and explain the uncertainty value, (2) to provide a sound technical base for improved measurements, and (3) to propagate the uncertainty from measured parameters to performance parameters, and from performance parameters

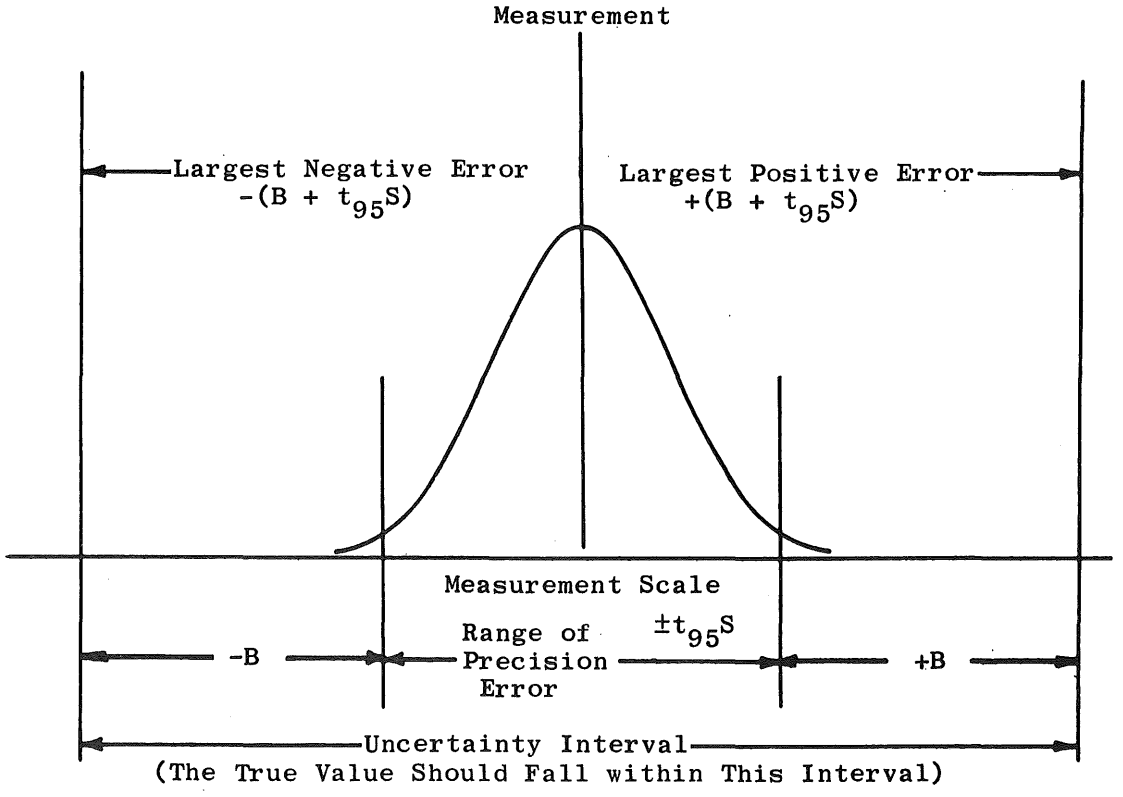

Fig. I-6 Measurement Uncertainty, Symmetrical Bias

to other more complex performance parameters (i.e. fuel flow to Thrust Specific Fuel Consumption (TSFC), TSFC to aircraft range, etc.). Although uncertainty is not a statistical confidence interval, it is an arbitrary substitute which is probably best interpreted as the largest error expected. Under any reasonable assumption for the distribution of bias, the coverage of U is greater than 95 percent, but this cannot be proved as the distribution of bias is both unknown and unknowable.

If there is a nonsymmetrical bias limit (Fig. I-7), the uncertainty U is no longer symmetrical about the measurement. The upper limit of the interval is defined by the upper limit of the bias interval (B^+). The lower limit is defined by the lower limit of the bias interval (B^-).

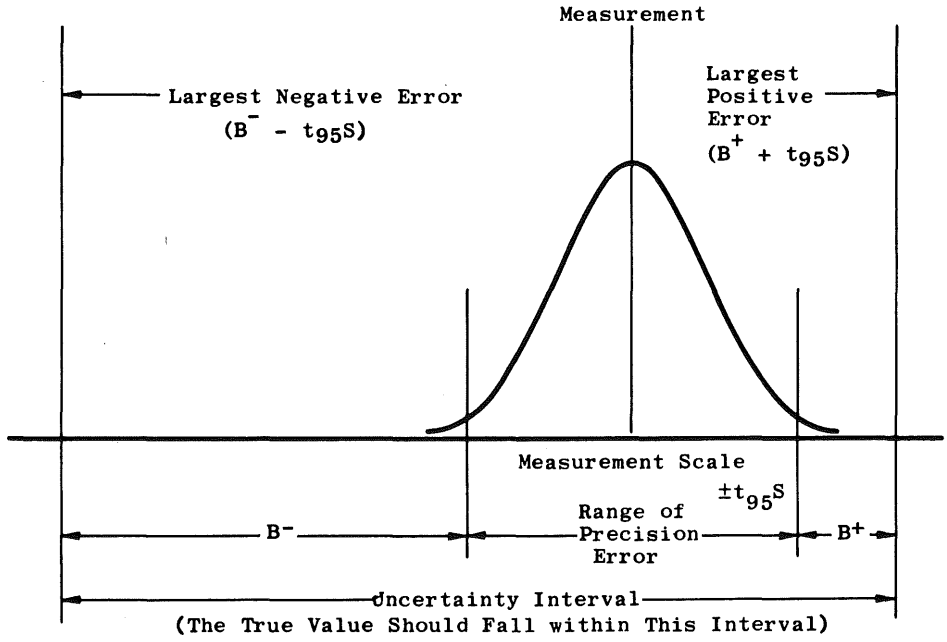

Fig. I-7 Measurement Uncertainty, Nonsymmetrical Bias

The uncertainty interval U is $U^- = B^- - t_{95}S$ to $U^+ = B^+ + t_{95}S$.

Table II shows the uncertainty U for the nonsymmetrical bias limits of Table I. The S and t_{95} are assumed to be 1 unit and 2 units for each case.

Table II Uncertainty Intervals Defined by Nonsymmetrical Bias Limits

B^-	B^+	$t_{95}S$	U^- (Lower limit for U)	U^+ (Upper limit for U)
0 deg	+10 deg	2 deg	-2 deg	+12 deg
-5 lb	+15 lb	2 lb	-7 lb	+17 lb
+3 psia	+7 psia	2 psia	+1 psia	+9 psia
-8 deg	-3 deg	2 deg	-10 deg	-1 deg

The proper method for combining elemental measurement uncertainty values is to determine the root-sum-square values of the elemental bias limits and the elemental precision indices separately. Then, apply the uncertainty formula to the combined bias limits and precision indices. In some cases, the same value will be obtained if the uncertainties are root-sum-squared directly. However, this is not a general rule, and large errors in the combined uncertainty (10 to 25 percent) can result. Further, the root-sum-squared uncertainty value will be smaller (optimistic) than the proper uncertainty estimate, and the estimate is a significant underestimate of the true measurement error.

For example, in combining the following uncertainties the root-sum-square of the uncertainties was 18.38 units. The correct value was 23.21 units.

Bias Limit (B)	Precision Index (S)	Uncertainty
1	6	±13
11	1	±13

where Uncertainty = ±(B + 2S).

Now the bias limit for the combined parameter is the root-sum-square of 1 and 11:

$$B = \sqrt{1^2 + 11^2} = \sqrt{122} = 11.05$$

The precision index for the combined parameter is the root-sum-square of 6 and 1:

$$S = \sqrt{6^2 + 1^2} = \sqrt{37} = 6.08$$

The Uncertainty is thus:

$$U = \pm(B + 2S) = \pm[11.05 + 2(6.08)] = \pm 23.21$$

The root-sum-square of the original uncertainties is

$$\sqrt{(13)^2 + (13)^2} = \sqrt{169 + 169} = \sqrt{338} = 18.38$$

Now,

$$\frac{23.21 - 18.38}{18.38} \times 100 = 26.3\%$$

and over 25 percent error has been introduced just because of the wrong propagation of error formula.

1.5 PROPAGATION OF MEASUREMENT ERRORS

Rarely are performance parameters measured directly; usually more basic quantities such as temperature, force, pressure, and fuel flow are measured, and the performance parameter is calculated as a function of the measurements. Error in the measurements is propagated to the parameter through the function. The effect of the propagation may be approximated with the Taylor's series methods.

1.5.1 Engine Inlet Airflow

Engine inlet airflow is determined by the use of a choked venturi and measurements of upstream temperature and stagnation pressure (Fig. I-8).

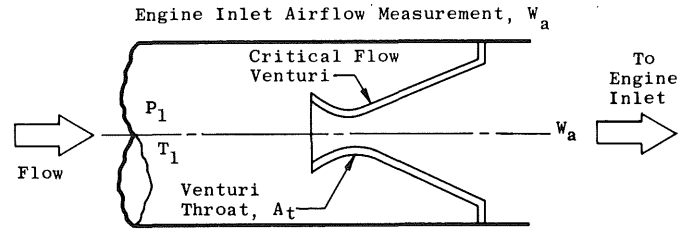

Fig. I-8 Flow through a Choked Venturi

The flow (W_a) is calculated from

$$W_a = F_A C^* A_{eff} P_1 / \sqrt{T_1} \quad \text{(I-4)}$$

where

F_A is the factor to account for thermal expansion of the venturi
A_{eff} is the effective venturi throat area
P_1 is the total (stagnation) pressure upstream
T_1 is the total temperature upstream
C^* is the factor to account for the properties of the air (critical flow constant)

The precision index for the flow (S_{W_a}) is calculated using the Taylor's series expansion (this method is derived in Appendix B):

$$S_{W_a} = \sqrt{\left(\frac{\partial W_a}{\partial F_A} S_{F_A}\right)^2 + \left(\frac{\partial W_a}{\partial C^*} S_{C^*}\right)^2 + \left(\frac{\partial W_a}{\partial A_{eff}} S_{A_{eff}}\right)^2 + \left(\frac{\partial W_a}{\partial P_1} S_{P_1}\right)^2 + \left(\frac{\partial W_a}{\partial T_1} S_{T_1}\right)^2} \quad \text{(I-5)}$$

where

$\frac{\partial W_a}{\partial F_A}$ denotes the partial derivative of W_a with respect to F_A.

Taking the necessary derivatives gives

$$S_{W_a} = \sqrt{\left(\frac{C^* A_{eff} P_1}{\sqrt{T_1}} S_{F_A}\right)^2 + \left(\frac{F_a A_{eff} P_1}{\sqrt{T_1}} S_{C^*}\right)^2 + \left(\frac{F_a C^* P_1}{\sqrt{T_1}} S_{A_{eff}}\right)^2 + \left(\frac{F_a C^* A_{eff}}{\sqrt{T_1}} S_{P_1}\right)^2 + \left(\frac{F_a C^* A_{eff} P_1}{-2\sqrt{T_1^3}} S_{T_1}\right)^2} \quad \text{(I-6)}$$

By inserting the nominal values and precision errors from Table III into Eq. (I-6), the precision index of 0.3658 lb/sec for engine airflow is obtained.

The bias limit in the flow calculation is propagated from the bias limits of the measured variables. Using the Taylor's series formula gives

$$B_f = \sqrt{\left(\frac{\partial f}{\partial x_1} B_{x_1}\right)^2 + \left(\frac{\partial f}{\partial x_2} B_{x_2}\right)^2 + \left(\frac{\partial f}{\partial x_3} B_{x_3}\right)^2 + \cdots + \left(\frac{\partial f}{\partial x_n} B_{x_n}\right)^2} \quad \text{(I-7)}$$

For this example, where $W_a = F_A C^* A_{eff} P_1 / \sqrt{T_1}$:

$$B_{W_a} = \sqrt{\left(\frac{\partial W_a}{\partial F_a} B_{F_a}\right)^2 + \left(\frac{\partial W_a}{\partial C^*} B_{C^*}\right)^2 + \left(\frac{\partial W_a}{\partial A_{eff}} B_{A_{eff}}\right)^2 + \left(\frac{\partial W_a}{\partial P_1} B_{P_1}\right)^2 + \left(\frac{\partial W_a}{\partial T_1} B_{T_1}\right)^2} \quad \text{(I-8)}$$

Taking the necessary derivatives gives

$$B_{W_a} = \sqrt{\left(\frac{C^* A_{eff} P_1}{\sqrt{T_1}} B_{F_A}\right)^2 + \left(\frac{F_a A_{eff} P_1}{\sqrt{T_1}} B_{C^*}\right)^2 \left(\frac{F_a C^* P_1}{\sqrt{T_1}} B_{A_{eff}}\right)^2 + \left(\frac{F_a C^* A_{eff}}{\sqrt{T_1}} B_{P_1}\right)^2 + \left(\frac{-F_a C^* A_{eff}}{-2\sqrt{T_1^3}} B_{T_1}\right)^2} \quad \text{(I-9)}$$

By inserting the nominal values and bias limits of the measured parameters from Table III into Eq. (I-9), a bias limit of 0.6987 lb/sec is obtained for a nominal engine airflow of 248.23 lb/sec.

Table III Flow Data

$W_a = F_A C^* A_{eff} P_1 / \sqrt{T_1}$

Parameter	Units	Nominal	Precision Index (One Standard Deviation)	Bias Limit
F_A	---	1.00	0.0	0.001
C^*	$\frac{\text{lbm } R^{1/2}}{\text{lb sec}}$	0.532	0.0	0.000532
A_{eff}	$in.^2$	296.	0.148	0.592
P_1	psia	36.8	0.05	0.05
T_1	°R	545.	0.3	0.3
$\therefore W_a$	$\frac{\text{lbm}}{\text{sec}}$	248.23	0.3658	0.6987

To propagate nonsymmetrical bias limits, the bias limit portion of the analysis must be completed for both the upper and the lower limits. Then, the two results are combined as illustrated in Table II. There is a more detailed illustration of propagation of nonsymmetrical bias limits in Section VIII.

1.5.2 Thrust Specific Fuel Consumption (TSFC)

The goal of any analysis of measurement system errors is to determine the resulting errors in the reduced parameters, for example TSFC, which is calculated as the ratio of fuel flow (W_f) to net thrust (F_N); TSFC = W_f/F_N. Net thrust and TSFC uncertainty calculations are described in Section VII. The technique for relating the errors of measurement to the errors in the reduced parameters is based on a Taylor's Series expansion from the calculus. The Taylor's expression for errors in thrust specific fuel consumption is

$$\Delta TSFC = \frac{\partial TSFC}{\partial W_f} \Delta W_f + \frac{\partial TSFC}{\partial F_N} \Delta F_N = \frac{1}{F_N} \Delta W_f - \frac{W_f}{F_N^2} \Delta F_N \qquad \text{(I-10)}$$

Where $\partial TSFC/\partial W_f$ and $\partial TSFC/\partial F_N$ are the partial derivatives of thrust specific fuel consumption with respect to fuel flow and net thrust. The precison index is approximated by

$$S_{TSFC} = \sqrt{\left(\frac{\partial TSFC}{\partial W_f} S_{W_f}\right)^2 + \left(\frac{\partial TSFC}{\partial F} S_F\right)^2} = \sqrt{\left(\frac{1}{F} S_{W_f}\right)^2 + \left(\frac{-W_f}{F^2} S_F\right)^2} \qquad \text{(I-11)}$$

For example, the following hypothetical data were used to estimate thrust specific fuel consumption uncertainty:

Parameter	Nominal	Bias Limit	Precision Index	Degrees of Freedom	Uncertainty Limit
Thrust (F_N)	10,000	18.1 lbf	37.8 lbf	57	93.7 lbf
Fuel Flow (W_f)	10,000	50 lbm/hr	50 lbm/hr	60	150 lbm/hr

The nominal thrust specific fuel consumption is calculated from W_f/F_N:

$$\frac{W_f}{F_N} = \frac{10{,}000}{10{,}000} \frac{\text{lbm/hr}}{\text{lbf}} = 1.0 \text{ lbm/lbf-hr}$$

The precision index of thrust specific fuel consumption is

$$S_{TSFC} = \sqrt{\left(\frac{1}{F_N} S_{W_f}\right)^2 + \left(\frac{-W_f}{F_N^2} S_{F_N}\right)^2} = \sqrt{\left(\frac{50}{10{,}000}\right)^2 + \left(\frac{-10{,}000}{10{,}000^2} \times 37.8\right)^2}$$

$$= \pm 0.0063 \text{ lbm/lbf-hr}$$

The propagation formula is similar for bias

$$B_{TSFC} = \sqrt{\left(\frac{\partial TSFC}{\partial W_f} B_{W_f}\right)^2 + \left(\frac{\partial TSFC}{\partial F_N} B_{F_N}\right)^2} \qquad \text{(I-12)}$$

$$B_{TSFC} = \sqrt{\left(\frac{1}{F_N} B_{W_f}\right)^2 + \left(\frac{-W_f}{F_N^2} B_{F_N}\right)^2} \qquad \text{(I-13)}$$

$$B_{TSFC} = \sqrt{\left(\frac{50}{10{,}000}\right)^2 + \left(\frac{-10{,}000}{10{,}000^2} 18.1\right)^2}$$

$$= \pm 0.0053 \text{ lbm/lbf-hr}$$

The degrees of freedom for the TSFC precision index can be found using the Welch-Satterthwaite technique. In this situation, the partial derivative weighting factors, which are used in the calculation of the precision index, must also be used in the Welch-Satterthwaite formula. Note: The calculation is carried out to illustrate the use of the partial derivatives with the Welch-Satterthwaite. It is not necessary to calculate the degrees of freedom for TSFC since the degrees of freedom for thrust and fuel flow are 57 and 60, respectively. The expected minimum result would be 57. The t multiple is essentially 2.0 for degrees of freedom greater than thirty (Section 1.4). When the degrees of freedom for each component are greater than 30, the Welch-Satterthwaite procedure can be omitted and t = 2.0 can be used.

$$df_{TSFC} = \frac{\left[\left(\frac{\partial TSFC}{\partial W_f} S_{W_f}\right)^2 + \left(\frac{\partial TSFC}{\partial F_N} S_{F_N}\right)^2\right]^2}{\frac{\left(\frac{\partial TSFC}{\partial W_f} S_{W_f}\right)^4}{df_{W_f}} + \frac{\left(\frac{\partial TSFC}{\partial F_N} S_{F_N}\right)^4}{df_{F_N}}} \tag{I-14}$$

$$= \frac{\left[\left(\frac{1}{F_N} S_{W_f}\right)^2 + \left(\frac{-W_f}{F_N^2} S_{F_N}\right)^2\right]^2}{\frac{\left(\frac{1}{F_N} S_{W_f}\right)^4}{df_{\dot{W}_f}} + \frac{\left(\frac{-W_f}{F_N^2} S_{F_N}\right)^4}{df_{F_N}}} \tag{I-15}$$

$$= \frac{\left[\left(\frac{1}{10{,}000} \times 50\right)^2 + \left(\frac{-10{,}000}{10{,}000^2} \times 37.8\right)^2\right]^2}{\frac{\left(\frac{1}{10{,}000} \times 50\right)^4}{60} + \frac{\left(\frac{-10{,}000}{10{,}000^2} \times 37.8\right)^4}{57}}$$

$$= 110$$

The t value is 2, and the uncertainty is

$$U = \pm(B + t_{95}S) = \pm[0.0053 + (2.0)(0.0063)] = \pm 0.0179 \text{ lbm/lbf-hr}$$

The results of the error analysis are presented in Table IV.

The uncertainty limit as a percent of the nominal value may be calculated by dividing the uncertainty limit in engineering units by the corresponding nominal value and then multiplying by 100.

The propagation of error formulas used in this section are derived and discussed in Appendix B.

Table IV Uncertainty Components

Parameter	Nominal Value	Bias Limit	Precision Error	Degrees of Freedom	Uncertainty
Thrust, F_N	10,000 lbf	18.1 lbf	37.8 lbf	57	93.7 lbf
Fuel Flow, W_f	10,000 lbm/hr	50 lbm/hr	50 lbm/hr	60	150 lbm/hr
Thrust Specific Fuel Consumption	1.0 lbm/lbf-hr	0.0053 lbm/lbf-hr	0.0063 lbm/lbr-hr	110	0.018 lbm/lbf-hr

1.6 MEASUREMENT PROCESS

In making uncertainty analyses, definition of the measurement process is of utmost importance. Uncertainty statements are based on a well-defined measurement process. A typical process is the measurement of thrust specific fuel consumption (TSFC) for a given gas turbine engine at a given test facility. The uncertainty of this measurement process will contain precision errors due to variations between installations, test stands, and measurement instruments. This uncertainty will be greater than the uncertainty for comparative tests to measure TSFC on a single test stand for a single engine, a different measurement process. The single stand, single engine, back-to-back test would assume that most installation and calibration errors would be biases rather than precision errors. Biases may be ignored in comparative testing in that the same equipment is used for all testing, and biases do not affect the comparison of one test with another (the test objective being to determine if a design change is beneficial). The single stand, single engine model and other comparative tests are treated in Section 8.3.

Because the definition of the measurement process is a prerequisite to defining the mathematical model, all the elemental bias and precision error sources which affect the measurements must be listed. Then, it must be determined how the bias and precision errors are related to the engine performance parameter. Based on this defined measurement process, the errors may be biases or precision errors.

The bias and precision errors related to the defined measurement process for thrust specific fuel consumption are listed in Section II. Uncertainty analyses should be repeated periodically. Continuous validation is essential.

1.7 REPORTING ERROR

The definition of the components, bias limit, precision index, and the limit (U) suggests a format for reporting measurement error. The format will describe the components of error, which are necessary to estimate further propagation of the errors, and a single value (U) which is the largest error expected from the combined errors. Additional information, degrees of freedom for the estimate of S, is required to use the precision index. These numbers provide all the information necessary to describe and use the measurement error. The reporting format is:

1. S, the estimate of the precision index, calculated from data.

2. df, the degrees of freedom associated with the estimate of the precision index (S).

3. B, the upper limit of the bias error of the measurement process or B^- and B^+ if the bias limit is nonsymmetrical.

4. $U = \pm(B + t_{95} S)$, the uncertainty limit, beyond which measurement errors would not reasonably fall. The t value is the 95th percentile of the two-tailed Student "t" distribution.

5. U, the interval between $U^- = B^- - t_{95} S$ and $U^+ = B^+ + t_{95} S$. These limits should be reported when the bias limit is nonsymmetrical.

The model components, S, df, B, and U, are required to report the error of any measurement process. As recommended in Section 1.4, for simplification, the first three components may be relegated to the detailed sections of uncertainty reports and presentations. The first three components, S, df, and B, are necessary to propagate the errors further, to propagate the uncertainty to more complex parameters, and to substantiate the uncertainty limit.

1.8 TRACEABILITY

In recent years the demanding requirements of military and commercial aircraft have led to the establishment of extensive hierarchies of standards laboratories within the military and the aerospace industry. The NBS is at the apex of these hierarchies, providing the ultimate reference for each standards laboratory. It has become commonplace for Government contracting agencies to require contractors to establish and prove traceability of their measurements to the NBS. This requirement has created even more extensive hierarchies of standards within the individual standards laboratories. At each level of these hierarchies, formal calibration procedures are used. These procedures not only define calibration methods and intervals but also specify just what information must be recorded during a calibration, i.e., meter model, serial number, calibration date, etc., in addition to actual measurement data.

The measurement process takes place over a long period of time. During this period, many calibrations occur at each level. Therefore, the precision errors of each comparison are precision errors affecting the measurement process. The overall effect on the measurement of force is a random (precision error) one. Therefore, the resultant overall precision index is the root-sum-square of the individual precision indices. For each comparison, the resultant calibration value is usually the average of several readings. The associated precision index would be a standard error of the mean (or standard error of estimate) for that number of readings. The precision index is

$$S = \sqrt{s_1^2 + s_2^2 + s_3^2 + s_4^2} \tag{I-16}$$

for four steps in the calibration process.

The degrees of freedom for each precision index may be combined using the Welch-Satterthwaite formula to provide an estimate of the degrees of freedom for the combined precision index.

$$df = \frac{\left(s_1^2 + s_2^2 + s_3^2 + s_4^2\right)^2}{\frac{s_1^4}{df_1} + \frac{s_2^4}{df_2} + \frac{s_3^4}{df_3} + \frac{s_4^4}{df_4}} \tag{I-17}$$

This technique was simulated for various sample sizes and provides the best known estimate of the equivalent degrees of freedom. The results of the simulation and the further use of the technique are discussed in CPIA No. 180 (AD855130). If non-integral values of df result from the Welch-Satterthwaite estimate, appropriate Student's t values can be found by interpolating from the table in Appendix E.

The unknown bias error limit for the end instrument is usually a function of many elemental bias limits, perhaps ten or twenty. It is unreasonable to assume that all of these biases are cumulative. There must be a cancelling effect because some are positive and some are negative. For this reason, the arbitrary rule that the bias limit B will be the root-sum-square of the elemental bias limit estimates was adopted:

$$B = \sqrt{b_1^2 + b_2^2 + b_3^2 + \cdots + b_L^2} \tag{I-18}$$

(where L is the number of sources of bias.)

In combining elemental nonsymmetrical bias limits, the upper limits should be root-sum-squared to determine the combined upper limit. The lower limits should be root-sum-squared to determine the combined lower limit. The resulting will be nonsymmetrical bias limits. An example of an error analysis containing nonsymmetrical bias limits is given in Section VIII.

The uncertainty in the measurement instrument due to calibration is calculated using the uncertainty formula:

$$U = \pm(B + t_{95}S) \tag{I-19}$$

where S is the precision index calculated from Eq. (I-16).

List of References on Statistical Quality Control Charts

Basic References

"ASTM Manual on Quality Control of Materials." ASTM STP 15-C (Available from American Society for Testing Materials, 1916 Race Street, Philadelphia, Pennsylvania 19103).

ASQC Standard B1, B2-1958. "Guide for Quality Control and Control Chart Method for Analyzing Data." ANSI Standard Z1.1, Z1.2, 1958.

ASQC Standard B3-1958. "Control Chart Method of Controlling Quality during Production." ANSI Standard Z1.3, 1958. (Available from American Society for Quality Control, 161 West Wisconsin Avenue, Milwaukee, Wisconsin 53203 or from American National Standards Institute, 1430 Broadway, New York, New York, 10018).

Duncan, A. J. Quality Control and Industrial Statistics. Third Edition, Richard D. Irwin, Incorporated, Homewood, Illinois, 1965.

Cowden, D. J. Statistical Methods in Quality Control. Prentice-Hall, Incorporated, Englewood Cliffs, New Jersey, 1957.

Juran, J. M., Editor. Quality Control Handbook. Second Edition, McGraw-Hill Book Company, New York, New York, 1962.

Examples of Control Charts in Metrology

Ku, H. H. "Statistical Concepts in Metrology." Chapter 2, Handbook of Industrial Metrology. American Society of Tool and Manufacturing Engineers, Prentice-Hall, Incorporated, New York, New York, 1967. (Reprinted in NBS SP 300-Vol. 1, "Precision Measurement and Calibration–Statistical Concepts and and Procedures." Available from the Superintendent of Documents, United States Government Printing Office, Washington, D.C. 20402).

Pontius, P. E. "Measurement Philosophy of the Pilot Program for Mass Calibration." NBS Technical Note 288, (Available from the Superintendent of Documents, United States Government Printing Office, Washington, D.C. 20402).

Pontius, P. E. and Cameron, J. M. "Realistic Uncertainties and the Mass Measurement Process." NBS Monograph 103, (Available from the Superintendent of Documents, United States Government Printing Office, Washington, D.C. 20402).

SECTION II
UNCERTAINTY MODEL

2.1 GENERAL

Terms such as bias[3], precision error, uncertainty, standard deviation, NBS, traceability, calibration, and degrees of freedom and the statistical concepts and mathematical procedures to be employed were introduced in Section I. This section will describe the mathematical model with words, illustrations, and an example.

It is intended that the examples given will closely fit typical applications. However, the model is general, and if specific calibration hierarchies are more or less extensive than the examples, simply add or omit levels and apply the model as shown; if specific measurement systems are different from the examples, substitute the bias limit and precision index terms for the system components and apply the model.

To review briefly, there are two types of measurement error: precision and bias. Precision error is the variation of repeated measurements of the same quantity. The sample standard deviation (S) is used as an index of the precision. Bias is the difference between the true value and the average of many repeated measurements. A limit (B) for the bias is estimated based on judgment, experience, and testing. The formula for combining these into uncertainty (U) is

$$U = \pm(B + t_{95}S) \tag{II-1}$$

or

$$U^- = B^- - t_{95}S \text{ and } U^+ = B^+ + t_{95}S$$

when nonsymmetrical biases are present.

Note that throughout this Handbook lower case notation always indicates elemental errors, i.e., s and b for elemental precision and bias, and upper case notation indicates the root-sum-square (RSS) combination of several errors, e.g.,

$$S = \pm\sqrt{s_1^2 + S_2^2 + s_3^2}$$

$$B = \pm\sqrt{b_1^2 + B_2^2 + b_3^2}$$

where

$$S_2 = \pm\sqrt{\Sigma_i\, s_i}$$

$$B_2 = \pm\sqrt{\Sigma_i\, b_i}$$

[3]For a definition of terms used in this Handbook, see the Glossary in Section IX.

The remainder of this section is devoted to illustration of a typical measurement uncertainty analysis and the propagation of errors to performance parameters.

2.2 MEASUREMENT ERROR SOURCES

For purposes of illustration, the elemental error sources for the force measurement system will be treated in this section. These error sources fall into three categories:

1. Calibration Hierarchy Errors (2.2.1)
2. Data Acquisition Errors (2.2.2)
3. Data Reduction Errors (2.2.3)

Elemental error sources for other measurements will be enumerated in the section dealing with each measurement.

2.2.1 Calibration Hierarchy Errors

To demonstrate traceability of measurements to the NBS, whose standards are by definition the "truth," it is necessary to establish calibration hierarchies. Each level in the hierarchy, including NBS, constitutes an error source which contributes to the error in the final measurement. Calibration of all measurement instruments at the NBS is possible;

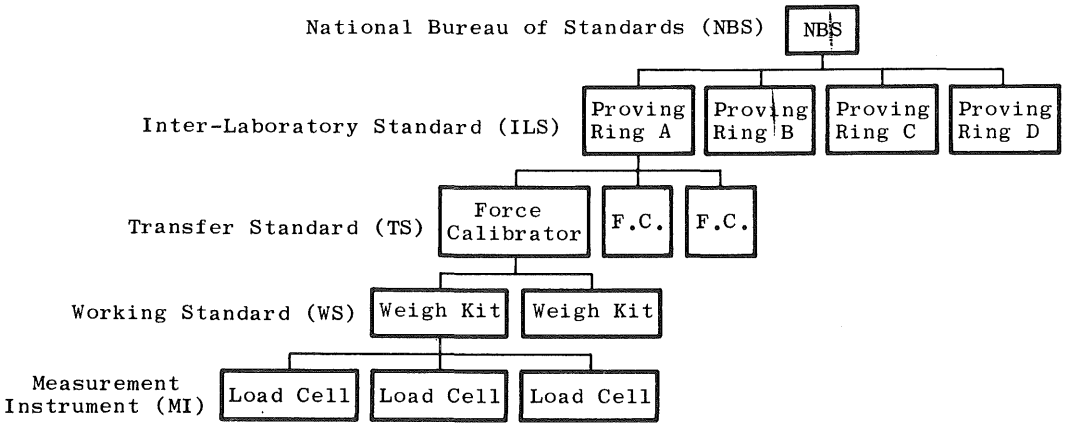

Fig. II-1 Force Measurement Calibration Hierarchy

however, such calibrations would be inconvenient, time consuming, and very expensive. The purpose here is to illustrate a typical hierarchy and to enumerate the error sources within. Figure II-1 is a typical force transducer calibration hierarchy. Associated with each comparison in the calibration hierarchy is a pair of elemental errors. These errors are the unknown bias and the precision index in each process. Note that these elemental errors are independent, e.g., b_{21} is not a function of b_{11}. The error sources are listed in Table V.

Table V Calibration Hierarchy Error Sources

Calibration	Bias Limit	Precision Index	Degrees of Freedom
NBS – ILS	b_{11}	s_{11}	df_{11}
ILS – TS	b_{21}	s_{21}	df_{21}
TS – WS	b_{31}	s_{31}	df_{31}
WS–MI	b_{41}	s_{41}	df_{41}

2.2.2 Data Acquisition Errors

Data are acquired by measuring the electrical output resulting from force applied to a strain-gage-type force measurement instrument. Figure II-2 illustrates some of the error sources associated with data acquisition. Other error sources such as electrical simulation, thrust bed mechanics, and environmental effects are also present. The best method to determine the effects of all of these error sources is to perform end-to-end calibrations and compare known applied forces with measured values. However, it is not always possible or even desirable to do this, and if this is the case, it is necessary to evaluate each of the elemental errors and combine them to determine the overall error.

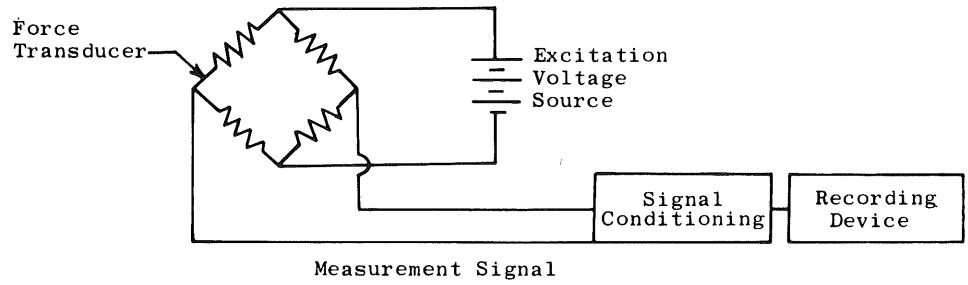

Fig. II-2 Data Acquisition System

All the data acquisition error sources are listed in Table VI. Symbols for the elemental bias and precision errors and for the degrees of freedom are shown.

2.2.3 Data Reduction Errors

Computers operate on raw data to produce output in engineering units. The errors in this process stem from calibration curve fits (Fig. II-3) and computer resolution.

Symbols for the data reduction error sources are listed in Table VII. These errors are often negligible in each process.

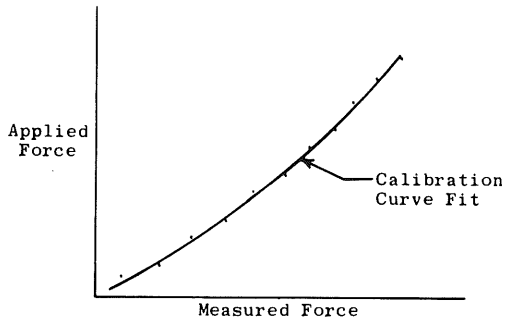

Fig. II-3 Calibration Curve

Table VI Data Acquisition Error Sources

Error Source	Bias Limit	Precision Index	Degrees of Freedom
Excitation Voltage	b_{12}	s_{12}	df_{12}
Electrical Simulation	b_{22}	s_{22}	df_{22}
Signal Conditioning	b_{32}	s_{32}	df_{32}
Recording Device	b_{42}	s_{42}	df_{42}
Force Transducer	b_{52}	s_{52}	df_{52}
Thrust Bed Mechanics	b_{62}	s_{62}	df_{62}
Environmental Effects	b_{72}	s_{72}	df_{72}

Table VII Data Reduction Error Sources

Error Source	Bias Limit	Precision Index	Degrees of Freedom
Calibration Curve Fit	b_{13}	s_{13}	df_{13}
Computer Resolution	b_{23}	s_{23}	df_{23}

2.3 MEASUREMENT UNCERTAINTY MODEL

The measurement process, defined for an entire engine test facility, is the totality of all the individual subprocesses and steps in the measurement system for a given engine type. That is, the process is the total of all the calibrations, all data acquisitions and all data reductions. Therefore, the precision error in each step of each subprocess is reflected as a precision error in the total process. The bias error in each subprocess is a bias error in the total process. (Another definition for the measurement process is discussed in Section VIII).

The precision index (S) at any stage in the total process is the root-sum-square of the elemental precision indices for that stage with the elemental precision indices for all of the preceding steps.

$$S = \pm\sqrt{\sum_j \sum_i s_{ij}^2} \tag{II-2}$$

where j defines the subprocesses calibration, data acquisition, and data recording and i defines the steps within the subprocess.

For example: The precision index for the calibration process is the root-sum-square of the elemental precision indices of Table V.

$$S_{cal} = \pm\sqrt{s_{11}^2 + s_{21}^2 + s_{31}^2 + s_{41}^2} \tag{II-3}$$

The precision index for the data acquisition process is the root-sum-square of the precision indices of Table VI.

$$S_{\substack{\text{Data} \\ \text{Acquisition}}} = \pm\sqrt{s_{12}^2 + s_{22}^2 + s_{32}^2 + s_{42}^2 + s_{52}^2 + s_{62}^2 + s_{72}^2} \tag{II-4}$$

The precision index for the data reduction process is the root-sum-square of the precision indices of Table VII.

$$S_{\substack{\text{Data} \\ \text{Reduction}}} = \pm\sqrt{s_{13}^2 + s_{23}^2} \tag{II-5}$$

The force measurement precision index is the root-sum-square of all the elemental precision indices in the force measurement system.

$$S_{Force} = \sqrt{s_{11}^2 + s_{21}^2 + s_{31}^2 + s_{41}^2 + s_{12}^2 + s_{22}^2 + s_{32}^2 + s_{42}^2 + s_{52}^2 + s_{62}^2 + s_{72}^2 + s_{13}^2 + s_{23}^2} \tag{II-6}$$

The bias limit for any stage in the process is the root-sum-square of the elemental errors in the preceding steps of the process.

For example: The bias limit for the calibration hierarchy is

$$B_{Cal} = \pm\sqrt{b_{11}^2 + b_{21}^2 + b_{31}^2 + b_{41}^2} \tag{II-7}$$

The bias limit for the data acquisition process is

$$B_{\substack{Data \\ Acquisition}} = \pm\sqrt{b_{12}^2 + b_{22}^2 + b_{32}^2 + b_{42}^2 + b_{52}^2 + b_{62}^2 + b_{72}^2} \tag{II-8}$$

The bias limit for the data reduction process is

$$B_{\substack{Data \\ Reduction}} = \pm\sqrt{b_{13}^2 + b_{23}^2} \tag{II-9}$$

The bias limit for the force measurement process is

$$B_{Force} = \sqrt{b_{11}^2 + b_{21}^2 + b_{31}^2 + b_{41}^2 + b_{12}^2 + b_{22}^2 + b_{32}^2 + b_{42}^2 + b_{52}^2 + b_{62}^2 + b_{72}^2 + b_{13}^2 + b_{23}^2} \tag{II-10}$$

Biases associated with force measurement are equally likely in either the plus or minus directions, i.e., there are no nonsymmetrical bias limit estimates.

The degrees of freedom (df) associated with the precision index at any step in the process are calculated using the Welch-Satterthwaite formula. It is a function of the degrees of freedom and magnitude of each elemental precision index.

For example: The degrees of freedom for the calibration precision index (S_{Cal}) is

$$df = \frac{\left[s_{11}^2 + s_{21}^2 + s_{31}^2 + s_{41}^2\right]^2}{\left[\frac{s_{11}^4}{df_{11}} + \frac{s_{21}^4}{df_{21}} + \frac{s_{31}^4}{df_{31}} + \frac{s_{41}^4}{df_{41}}\right]} \tag{II-11}$$

The degrees of freedom for the force measurement precision index is

$$df = \frac{\left[s_{11}^2 + s_{21}^2 + s_{31}^2 + s_{41}^2 + s_{12}^2 + s_{22}^2 + s_{32}^2 + s_{42}^2 + s_{52}^2 + s_{62}^2 + s_{72}^2 + s_{13}^2 + s_{23}^2\right]^2}{\left[\frac{s_{11}^4}{df_{11}} + \frac{s_{21}^4}{df_{21}} + \frac{s_{31}^4}{df_{31}} + \frac{s_{41}^4}{df_{41}} + \frac{s_{12}^4}{df_{12}} + \frac{s_{22}^4}{df_{22}} + \frac{s_{32}^4}{df_{32}} + \frac{s_{42}^4}{df_{42}} + \frac{s_{52}^4}{df_{52}} + \frac{s_{62}^4}{df_{62}} + \frac{s_{72}^4}{df_{72}} + \frac{s_{13}^4}{df_{13}} + \frac{s_{23}^4}{df_{23}}\right]} \tag{II-12}$$

The uncertainty parameter (U) at any stage is the sum of the bias limit (B) for that stage and the precision limit ($t_{95}S$). The precision limit ($t_{95}S$) for any stage is the precision index (S) for that stage times the 95th percentile of the student's "t" distribution (when the degrees of freedom are greater than 30, 2.0 is used for the "t" value). The uncertainty parameter (U) defines the limits of the measurement error that might reasonably be expected in a well-defined measurement process:

$$U = \pm(B + t_{95}S) \tag{II-13}$$

Figure II-4 illustrates the uncertainty parameter (U).

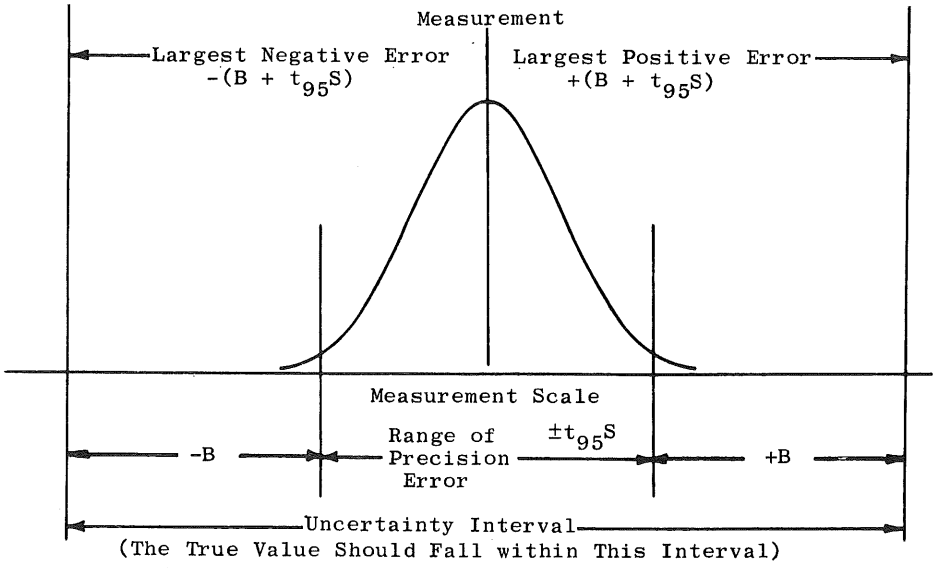

Fig. II-4 Uncertainty Parameter U = $\pm(B + t_{95}S)$

2.4 EXAMPLE OF THE MODEL

Figure II-5a is a block diagram showing the overall model for determining the uncertainty in gas turbine engine thrust specific fuel consumption. The blocks identify the two major parameters: net thrust and fuel flow. The dotted lines indicate the calculation of uncertainty for each parameter; solid lines indicate the propagation of bias limits and precision indices to the bias limit and precision index for thrust specific fuel consumption using Taylor's series methods. Detailed treatment of fuel flow measurement uncertainty and net thrust determination uncertainty is contained in Sections IV and VII, respectively.

In Fig. II-5b, it is seen that each parameter block contains three general types of errors: calibration errors, data acquisition errors, and data reduction errors. These are identified by S_1, S_2, and S_3, respectively, for precision indices and B_1, B_2, and B_3, respectively, for bias limits. The lines within each parameter indicate the calculation of uncertainty (U_1, U_2, and U_3) for each type of measurement. Other lines indicate the calculation of bias limits and precision indices for the individual parameters.

The final figure of the series (Fig. II-5c) illustrates the fact that each measurement is made up of several elemental sources of error. Examples of these are tabulated in Tables V, VI, and VII. In the figure, blocks indicate the formulas for the calculation of bias limits and precision indices at each level in the measurement process. The lines point out the procedures for determining bias limit (B), precision index (S), and uncertainty (U) for each process in the measurement chain and also for the calculated parameter, thrust specific fuel consumption.

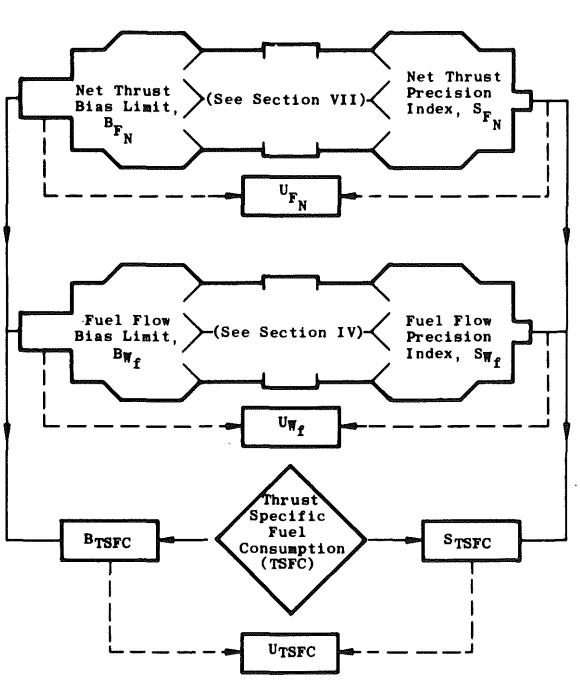

a. General View

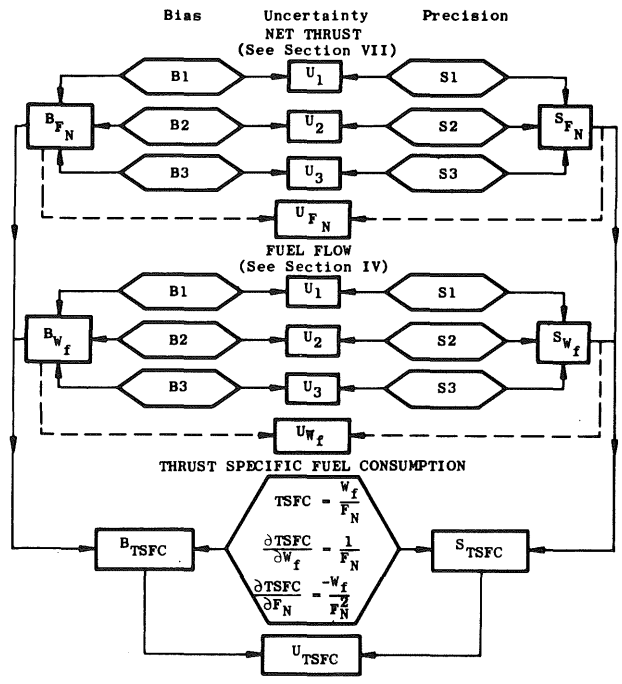

b. Propagation of Errors

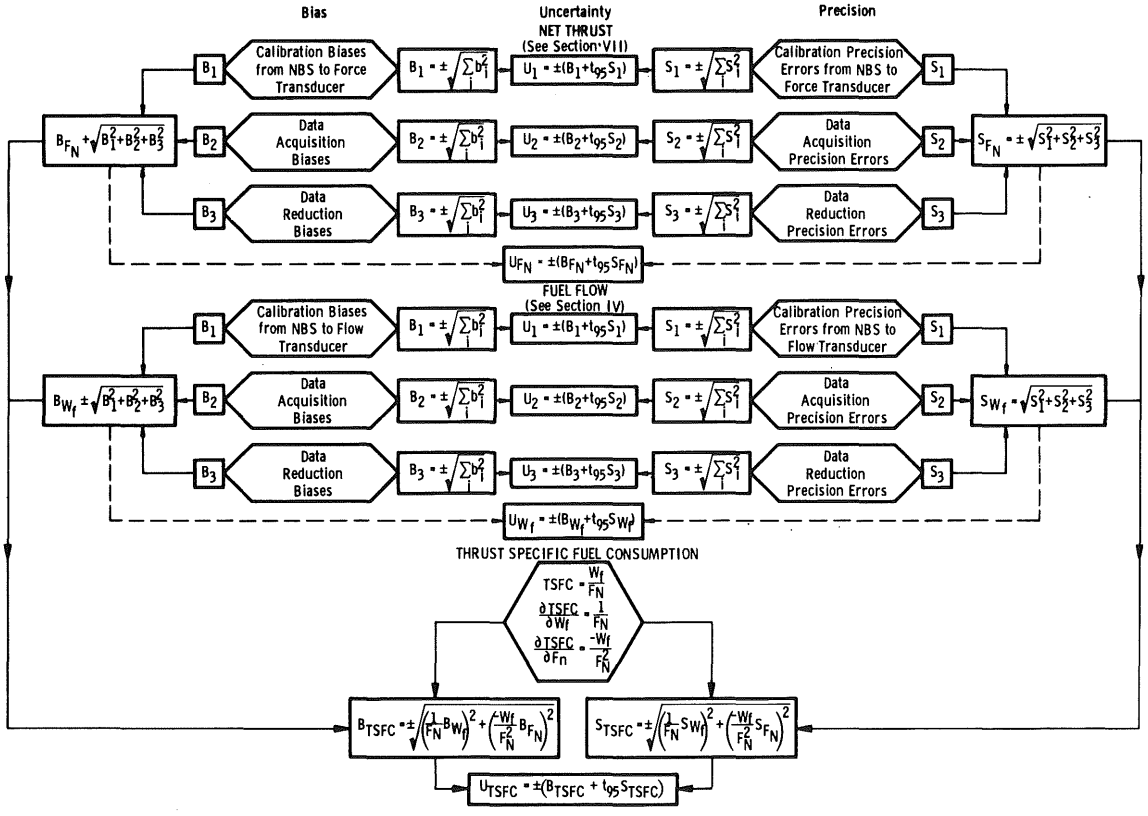

c. Elemental Errors

Fig. II-5 Overall Uncertainty Model

As an example, the uncertainty in the thrust specific fuel consumption of a gas turbine engine will be calculated. Test conditions are that the engine is being tested on an outdoor sea-level test stand. Assume a nominal sea-level thrust specific fuel consumption of 1.0 lbm/lbf-hr and 10,000 lbf and 10,000 lbm/hr for net thrust and fuel flow, respectively. Detailed treatment of the errors in net thrust determination may be found in Section 3.3 for sea-level testing which applies to this example. Section VII details the treatment of errors in net thrust determination at altitude conditions. For simplicity, values for the bias and precision index for fuel flow have been assumed.

2.4.1 Net Thrust Measurement

It is assumed that:

1. The net thrust bias limit is

$$B_{F_N} = \pm 18.1 \text{ lbf}$$

2. The net thrust precision index is

$$S_{F_N} = \pm 37.8 \text{ lbf}$$

3. The net thrust nominal level = 10,000 lbf

Then,

4. Net thrust uncertainty is

$$U_{F_N} = \pm(B_{F_N} + t_{95}S_{F_N}), \quad t_{95} = 2.00 \text{ because df} > 30 \text{ for } S_{F_N}$$

$$U_{F_N} = \pm(18.1 + 2.00 \times 37.8)$$

$$= \pm 93.7 \text{ lbf}$$

2.4.2 Fuel Flow Measurement

It is assumed that:

1. The fuel flow bias limit is

$$B_{W_f} = \pm 50 \text{ lb/hr}$$

2. The fuel flow precision index is

$$S_{W_f} = \pm 50 \text{ lb/hr}, \quad df_{W_f} = 60$$

3. The fuel flow nominal level = 10,000 lb/hr

Then,

4. Fuel flow uncertainty is

$$U_{W_f} = \pm\left(B_{W_f} + t_{95}S_{W_f}\right), t_{95} = 2.00 \text{ because df} > 30 \text{ for } S_{W_f}$$

$$U_{W_f} = \pm(50 + 2.00 \times 50)$$

$$= \pm 150 \text{ lb/hr}$$

2.4.3 Thrust Specific Fuel Consumption

The TSFC bias limit is

$$B_{TSFC} = \pm\sqrt{\left(\frac{1}{F_N}B_{W_f}\right)^2 + \left(\frac{-W_f}{F_N^2}B_{F_N}\right)^2}$$

$$B_{TSFC} = \pm\sqrt{\left(\frac{1}{10,000} \times 50\right)^2 + \left(\frac{-10,000}{10,000^2} \times 18.1\right)^2}$$

$$= \pm 0.0053 \text{ lbm/lbf-hr}$$

The TSFC precision index is

$$S_{TSFC} = \pm\sqrt{\left(\frac{1}{F_N}S_{wf}\right)^2 + \left(\frac{-W_f}{F_N{}^2}S_{F_N}\right)^2}$$

$$S_{TSFC} = \pm\sqrt{\left(\frac{1}{10,000} \times 50\right)^2 + \left(\frac{-10,000}{10,000^2} \times 37.8\right)^2}$$

$$= \pm 0.0063 \text{ lbm/lbf-hr}$$

The TSFC degree of freedom is

$$df_{TSFC} = \frac{\left[\left(\frac{\partial TSFC}{\partial W_f}S_{wf}\right)^2 + \left(\frac{\partial TSFC}{\partial F_N}S_{F_N}\right)^2\right]^2}{\frac{\left(\frac{\partial TSFC}{\partial W_f}S_{wf}\right)^4}{df_{wf}} + \frac{\left(\frac{\partial TSFC}{\partial F_N}S_{F_N}\right)^4}{df_{F_N}}}$$

$$df_{TSFC} = \frac{\left[\left(\frac{1}{F_N} S_{W_f}\right)^2 + \left(\frac{-W_f}{F_N^2} S_{F_N}\right)^2\right]^2}{\frac{\left(\frac{1}{F_N} S_{W_f}\right)^4}{df_{W_f}} + \frac{\left(\frac{-W_f}{F_N^2} S_{F_N}\right)^4}{df_{F_N}}}$$

When the degrees of freedom for each source of error are greater than thirty, the resultant degrees of freedom will also be greater than thirty. For illustrative purposes, the calculation of degrees of freedom are:

$$df_{TSFC} = \frac{\left[\left(\frac{1}{10,000} \times 50\right)^2 + \left(\frac{-10,000}{10,000^2} \times 37.8\right)^2\right]^2}{\frac{\left(\frac{1}{10,000} \times 50\right)^4}{60} + \frac{\left(\frac{-10,000}{10,000^2} \times 37.8\right)^4}{57}}$$

$$= 110$$

The result is greater than thirty, as expected. Therefore, $t_{95} = 2.00$.

The TSFC uncertainty is

$$U_{TSFC} = \pm(B_{TSFC} + t_{95} S_{TSFC})$$

$$U_{TSFC} = \pm(0.0053 + 2.00 \times 0.0063)$$

$$= \pm 0.018 \text{ lbm/lbf-hr}$$

2.5 SUMMARY

The statistical concepts and mathematical procedures used to develop the models are set forth in Section I.

In Section II, the uncertainty model is presented in mathematical, graphical, and block diagram form with a numerical example of how the model is to be used. These methods are summarized in Fig. II-6, a logic decision diagram. However, Sections I and II by no means provide full treatment of the problem of determining uncertainty in the gas turbine engine performance parameter, thrust specific fuel consumption. Some things which have not been treated in this section are:

1. Multiple measurements (see Appendix III)
2. Evaluation of elemental errors (see Sections III through VII)
3. Signed bias (see Section I).

To Estimate	Use	Formula
Bias Limit	(For Treatment of Signed Biases, see Section 1.3.2)	
1. Elemental (b)	Judgment Supported by Special Test Data	Estimate a Reasonable Limit for Each Bias Error
2. Measurement Bias	Estimated Elementals	$B_j = \sqrt{\sum_i b_i^2}$
3. Performance Parameter Bias	Measurement Bias and the Propagation of Error (Taylor Series)	$B_F = \sqrt{\sum_j \left(\frac{\partial F}{\partial j} B_j\right)^2}$ F Denotes Performance Parameter Function
Precision Index		
1. Elemental s_i	Data from Multiple Measurements	$S_i = \sqrt{\frac{\sum_L (X_L - X)^2}{N_L - 1}}$, $df = N_L - 1$
2. Measurement Precision Index	Calculated Elementals and Data	$S_j = \sqrt{\sum_i S_i^2}$, $df = \frac{\left[\sum_i S_i^2\right]^2}{\sum_i \left[\frac{S_i^4}{df_i}\right]}$
3. Performance Parameter Precision Index	Measurement Precision Indices and the Propagation of Error (Taylor Series)	$S_F = \sqrt{\sum_j \left(\frac{\partial F}{\partial j}\right) S_j^2}$ $df_F = \frac{\left[\sum_i \left(\frac{\partial F}{\partial j}\right) S_j^2\right]^2}{\sum_j \left[\frac{\left(\frac{\partial F}{\partial j} S_j\right)^4}{df_j}\right]}$
t_{95} Value	Degrees of Freedom Less Than 30 (df < 30)	Interpolate in Two-Tailed Student's "t" Table for t
	Degrees of Freedom Greater Than or Equal to 30 (df ≥ 30)	Use t = 2.0
Uncertainty		
1. Elemental	Elemental Bias Limit and Precision Index	$U_i = \pm\left[B_i + t_{95} S_i\right]$
2. Measurement	Measurement Bias Limits and Precision Indices	$U_j = \pm\left[B_j + t_{95} S_j\right]$
3. Performance Parameter	Performance Parameter Bias Limit and Precision Index	$U_F = \pm\left[B_F + t_{95} S_F\right]$

Fig. II-6 Logic Decision Diagram

SECTION III
FORCE MEASUREMENT

3.1 GENERAL

The purpose of this section is to illustrate the measurement uncertainty[4] model as applied to a typical force measuring system. Figure III-1 illustrates the system and will be the basis for all examples in this section. The propagation of force measurement and other parameter measurement uncertainties to obtain net thrust uncertainty are discussed in Section VII.

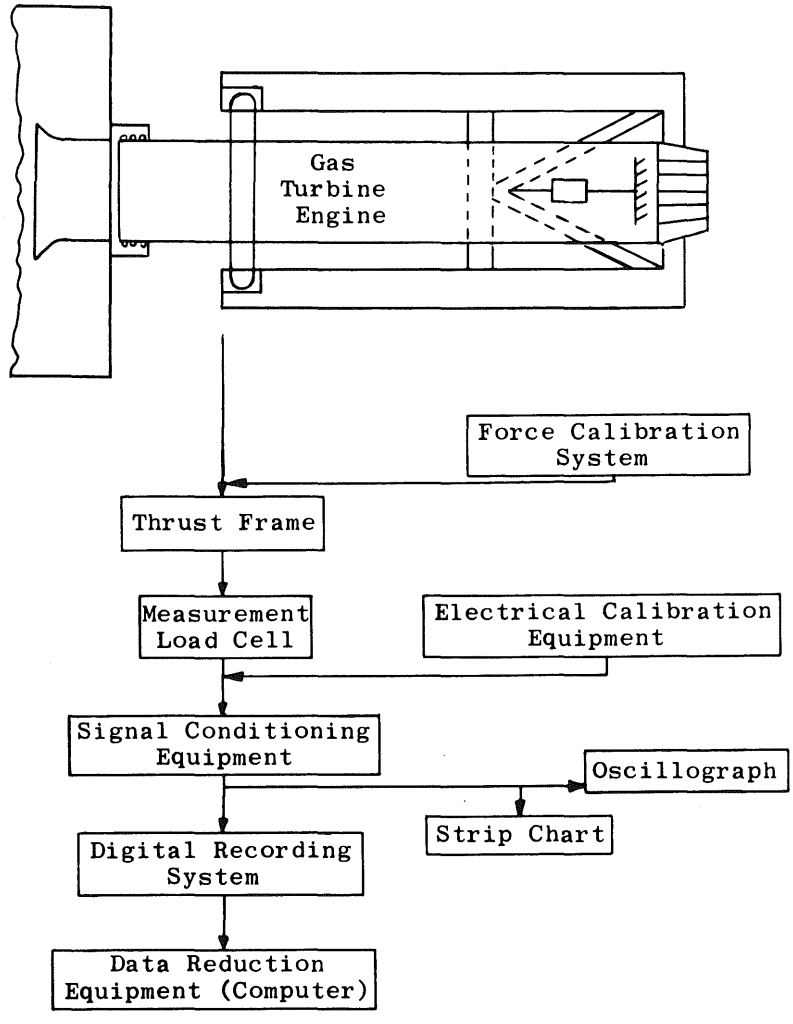

Fig. III-1 Force Measurement System

[4]For a definition of terms used in this handbook, see the Glossary in Section IX.

3.2 FORCE MEASUREMENT ERROR SOURCES

Error sources for any measurement fall into three categories: (1) calibration, (2) data acquisition, and (3) data reduction. These categories will be discussed in this order describing methods for determining values for the elemental errors.

3.2.1 Force Transducer Calibration Hierarchy

Figure III-2 illustrates a typical force transducer calibration hierarchy.

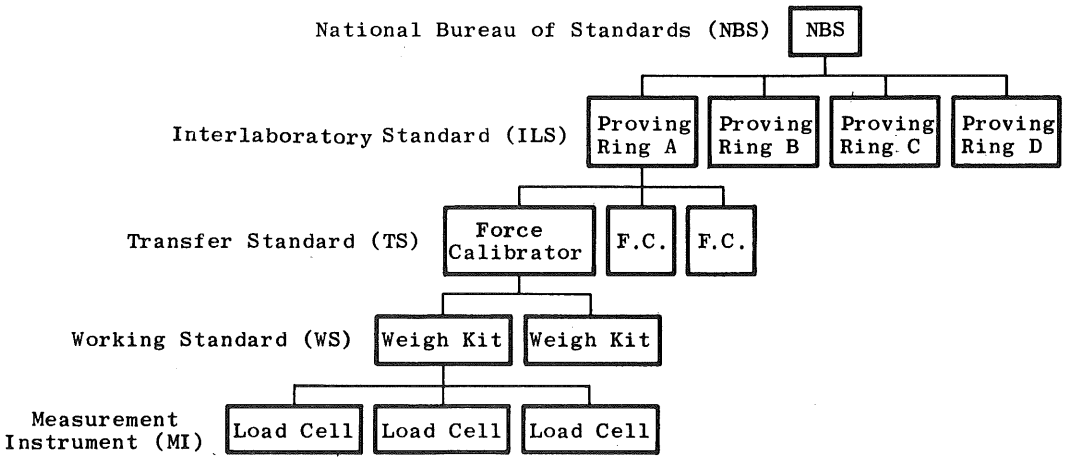

Fig. III-2 Force Transducer Calibration Hierarchy

Associated with each comparison in the calibration hierarchy is a pair of elemental errors. These errors are the unknown bias and the precision index in each process. Note that these elemental errors are not cumulative, e.g., b_{21} is not a function of b_{11}. The error sources are listed in Table VIII.

Table VIII Calibration Hierarchy Error Sources

Calibration	Bias Limit	Precision Index	Degrees of Freedom
NBS – ILS	b_{11}	s_{11}	df_{11}
ILS – TS	b_{21}	s_{21}	df_{21}
TS – WS	b_{31}	s_{31}	df_{31}
WS–MI	b_{41}	s_{41}	df_{41}

The bias limit for the calibration process is the root-sum-square of the elemental errors in the preceding steps of the process.

$$B_1 = \pm\sqrt{b_{11}^2 + b_{21}^2 + b_{31}^2 + b_{41}^2} \quad \text{(III-1)}$$

The precision index for the calibration process is the root-sum-square of the elemental precision indices in the preceding steps of the process.

$$S_1 = \pm\sqrt{s_{11}^2 + s_{21}^2 + s_{31}^2 + s_{41}^2} \quad \text{(III-2)}$$

Calibrations are accomplished by applying known forces to the instrument being calibrated and recording the output. The output may be inches deflection, millivolts,

pounds force, or other measurement units. Several known forces (usually eleven or more) are applied over the range of the instrument being calibrated as indicated in Table IX. The forces are applied first going up scale and then going down to determine the hysteresis errors.

Table IX Calibration Data

Applied Force Levels, F	Calibration One			Calibration Two		
	Measured Force		Calculated Force (From Curve Fit of Cal 1 Data)	Measured Force		Calculated Force (From Curve Fit of Cal 2 Data)
	Up	Down		Up	Down	
0	0.00	0.20	0.105	0.00	0.20	0.11
2	1.00	1.60	1.30	1.25	1.50	1.38
4	2.20	3.10	2.65	2.50	2.90	2.70
6	3.75	4.82	4.29	4.00	4.60	4.30
8	5.77	6.77	6.29	5.90	6.50	6.20
10	9.30		9.30	9.30		9.29

The data from Table IX are plotted in Fig. III-3. The calculated values are determined from a polynomial curve fit of the data. All four curves demonstrate the nonlinearity of the calibration (exaggerated for this example). The difference between the upscale lines and the downscale lines demonstrates the hysteresis of the system. Note that the contribution to overall uncertainty by transducer nonlinearity and hysteresis can be minimized by considering system performance over a relatively small range near nominal.

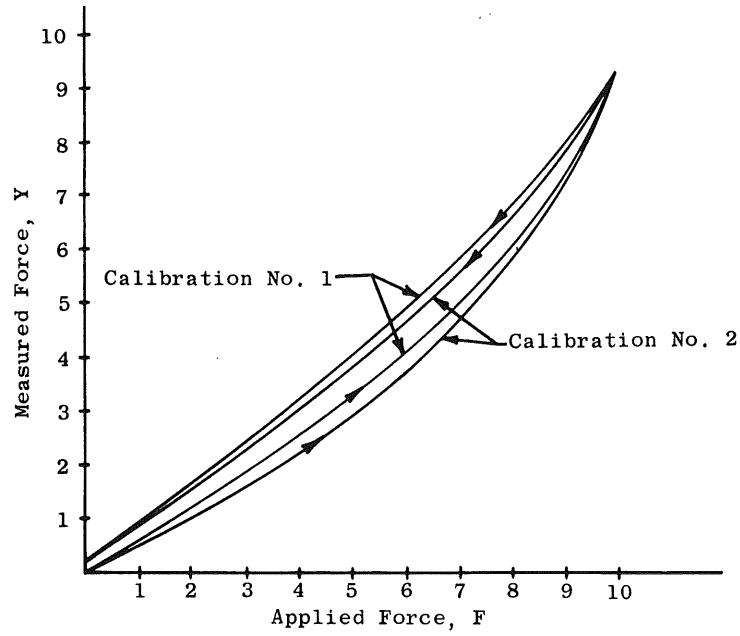

Fig. III-3 Calibration Curves

3.2.1.1 Precision Index

A least squares polynomial curve (Y) is fitted to the calibration data:

$$Y = A_o + A_1F + A_2F^2 + \cdots + A_kF^k \qquad \text{(III-3)}$$

where Y = calculated force with F pounds force applied

k = degree of curve fit, i.e., largest exponent of F

A_o through A_k are curve coefficients.

Figure III-4 illustrates a plot of calibration data with the dashed line representing a least squares polynomial curve fit. The Y value is the force calculated from the curve fit and corresponding to the applied force F in Eq. (III-3). The Y_j values are calculated from curve fits of previous calibrations establishing a set of Y_j, j = 1, ... N, where each Y_j represents a calibration and curve fit. The precision index at any particular point F_i on the curve is calculated by

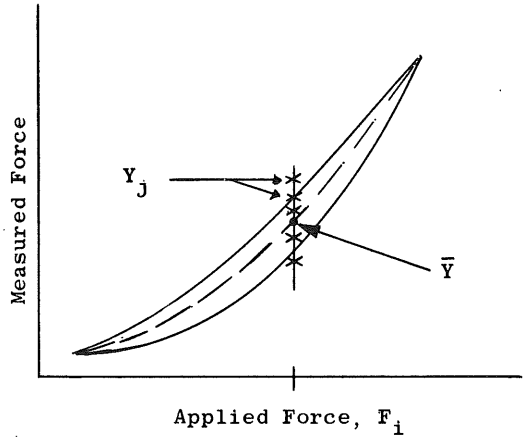

Fig. III-4 Scatter in Measured Force

$$s_i = \pm \sqrt{\frac{\sum_{j=1}^{N} (Y_j - \bar{Y})^2}{N-1}} \qquad \text{(III-4)}$$

where $\bar{Y}$ = the average of all Y_j values for this transducer at F_i

s_i = the precision index for Y with F_i pounds force applied

N = the number of calibrations in the estimate

Equation (III-4) yields the precision index for any value of F_i for any number of calibrations. For example, Fig. III-3 exhibits the data from two calibrations of one device, say an interlab standard. Table IX lists calculated values of $\bar{Y}$ from the data from both calibrations. At F_i = 4, Y = 2.675 and the Y_j values are 2.65 and 2.70. These data along with Eq. (III-4) yield

$$s_i = \pm \sqrt{\frac{(2.65 - 2.675)^2 + (2.70 - 2.675)^2}{(2-1)}}$$

$$s_i = \pm 0.034$$

Note that Eq. (III-4) yields the precision index for each value of F_i, but there are many values of F_i. The precision index for a given F_i value will apply over a narrow range of F, possibly ±10 percent of full scale from the point of interest. Generally, it should not be assumed that the precision index for 80 percent of full scale is the same as that for 10, 20, 30 percent and so on. Equation (III-4) applies in all of these cases, but the

differences $(Y_j - \overline{Y})^2$ must be summed for the different values of F_i and the largest reported as the precision index for the calibration process. Equations (III-3) and (III-4) and all of the rules presented above will apply to each level in the calibration hierarchy. The precision index for the complete hierarchy is calculated as indicated by Eq. (III-5):

$$S_1 = \pm\sqrt{\sum_i s_i^2} \qquad \text{(III-5)}$$

where S_1 = calibration hierarchy precision index

s_i = precision index for the individual levels in the hierarchy

3.2.1.2 Degrees of Freedom

The degrees of freedom (df_i) associated with the precision index (s_i) is one less than the number (N) of Y observations used to determine the precision index:

$$df_i = N-1 \qquad \text{(III-6)}$$

Degrees of freedom (df_i) may be calculated at each level in the calibration hierarchy. When the precision index (S_1) is calculated for the complete hierarchy, also calculate df_1 for the hierarchy utilizing the Welch-Satterthwaite technique (see example in Section 2.3) if any of the degrees of freedom are less than 30.

3.2.1.3 Bias

The bias for each level in the calibration hierarchy should be reported as plus or minus the largest unknown fixed error expected. At the first level in the hierarchy (NBS versus interlab standard), the NBS will state an upper limit of bias for the deadweights,

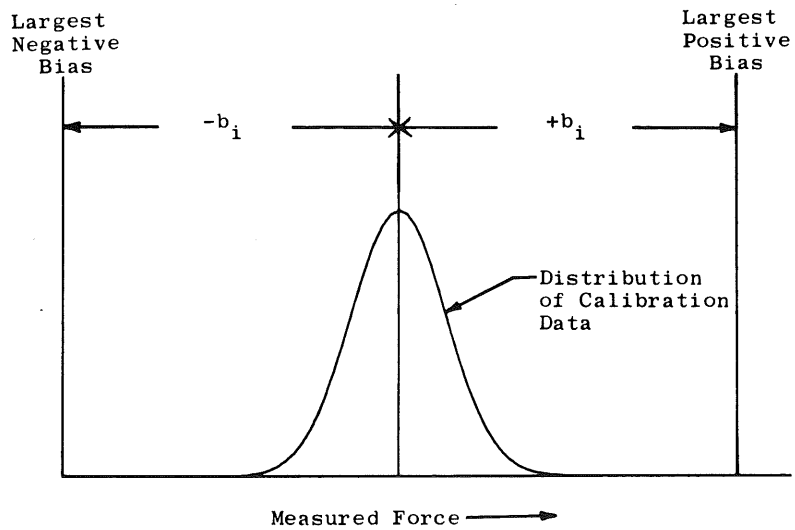

Fig. III-5 Calibration Hierarchy Elemental Bias

e.g., "the errors of the applied loads did not exceed 0.002 percent," quoted for the calibration of an interlab standard with a 60,000-lb capacity. This, however, is only the bias in the applied forces. There will be additional biases resulting from the calibration process. The estimate of the bias limits for the calibration process must be based on careful analysis of the calibration data and any other available information tempered by engineering judgment. For example, the data from an extremely large calibration history may lead to a bias estimate no greater than that reported at the preceding level in the hierarchy. On the other hand, if only one calibration is available to use as a guide to the bias estimate, the estimate from the preceding level in the hierarchy might be increased by an order of magnitude.

When bias limits (b_i) have been established for each level of the calibration hierarchy, a bias limit B_1 for the total hierarchy may be calculated, i.e.,

$$B_1 = \pm\sqrt{\sum_i b_i^2} \tag{III-7}$$

3.2.1.4 Uncertainty

Uncertainty in the calibration process is now obtained by a simple combination of the precision index and bias limit (see example in Section 2.3).

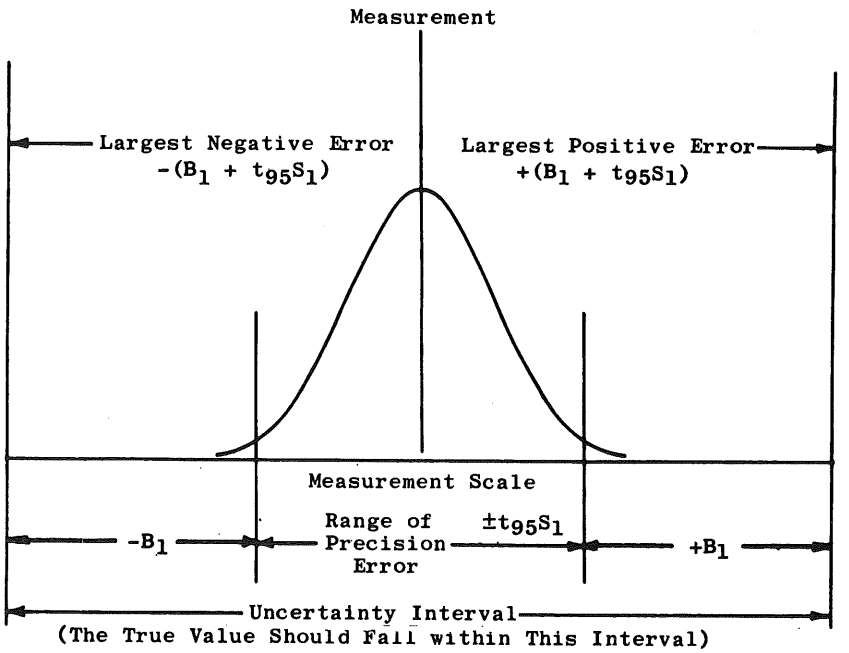

Fig. III-6 Calibration Process Uncertainty Parameter $U_1 = \pm(B_1 + t_{95}S_1)$

As indicated in Fig. III-6,

$$U_1 = \pm(B_1 + t_{95}S_1) \tag{III-8}$$

where U_1 = calibration hierarchy uncertainty

B_1 = calibration hierarchy bias limit

S_1 = calibration hierarchy precision index

t_{95} = 95th percentile of the "Student's" t distribution with df_1 degrees of freedom

3.2.2 Data Acquisition and Reduction Errors

The best method of evaluating the net effect of data acquisition and reduction errors is to periodically perform applied load tests. These tests will evaluate all data acquisition and reduction errors including errors due to force transducer temperature variations, fuel line temperature and pressure variations, fuel flow and environmental effects on the thrust bed.

All data acquisition error sources are listed in Table X. Symbols for the elemental bias and precision errors and for the degrees of freedom are also shown.

Table X Data Acquisition Error Sources

Error Source	Bias Limit	Precision Index	Degrees of Freedom
Excitation Voltage	b_{12}	s_{12}	df_{12}
Electrical Simulation	b_{22}	s_{22}	df_{22}
Signal Conditioning	b_{32}	s_{32}	df_{32}
Recording Device	b_{42}	s_{42}	df_{42}
Force Transducer	b_{52}	s_{52}	df_{52}
Thrust Bed Mechanics	b_{62}	s_{62}	df_{62}
Environmental Effects	b_{72}	s_{72}	df_{72}

The bias limit for the data acquisition process is

$$B_2 = \pm\sqrt{b_{12}^2 + b_{22}^2 + b_{32}^2 + b_{42}^2 + b_{52}^2 + b_{62}^2 + b_{72}^2} \qquad \text{(III-9)}$$

The precision index for the data acquisition process is

$$S_2 = \pm\sqrt{s_{12}^2 + s_{22}^2 + s_{32}^2 + s_{42}^2 + s_{52}^2 + s_{62}^2 + s_{72}^2} \qquad \text{(III-10)}$$

The computer operates on the raw data to produce output in engineering units. The errors in this process stem from the calibration curve fits and the computer resolution.

Symbols for the data reduction error sources are listed in Table XI. These errors are often negligible in each process.

Table XI Data Reduction Error Sources

Error Source	Bias Limit	Precision Index	Degrees of Freedom
Calibration Curve Fit	b_{13}	s_{13}	df_{13}
Computer Resolution	b_{23}	s_{23}	df_{23}

The bias limit for the data reduction process is

$$B_3 = \pm\sqrt{b_{13}^2 + b_{23}^2} \qquad \text{(III-11)}$$

The precision index for the data reduction process is

$$S_3 = \pm\sqrt{s_{13}^2 + s_{23}^2} \qquad \text{(III-12)}$$

3.2.2.1 Applied Load Tests

Applied load tests are performed as follows:

1. Install an engine in the test stand.
2. Connect all service lines (fuel, instrumentation, water, etc.) and other restraints to the engine.
3. Perform an end-to-end calibration of the force measurement system in the usual manner (with all service systems operating at nominal levels if practical).
4. Evaluate the calibration data and perform a curve fit according to normal procedures.
5. Perform the usual pre-run set-up procedures as if preparing for an engine run. Just prior to an engine run is an excellent time to perform an applied load test.
6. Apply a known force by means of the force calibration system equal to the nominal expected when the engine is delivering rated thrust.
7. Record digital data at a sampling rate and for a period which is normal for steady-state engine conditions; also, record the applied force (X) indicated by the standard.
8. Make several (ten or more) recordings as defined in (7) above.
9. Reduce the data by means of the engine data reduction program.
10. Regardless of the number of measuring devices used (multiple bridge load cells, multiple load cells, etc.), calculate multiple sample average Y_{kj} for each steady-state recording. The average of the ten or more recordings ($\bar{Y}_j$) for the jth bridge or transducer is

$$\bar{Y}_j = \frac{\sum_{k=1}^{M} Y_{kj}}{M} \qquad \text{(III-13)}$$

where M = number of steady-state recordings.

The grand average $\overline{\overline{Y}}$ is then calculated for all load cells

$$\overline{\overline{Y}} = \frac{\sum_{i=1}^{N} \overline{Y}_j}{N} \tag{III-14}$$

where N = number of bridges

11. This grand average ($\overline{\overline{Y}}$) represents a measurement of the known input. The precision index (s_i) for this average is estimated from the precision error of the bridges and/or load cells (s_b):

$$s_b = \pm\sqrt{\frac{\sum_{j=1}^{N} (\overline{Y}_j - \overline{\overline{Y}})^2}{N-1}} \tag{III-15}$$

The estimate of s_i is s_b divided by the square root of the number of bridges (N):

$$s_i = \pm \frac{s_b}{\sqrt{N}} = \pm\sqrt{\frac{\sum_{j=1}^{N} (\overline{Y}_j - \overline{\overline{Y}})^2}{N(N-1)}} \tag{III-16}$$

12. If several applied load tests are performed, the precision index of the data acquisition and reduction process is calculated by pooling the estimates (s_i) from each test:

$$s_{ip} = \pm\sqrt{\frac{\Sigma s_i^2}{K}} \tag{III-17}$$

where K tests have been performed.

13. The bias limit for data acquisition and reduction may be estimated through careful analysis of ancillary data such as applied load test histories tempered by the judgment of the most knowledgeable force measurement engineer.

Applied load tests performed in the preceding manner will evaluate the net effect of the following error sources:

1. Excitation voltage
2. Electrical calibration of the data recording system
3. Analog to digital conversion

4. Stand mechanics

5. Calibration curve fit

6. Computer resolution

Performance of additional applied load tests at the conclusion of engine runs will provide evaluation of the net effects of:

1. Environmental effects on force transducer

2. Effects of fuel line temperature and pressure variations

3. Environmental effects on the thrust bed

Post-run applied load tests are performed immediately after engine shutdown as follows:

1. Ensure that fuel lines are at nominal run temperatures and pressures

2. If practical, flow fuel at nominal flow rates

3. Ascertain that the force measurement system is at run temperature

4. Apply a known force as described in the pre-run applied load test

5. Record test data as described in pre-run test procedures

6. Record an electrical calibration of the data recording system to ensure no change since the pre-run calibration

7. Reduce data as described in pre-run test procedures

8. Calculate precision index using Eqs. (III-15) through (III-17)

9. Estimate bias limit

3.2.2.2 Elemental Error Evaluation

If it is undesirable or impractical to perform applied load tests frequently, the alternative is to evaluate individually all elemental errors and combine them statistically. The complete list of data acquisition and reduction elemental errors is:

1. Stand mechanics

2. Fuel line temperature variations

3. Fuel line pressure variations
4. Force transducer temperature variations
5. Excitation voltage
6. Recording system electrical calibration
7. Analog-to-digital converter nonlinearity and drift
8. Recording system resolution
9. Electrical noise
10. Tare evaluation (thrust stand losses)
11. Computer resolution

In the following sections, the above errors are discussed in enough detail to evaluate them and combine them statistically.

3.2.2.2.1 Stand Mechanics

Several mechanical features of the thrust stand (Fig. III-7) must be considered and their effects evaluated. These features are:

1. Design of thrust bed support system
2. Flexure design
3. How much deflection can be expected in the thrust bed and measurement linkage when a force equal to nominal rated thrust is applied at the point(s) of engine support?

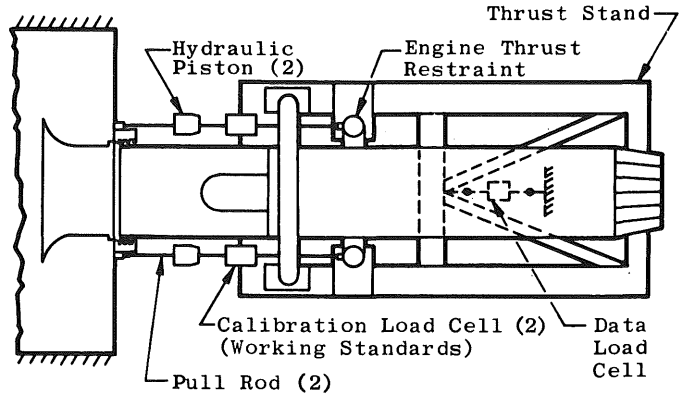

Fig. III-7 Gas Turbine Thrust Measurement System Calibration Configuration

4. How are fuel lines supported?

5. How are fuel lines and other restraints oriented with relation to the axial force vector?

6. What is the effect of engine and instrumentation weight on force measurement?

Some of these are simply considerations to be made, with improvements to minimize the effects being the obvious course of action. Errors caused by stand mechanics will always exist to some degree.

If in-place calibrations are not performed, i.e., only laboratory calibrations of the force measurement transducers are performed, then applied load tests are required to evaluate errors caused by stand mechanics. For example, if applied load tests are performed with and without the weight of the engine and instrumentation on the thrust bed and the load cell output is measured by means of a laboratory potentiometer to eliminate recording system errors, then the difference between measured force and applied force with no engine installed is the error due to thrust bed design. The difference between measured force and applied force with an engine and instrumentation installed is the error caused by test stand design and the additional weight. If several tests of this nature are performed, distributions of data can be developed and handled statistically. Figure III-8 illustrates data distribution X_1 without the engine installed, and

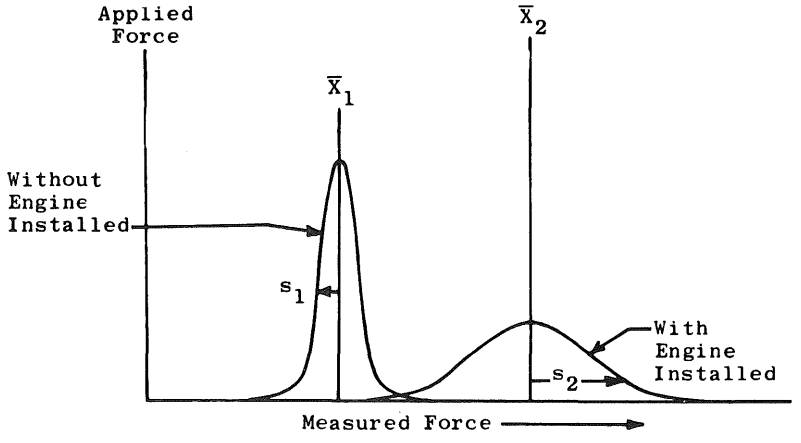

Fig. III-8 Precision Errors

data distribution X_2 with the engine installed. The precision index for tests without the engine installed is

$$s_1 = \sqrt{\frac{\Sigma(X_i - \bar{X}_1)^2}{(N-1)}} \qquad \text{(III-18)}$$

The precision index for tests with the engine installed is

$$s_2 = \sqrt{\frac{\Sigma(X_i - \overline{X}_2)^2}{N-1}} \qquad \text{(III-19)}$$

where:

X = applied force

s_1 = precision index of tests without engine installed

s_2 = precision index of tests with engine installed

$\overline{X}_1$ = the average of all measured values without engine installed

$\overline{X}_2$ = the average of all measured value with engine installed

N = number of tests with engine installed or without engine installed

Unknown bias limit estimates may be made as indicated in Section 3.2.2.1, item 13. Similar tests can be designed to evaluate the effect of other error sources in this category.

3.2.2.2.2 Fuel Line Temperature Variations

Variations in fuel line temperature result in more or less restraint on the force measuring system, side loads, and possible axial loads. In-place calibration of the measurement load cell will not account for errors from this source, unless, of course, run temperature is maintained during calibration. Again, applied load tests are the best solution with data being evaluated as in the preceding section on stand mechanics. If in-place force transducer calibrations are performed, with the engine and all associated plumbing installed, errors from the above sources will be reflected as nonlinearity and hysteresis in the calibration data. These errors then become a part of the error attributed to the working standard versus force measurement transducer calibration process. Calculation of the precision index (s_i) at each operating point F is accomplished with Eq. (III-4).

$$s_i = \pm\sqrt{\frac{\sum_{j=1}^{N}(Y_j - \overline{Y})^2}{N-1}} \qquad \text{(III-4)}$$

where $\overline{Y}$ is the value of the calibration curve at the operation point F, and the N values (Y_j) are the calculated values at F as defined in Section 3.2.1.1 (Fig. III-4). The degrees of freedom associated with s_i are N-1.

3.2.2.2.3 Fuel Line Pressure Variations

Side loads and axial loads are the usual result of pressurizing fuel lines. Once again, in-place calibration will not account for this error unless the lines are pressurized during the calibration. Applied load tests will aid in evaluating this error. Data should be evaluated as discussed in Section 3.2.2.2.1.

3.2.2.2.4 Force Transducer Temperature and Ambient Pressure Variations

3.2.2.2.4.1 Temperature Variations

The best method for minimizing the effect of temperature variations is to minimize the variations through environmental control. This, however, is not always possible. Another way to combat this problem is to perform applied load tests in the laboratory at different fixed temperatures on individual load cells. Suppose a load cell is loaded to X pounds, N_1 times, at a constant temperature of 75°F, and the average of the N observations is $\overline{X}_1$. The precision index and the bias, which is correctable, may be established as follows:

$$s_{L1} = \pm\sqrt{\frac{\sum_{i=1}^{N_1}(X_i - \overline{X}_1)^2}{N_1 - 1}} \qquad \text{(III-20)}$$

$$b_{L1} = \geq \overline{X}_1 - X \qquad \text{(III-21)}$$

where

s_{L1} = precision index for the load cell

X_i = force indicated by the load cell

Now, if the same load X is applied, N_2 times, at a constant temperature of 40°F and the average of the N_2 observations is $\overline{X}_2$, then

$$s_{L2} = \pm\sqrt{\frac{\sum_{i=1}^{N_2}(X_i - \overline{X}_2)^2}{N_2 - 1}} \qquad \text{(III-22)}$$

$$b_{L2} \geq \overline{X}_2 - X \qquad \text{(III-23)}$$

where

s_{L2} = precision index for the load cell

X_i = force indicated by the load cell

To be conservative, the largest of the two precision errors (s_{L1} and s_{L2}) is selected as the elemental error for this source. This will minimize the possibility that changes in conditions will invalidate the estimated uncertainty value. A relatively large change in bias and very little change in precision error is expected (Fig. III-9).

In evaluating the effect of temperature variations on load cells, it is very important to determine the temperature of the strain-gage bridge both in the laboratory and in the test environment. Large temperature gradients between the outer shell and inner working parts of a load cell may well result in serious errors in correction values.

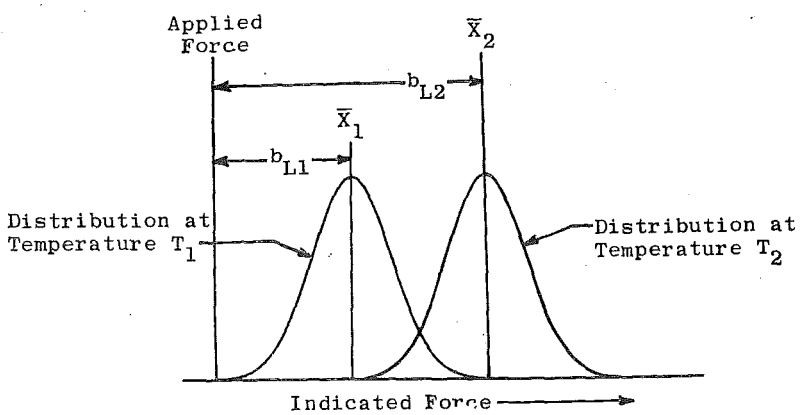

Fig. III-9 Temperature Bias Effect on Distributions of Errors

3.2.2.2.4.2 Ambient Pressure Variations

When used in altitude test chambers, load cells may be exposed to a range of ambient pressure levels from approximately 14.7 (one atmosphere) to about 0.5 psia. A typical variation of load cell output versus ambient pressure is shown in Fig. III-10. The sensitivity of the load cell to ambient pressure is, of course, a function of the load cell physical characteristics. Some load cells are compensated to nullify partially the effects of ambient pressure variation. Typically, load cells exhibit an increasing output in the tension direction with decreasing ambient pressure. Data reduction programs must correct for load cell ambient pressure effects to remove this bias error from the data. The data reduction program typically makes this correction based on a measurement of the load cell environmental pressure during altitude testing.

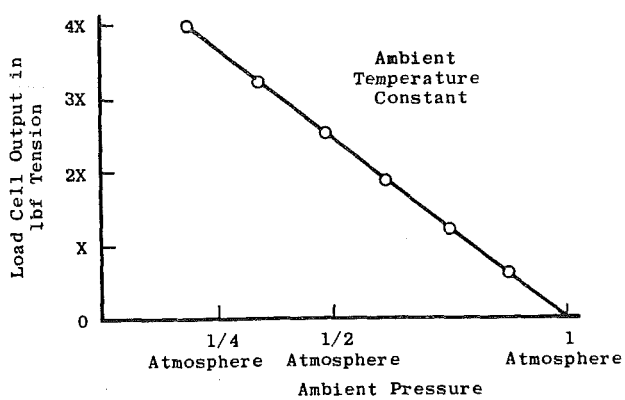

Fig. III-10 Ambient Pressure Effect on Load Cell Output

To determine the load cell sensitivity to ambient pressure, laboratory tests are performed with the load cell in a "bell jar." The pressure within the "bell Jar" is adjusted over the desired range, and load cell output is recorded at several discrete pressure levels. Each discrete pressure level is maintained for several minutes, and the load cell output is monitored to detect any significant pressure leaks in the load cell.

The elemental errors associated with the load cell ambient pressure calibration, the environmental pressure parameter measurement, and data reduction must be considered in determining the force measurement uncertainty.

3.2.2.2.5 Excitation Voltage Errors

Instrumentation excitation power supplies are usually purchased with rigid requirements on output voltage drift and regulation. If verification limits for excitation voltage are established, say ±0.05 percent of the output, and then laboratory tests are performed to ensure that the power supply produces the desired voltage within these limits; then the precision index is

$$s_i = \pm 0.0003 \times \text{desired voltage} \tag{III-24}$$

and the bias limit is

$$b_i = \pm 0.0005 \times \text{desired voltage} \tag{III-25}$$

where s_i is the calculated precision assuming a uniform distribution over the interval ±0.0005. Uniform is a conservative assumption for the errors. They probably will have a central tendency.

For any uniform interval, the precision index is calculated by taking the square root of the upper limit minus the lower limit squared divided by 12:

$$s_i = \sqrt{\frac{(\text{Upper} - \text{Lower})^2}{12}} \tag{III-26}$$

(See Appendix A for the derivation.)

Better estimates of the elemental bias and precision errors can be obtained by measuring the excitation voltage during a run. This can be done by randomly selecting a channel to be reserved to measure the voltage during the run. The uncertainty limit depends on the frequency of error variation in terms of test duration. The error could be largely precision (Fig. III-11a) and may be long term (drift) and/or short term (noise).

The error could be mostly bias (Fig. III-11b) with very little precision error (this could be long term drift which appears as bias during any one test). Another possibility is that the system could contain both bias and precision error (Fig. III-11c). The estimates from the recorded data would be

$$S_i = \sqrt{\frac{\sum_{i=1}^{N}(X_i - \overline{X})^2}{N-1}} \tag{III-27}$$

and

$$b_i \geq \pm|\text{desired voltage} - \overline{X}| \tag{III-28}$$

where $\overline{X}$ = the average value recorded during the run.

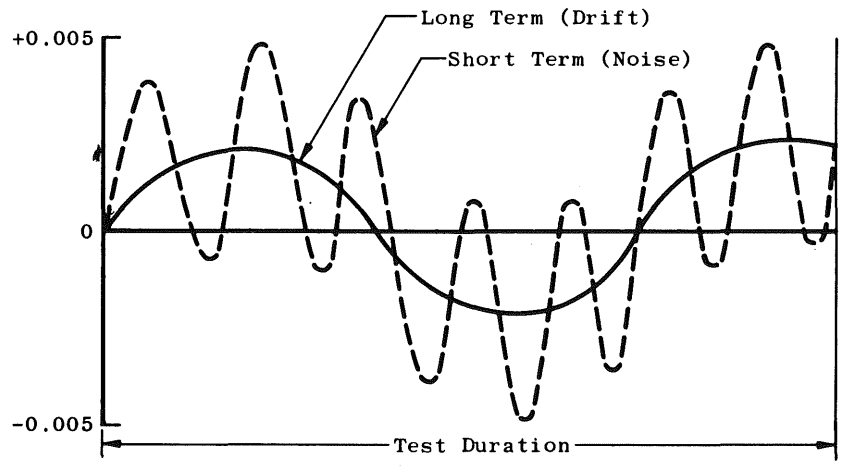

a. Precision Error

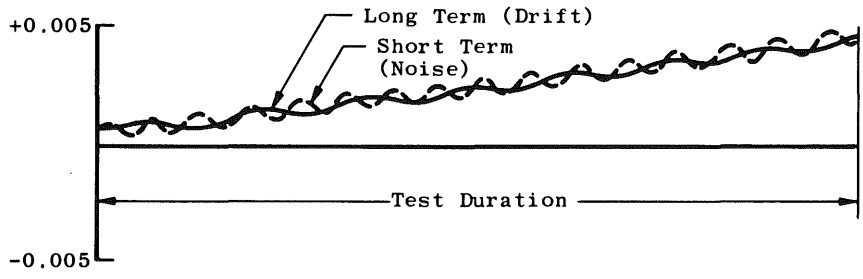

b. Bias Error

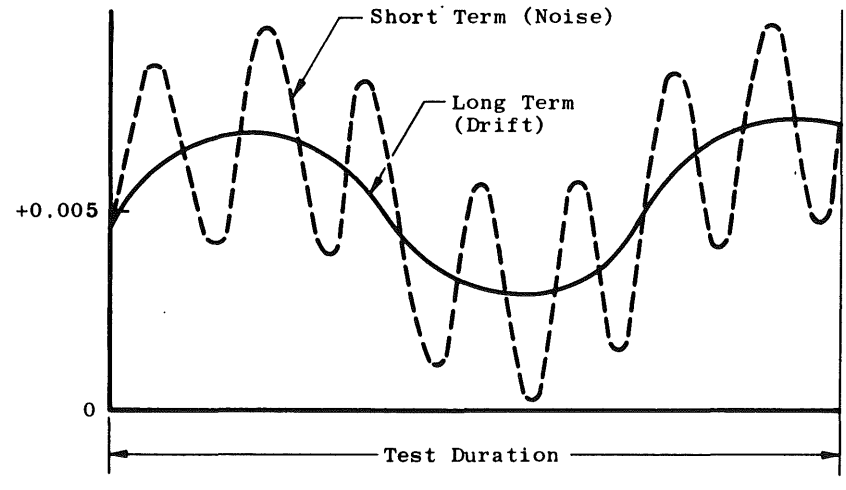

c. Both Bias and Precision Errors

Fig. III-11 Errors

3.2.2.2.6 Recording System Electrical Calibration

Recording system electrical calibrations for force measurements are performed by applying known voltages such as zero and full scale at the recording system input to determine system sensitivity to load cell analog voltages. Another method of electrical calibration is the shunt resistor calibration. This method employs precision resistors which, by means of switches, are placed in parallel with one or more of the active bridge legs in the load cell. These shunt resistors unbalance the load cell bridge and cause a resultant voltage output.

Errors associated with voltage calibration are:

	Precision Index	Bias
1. Calibration power supply	s_p	b_p
2. Analog to digital conversion 3. System resolution	s_k	b_k

Calibration power supply errors s_p and b_p are evaluated by the same procedure employed for excitation power supplies (see Section 3.2.2.2.5).

The net effect of errors from the other two sources can be evaluated by measuring the voltage output of the calibration power supply with a laboratory standard and the recording system. If this test is performed a number of times, a distribution can be developed similar to the one shown in Fig. III-12.

The precision index (s_k) is

$$s_k = \pm\sqrt{\frac{\sum_{j=1}^{N}(X_j - \bar{X})^2}{N-1}} \qquad \text{(III-29)}$$

where X_j = voltage indicated by the recording system

$\bar{X}$ = average of all recording system indications

N = number of observations of X_j

X = voltage indicated by the laboratory standard

The electrical calibration precision index (s_i) is

$$s_i = \pm\sqrt{s_p^2 + s_k^2} \qquad \text{(III-30)}$$

Estimating limits for the unknown biases b_p and b_k are left to the judgment of the most knowledgeable engineer. Of course, this judgment should be supported by an extensive history of special tests designed for this specific purpose.

In the case of shunt resistor calibration, recording system sensitivity is determined in terms of pounds per digital count. This is accomplished by recording the count level at some reference force level (for example, zero applied force) and then recording the count level with the resistor shunted across the bridge. The force equivalent of the bridge unbalance caused by the shunted resistor is known. Therefore, the change in recording system counts corresponding to this force change determines system sensitivity (pounds per count). The errors associated with this technique are

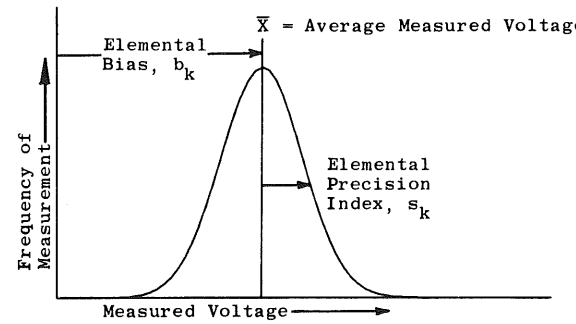

Fig. III-12 Elemental Precision Error of Calibration Power Supply

	Precision Index	Bias
1. Erroneous Shunt Resistance Values	---	b_s
2. Line Resistance	---	b_r
3. Reference Errors	s_p	b_p

Analog-to-digital conversion and system resolution errors may be evaluated by the technique described below. The reference errors (s_p and b_p) are evaluated by pre- and post-run tare investigations. The total effect of the first two error sources may be evaluated as follows:

1. Install a force transducer and connect to the recording system
2. Install a force standard in the system such that it senses the same force as the measurement transducer
3. Switch in the shunt resistor and make a multiple scan (ten or more) recordings (Y_i)
4. Apply a force equivalent to the shunt resistor as indicated by the force standard and established by calibration
5. Make a multiple scan (ten or more) recording (Y_k)
6. Repeat steps 3, 4, and 5 several times, say ten
7. Calculate a multiple scan average Y_i and Y_k for steps 3 and 5, respectively
8. Further calculate a $\overline{Y}_i$ and $\overline{Y}_k$ for the repeated recordings

The difference $\overline{Y}_i - \overline{Y}_k$ is correctable. Estimates of the limits of the unknown bias from these sources are left to engineering judgment supported by special test data.

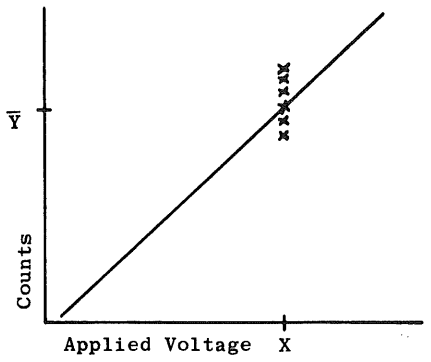

Fig. III-13 Sensitivity Curve

3.2.2.2.7 Analog-To-Digital Conversion Errors

This portion of the data acquisition system includes amplifier and analog-to-digital (A/D) converter. Consider these two components as a single unit, first because modern data recording systems employ only one amplifier which is a part of the A/D converter, and secondly, because the errors are more easily evaluated.

Analog-to-digital conversion error is evaluated by the following procedure:

1. Select a stable voltage source and a voltage standard

2. Connect the voltage source to the A/D converter such that it is common to several channels

3. Connect the voltage standard into the system such that it will have no effect on the recorded data

4. Make a multiple scan (ten or more) recording with the input to all channels shorted, i.e., with the input voltage equal to zero

5. Make a multiple scan (ten or more) recordings with the input at a level which will produce a digital indication slightly less than full scale

6. The data from 4 and 5 above will allow calculation of the sensitivity (Fig. III-13) of each channel to applied voltages. For example:

$$\text{Sensitivity } \left(\frac{\text{counts}}{\text{volt}}\right) = \frac{\text{digital output (counts)}}{\text{input (volts)}} \qquad \text{(III-31)}$$

7. Apply discrete voltages (typically eleven or more) in ascending and descending steps to the A/D conversion unit input and make multiple scan (typically ten or more) recordings at each level

8. Repeat 7 several times over a period of several hours (typically four or more). Calculate a multiple scan average (Y_{ij} counts) for each channel at each voltage level. The average ($\overline{Y}_j$) for each voltage level and for each channel is

$$\overline{Y}_j = \frac{\sum_{i=1}^{M} Y_{ij}}{M} \qquad \text{(III-32)}$$

where M = number of multiple scan averages at each voltage level for each channel. The grand average ($\bar{Y}$) at each voltage level is then calculated for all channels

$$\bar{Y} = \frac{\sum_{i=1}^{N} \bar{Y}_j}{N} \tag{III-33}$$

where N = number of channels. The precision index for A/D conversion is the within channel variation pooled for the N channels:

$$s_{A/D} = \pm \sqrt{\frac{\sum_{j=1}^{N} \sum_{i=1}^{M_j} (Y_{ij} - \bar{Y}_j)^2}{\sum_{j=1}^{N} (M_j - 1)}} \tag{III-34}$$

For an actual engine measurement, this precision index must be converted to the standard error of the mean by dividing by the square root of the number of recordings used:

$$S_{mean} = \frac{s_{A/D}}{\sqrt{K}} \tag{III-35}$$

where K recordings are used for each measurement. This test will yield a conservative estimate of the precision index because the precision index in the voltage standard will influence the data.

3.2.2.2.8 Recording System Resolution

This is primarily a fixed error in that for digital systems the resolution error is plus or minus one-half of one count. Whether the system is three digit or four digit, the error is still one-half of one count. What really happens is that, if a system is between digits, e.g., 5000.5, the indicator lights will alternate between 5000 and 5001. If ten recordings are made, the average will likely be 5000.5. However, suppose the system indicates a constant digital value of 5001 for an analog input equal to 5000.6. Nothing has been gained from multiple sampling and averaging in this case. The precision index for recording system resolution is

$$s_i = \pm 0.3 \text{ units}$$

and the bias limit is zero.

3.2.2.2.9 Electrical Noise

Electrical noise is an error which is generally purely random. The effect can best be described as a variable indication of an input which is constant. The effect of electrical noise can be minimized by making several measurements and averaging. Suppose the

digital indication of a constant 5-volt signal varies randomly over the interval from 4090 to 5010. If ten measurements are recorded and averaged, the answer will be very close to 5000. The precision error caused by electrical noise is

$$s_i = \pm\sqrt{\frac{\sum_{i=1}^{N}(Y_i - \bar{Y})^2}{N-1}} \qquad \text{(III-36)}$$

where s_i = electrical noise precision index

Y_i = individual recorded values

$\bar{Y}$ = the average of all measurements

N = the number of measurements

3.2.2.2.10 Tare Variations

If the measurement system output is recorded for each run after engine shutdown, with fuel line temperatures and pressures at run conditions, with the force transducer and thrust bed at run temperature and with fuel flowing at nominal rates if possible, most of the bias caused by these conditions will be eliminated. Tare variation history on any given test stand should yield a data distribution similar to Fig. III-14. The precision index for tare is then

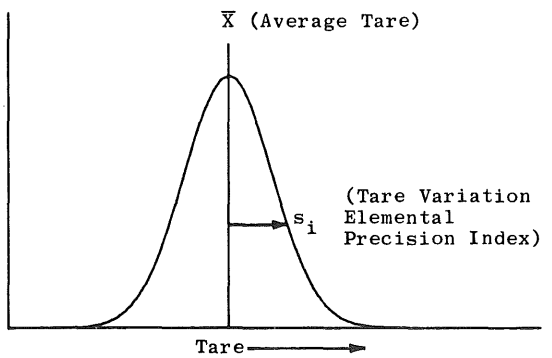

Fig. III-14 Tare History Showing Elemental Precision Error

$$s_i = \pm\sqrt{\frac{\sum_{i=1}(X_i - \bar{X})^2}{N-1}} \qquad \text{(III-37)}$$

The bias limits for tare measurement are estimated in the same manner as the bias limit for force measurement.

3.2.2.2.11 Computer Resolution

Computer resolution is the source of a small elemental error. Some of the smallest computers used in experimental test applications have six digits resolution. The resolution error is then plus or minus one in 10^6. Even though this error is probably negligible, some consideration should be given to it. For example, consideration should be given to rounding-off and truncating errors. Examples of rounding-off are

10.4 is rounded off to 10.0

10.6 is rounded off to 11.0

Rounding-off results in a precision error. Examples of truncating are

$$10.1 = 10.0$$
$$10.9 = 10.0$$

Truncating always results in a bias. Whenever faced with the choice of a small precision error versus a small bias, the precision error is generally chosen. Therefore, the computer resolution error is

$$s_i = \pm 0.3 \text{ digits (see Appendix A for derivation)}$$

3.3 FORCE MEASUREMENT ERROR ANALYSIS

By assuming completely hypothetical numbers for the elemental error terms for the calibration hierarchy, data acquisition, and data reduction processes, Table XII tabulates values for all elemental bias and precision error terms as defined in Tables VIII, X, and XI. Table XII also includes sample sizes for the calibration processes.

Table XII Force Measurement Elemental Error Values

Calibration Errors, lb			Data Acquisition Errors, lb		Data Reduction Errors, lb	
Bias	Precision	Sample Size	Bias	Precision	Bias	Precision
$b_{11} = \pm 0.2$	$s_{11} = \pm 10.0$	6	$b_{12} = \pm 5.0$	$s_{12} = \pm 5.0$	$b_{13} = \pm 10.0$	s_{13} = negligible
$b_{21} = \pm 0.2$	$s_{21} = \pm 10.0$	11	$b_{22} = \pm 5.0$	$s_{22} = \pm 5.0$	b_{23} = negligible	s_{23} = negligible
$b_{31} = \pm 0.4$	$s_{31} = \pm 14.1$	5	$b_{32} = \pm 5.0$	$s_{32} = \pm 5.0$		
$b_{41} = \pm 0.8$	$s_{41} = \pm 20.0$	17	$b_{42} = \pm 5.0$	$s_{42} = \pm 5.0$		
			$b_{52} = \pm 0.4$	$s_{52} = \pm 20.0$		
			$b_{62} = \pm 10.0$	$s_{62} = \pm 10.0$		
			$b_{72} = \pm 5.0$	$s_{72} = \pm 5.0$		
			(df = 31 for all elemental precision errors)			

The errors associated with the calibration hierarchy, data acquisition, and data reduction stages in the measurement process are calculated below and are identified by S_1, S_2, and S_3, respectively, for precision indices and B_1, B_2, and B_3, respectively, for bias limits and U_1, U_2, and U_3, respectively, for uncertainty intervals.

1. Calibration bias limit for the force transducer is

$$B_1 = \pm \sqrt{\sum_i b_i^2}$$

$$B_1 = \pm \sqrt{(0.2)^2 + (0.2)^2 + (0.4)^2 + (0.8)^2} \qquad \text{(III-38)}$$

$$B_1 = \pm 0.94 \text{ lb}$$

2. Calibration precision index estimate for the force transducer is

$$S_1 = \pm\sqrt{\sum_i s_i^2}$$

$$S_1 = \pm\sqrt{(10)^2 + (10)^2 + (14.1)^2 + (20)^2} \qquad \text{(III-39)}$$

$$S_1 = \pm 28.3 \text{ lb}$$

3. To demonstrate use of the Welch-Satterthwaite method for determining degrees of freedom (df), small sample sizes for the calibration processes in the force transducer calibration hierarchy have been assumed. Sample sizes are included along with the elemental errors in Table XII. From Section I,

$$df = \frac{\left(s_1^2 + s_2^2 + \cdots + s_n^2\right)^2}{\left(\frac{s_1^4}{df_1} + \frac{s_2^4}{df_2} + \cdots + \frac{s_n^4}{df_n}\right)} \qquad \text{(III-40)}$$

where df_n = sample size minus one for the nth calibration

$$df_1 = \frac{\left[(10)^2 + (10)^2 + (14.1)^2 + (20)^2\right]^2}{\frac{(10)^4}{5} + \frac{(10)^4}{10} + \frac{(14.1)^4}{4} + \frac{(20)^4}{16}}$$

$$= \frac{640 \times 10^3}{23 \times 10^3}$$

$$= 27.8$$

Under the "t" column in Table E-1 in Appendix E, t is 2.052 for 27 degrees of freedom and 2.048 for 28 degrees of freedom. Interpolating linearly gives a t of 2.049 for 27.8 degrees of freedom.

The calculation of calibration uncertainty (U_1) for the force transducer is then

$$U_1 = \pm(B_1 + t_{95}S_1)$$

$$= \pm(0.94 + 2.049 \times 28.3) \qquad \text{(III-41)}$$

$$= \pm 58.9 \text{ lb}$$

4. Data acquisition bias limit is

$$B_2 = \pm\sqrt{\sum_i b_i^2}$$
$$= \pm\sqrt{(5)^2 + (5)^2 + (5)^2 + (5)^2 + (0.4)^2 + (10)^2 + (5)^2} \quad \text{(III-42)}$$
$$= \pm 15.0 \text{ lb}$$

5. Data acquisition precision index estimate is

$$S_2 = \pm\sqrt{\sum_i s_i^2}$$
$$= \pm\sqrt{(5)^2 + (5)^2 + (5)^2 + (5)^2 + (20)^2 + (10)^2 + (5)^2} \quad \text{(III-43)}$$
$$= \pm 25.0 \text{ lb}$$

6. Data acquisition uncertainty is

$$U_2 = \pm(B_2 + t_{95}S_2)$$
$$= \pm(15.0 + 2 \times 25.0) \quad \text{(III-44)}$$
$$= 65.0 \text{ lb}$$

t_{95} = 2.00 because df > 30 for S_2

7. Data reduction bias limit is

$$B_3 = \pm\sqrt{\sum_i b_i^2}$$
$$= \pm 10.0 \text{ lb} \quad \text{(III-45)}$$

8. Data reduction precision index estimate is

$$S_3 = \pm\sqrt{\sum_i s_i^2}$$
$$= 0 \quad \text{(III-46)}$$

9. Data reduction uncertainty is

$$U_3 = \pm(B_3 + t_{95}S_3)$$
$$= \pm(10 + 0.0)$$
$$= \pm 10.0 \text{ lb} \quad \text{(III-47)}$$

t_{95} = 2.00 because df > 30 for S_3

10. Force measurement bias limit is

$$B_F = \pm\sqrt{B_1^2 + B_2^2 + B_3^2}$$
$$= \pm\sqrt{(0.9)^2 + (15)^2 + (10)^2} \quad \text{(III-48)}$$
$$= \pm 18.1 \text{ lb}$$

11. Force measurement precision index estimate is

$$S_F = \pm\sqrt{S_1^2 + S_2^2 + S_3^2}$$
$$= \pm\sqrt{(28.3)^2 + (25)^2 + 0^2} \qquad \text{(III-49)}$$
$$= \pm 37.8 \text{ lb}$$

12. Degrees of freedom for force measurement are

$$df_F = \frac{(S_1^2 + S_2^2 + S_3^2)^2}{\frac{S_1^4}{df_1} + \frac{S_2^4}{df_2} + \frac{S_3^4}{df_3}} \qquad \text{(III-50)}$$
$$= \frac{[(28.3)^2 + (25)^2]^2}{\frac{(28.3)^4}{27.8} + \frac{(25)^4}{31}}$$
$$= 57$$

13. Force measurement uncertainty is

$$U_F = \pm(B_F + t_{95}S_F)$$
$$= \pm(18.1 + 2.00 \times 37.8) \qquad df_F = 57, \quad t_{95} = 2.00 \qquad \text{(III-51)}$$
$$= \pm 93.7 \text{ lb}$$

3.4 END-TO-END CALIBRATION

A working standard which typically consists of a strain-gage load cell(s) with a precise read-out device may be obtained. The working standard is installed in the force measurement system such that the force applied to the measurement system will also be applied to the working standard (Fig. III-7). All electrical and mechanical service connections to the force measuring system should be intact, and all system pressures should be adjusted to the nominal levels incurred during engine testing. Care must be taken to ensure that those fluid systems which are pressurized but not flowing during calibration, especially the engine fuel system, are designed so that no fluid moments forces are applied to the thrust stand during testing with fluid flowing. Calibration is accomplished by applying several known forces in succession (usually eleven or more) to the measurement system and recording the results on a digital recording system. The data recorded are pounds of applied force as indicated by both the working standard and the resulting voltage output of the measurement transducer. Generally, the calibration cycle will be repeated one or more times.

Typical calibration data for a force measuring system used in engine sea-level static testing is as shown in Fig. III-15. During the course of sea-level static testing, the forces are always applied in one direction only.

Typical calibration data for a force measuring system used in engine altitude testing is as shown in Fig. III-16. During the course of altitude testing, the resulting forces experienced may be either "positive" or "negative" depending on the simulated flight and altitude conditions.

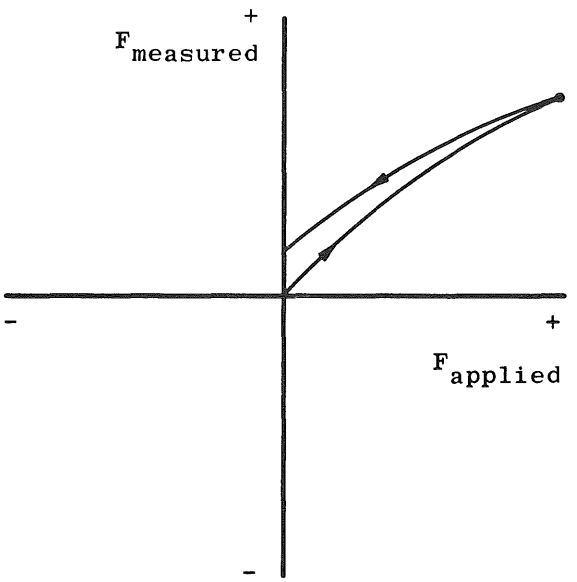

Fig. III-15 Typical Calibration Data from Force Measuring System Used in Engine Sea-Level Testing

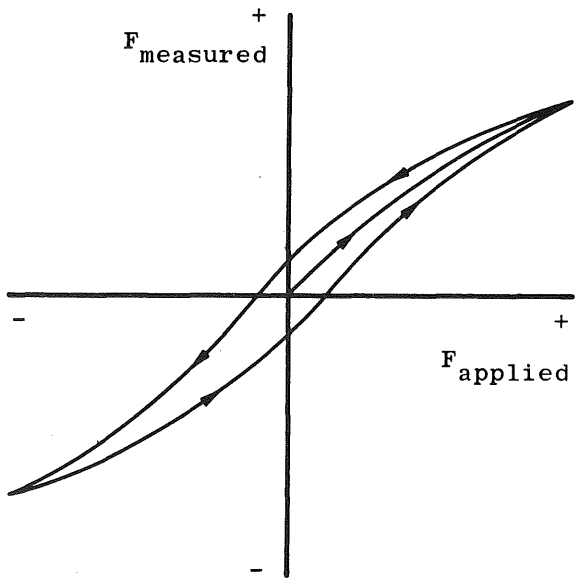

Fig. III-16 Typical Calibration Data from Force Measuring System Used in Engine Altitude Testing

A force calibration program is utilized in a digital computer to fit a least squares curve through the calibration data in Figs. III-15 and III-16. The curve-fit produces coefficients from which measured force may be determined. In practice, curve-fits are usually linear or second order. Occasionally, a third-order curve-fit may be used to represent a calibration. Higher order curve-fits should not be used without close examination. Without a keen knowledge of the relationship between data and a higher order curve-fit, unrepresentative values may result at interpolated points.

3.5 SUMMARY

Errors from calibration, data acquisition and data reduction processes must be evaluated by one of two methods:

1. Performance of end-to-end calibrations and pre- or post-run applied load tests

2. Evaluation of all elemental errors

In either case, the evaluated errors are combined by the methods outlined in Section 3.3, to determine the precision index (S_F), bias (B_F), and uncertainty (U_F) for measured force.

SECTION IV
FUEL FLOW MEASUREMENT

4.1 GENERAL

Fuel flow measurements are difficult because there is no standard for measuring volume per unit of time; therefore, the flow calibration[5] must be referenced to standards for weight or volume. Furthermore, there is no universal method for calibrating a flowmeter.

Turbine meters are the most widely used instruments for measuring fuel flows. They generate an alternating voltage with frequency proportional to the volumetric flow rate. The frequency of the output is converted to an analog voltage and then to digital counts. Another method for recording turbine meter signals is to count the voltage excursions (pulses) over some preset period of time to determine the signal frequency. Figure IV-1 illustrates a typical turbine meter signal.

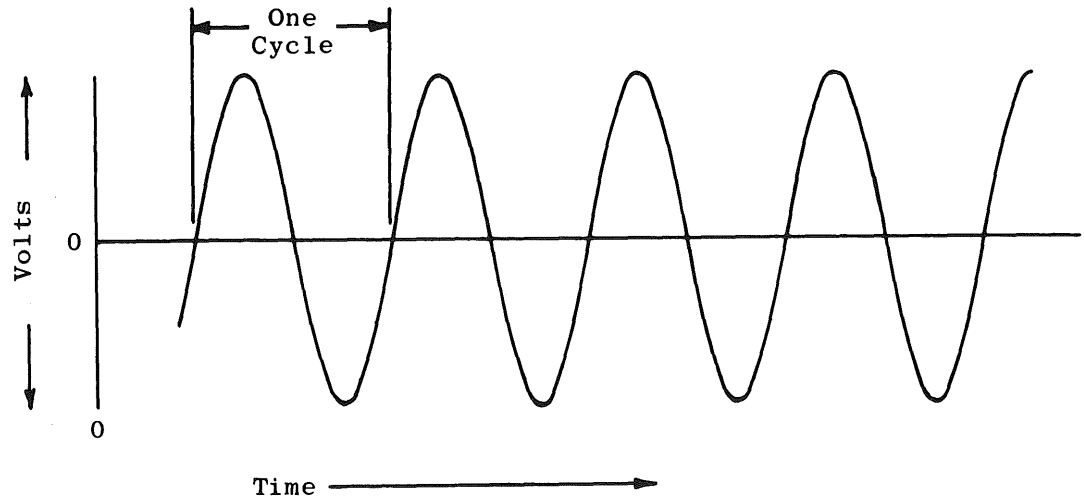

Fig. IV-1 Turbine Meter Signal

Turbine meters may be calibrated by three methods:

1. Volumetric: flowing a measured volume of fluid through the meter to establish a pulses-per-gallon factor,
2. Gravimetric: flowing a measured mass of fluid through the meter, determining the density, and converting the mass to volume to establish a pulses-per-gallon factor, and
3. Comparative calibration: comparing the meter against a master meter.

[5]For a definition of terms used in this Handbook, see the Glossary in Section IX.

Calibration factors are determined over a range of turbine meter frequencies to develop a calibration curve. Figure IV-2 is an illustration of a typical turbine meter calibration curve.

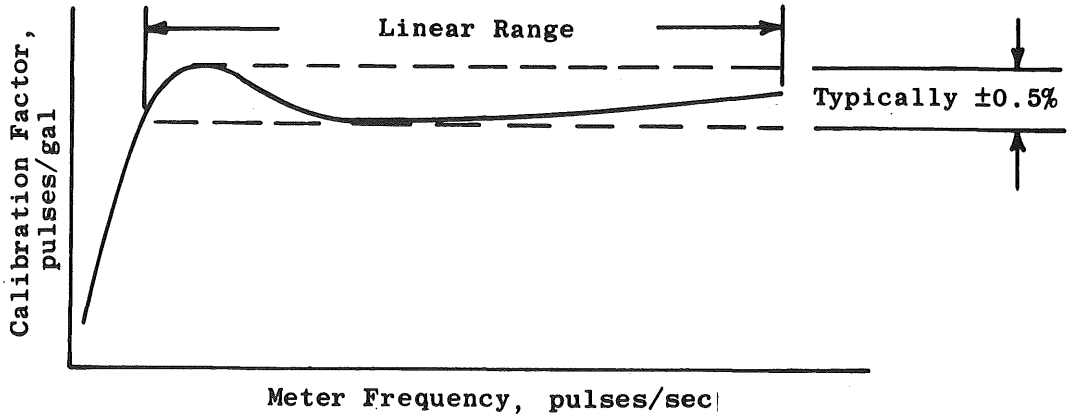

Fig. IV-2 Turbine Meter Calibration Curve

The range of calibration factors, over the linear range of a turbine meter, is typically ±0.5 percent. However, meter range may vary somewhat and is influenced by meter size and design, plus fluid viscosity. A complete analysis of turbine meter performance is given by the "Turbine Flowmeter Performance Model." (AD825354) prepared by the Greyrad Corporation.

Multiple measurement of fuel flow is recommended for several reasons, the chief ones being reliability and accuracy. Multiple measurements are readily accomplished by simply installing two or more turbine meters in series. The meters should have independent calibrations as far back in the calibration hierarchy as possible.

4.2 FUEL FLOW MEASUREMENT ERROR SOURCES

Errors in fuel flow measurement fall into three major categories: (1) calibration, (2) data acquisition, and (3) data reduction. The calibration elemental bias and precision error sources will vary according to the method of calibration used, while the data acquisition and reduction errors will not. The next section will contain three parts, one for each method of calibration. All three may not apply to a particular test facility. The ones that do not should be ignored. The remainder of the section will be devoted to discussions of the elemental errors in the data acquisition and data reduction processes.

4.2.1 Calibration Errors

Turbine meters are calibrated by three methods or a combination thereof. The first is volumetric calibration. It is accomplished by flowing a measured volume of fluid through the meter and recording the total number of turbine meter cycles (pulses) generated. The calibration factor (K factor) is then calculated

$$K = \frac{\text{total pulses}}{\text{total gallons}} = \frac{\text{pulses}}{\text{gallon}} \qquad \text{(IV-1)}$$

The second method, gravimetric calibration, is accomplished by flowing a measured mass of fluid through the meter and again recording the total number of turbine meter pulses. Measurement of fluid temperature and pressure will allow determination of fluid density. With these data, a meter K factor may be calculated:

$$K = \frac{\text{total pulses}}{\text{total pounds}} \times \frac{\text{pounds}}{\text{gallon}}$$

$$= \frac{\text{pulses}}{\text{gallon}} \qquad \text{(IV-2)}$$

where density = pounds per gallon.

The third method is comparative calibration. The meter being calibrated is compared against a working standard turbine meter. In some applications turbine meters are so repeatable that the greater part of any precision error incurred results from nonrepeatability of the calibrating device. In this case, better calibration results can be obtained by simply flowing the calibration fluid through a standard turbine meter in series with the meter being calibrated. Data recorded are frequency of each meter and the ratio (R) of total pulses from the meter being calibrated to total pulses from the standard meter. The calibration factor (K_{Cal}) for the meter being calibrated is

$$K_{Cal} \frac{\text{pulses}}{\text{gallon}} = (R)K_{standard} \qquad \text{(IV-3)}$$

where $K_{standard}$ = the $\frac{\text{pulses}}{\text{gallon}}$ factor for the standard meter at the set frequency.

4.2.1.1 Volumetric Calibration

At the apex of the calibration hierarchy, Fig. IV-3, for volumetric calibrations is the National Bureau of Standards Dynamic Weigh Calibrator. The Interlab Standard Turbine Meter is calibrated against this calibrator and in turn is used to calibrate the working standard volumetric calibrator in the company laboratory.

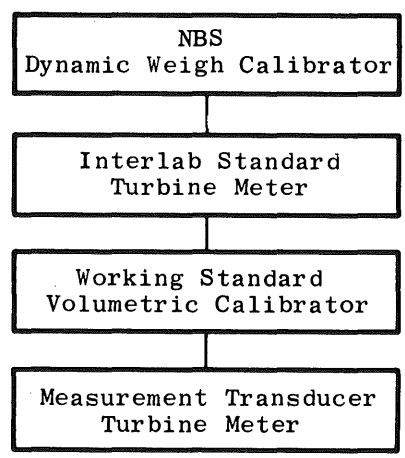

Fig. IV-3 Turbine Meter Volumetric Calibration Hierarachy

4.2.1.1.1 Calibration of the Interlab Standard

Beginning with the interlab standard, calibration methods and elemental error evaluation techniques at each level in the hierarchy will be discussed.

Turbine meters are calibrated at the NBS as follows:

1. At each pulse frequency, specified by the owner, and controlled to within one-half percent, the total number of pulses generated are counted during the period required to flow a weighed quantity of liquid through the meter.

2. Liquid density is determined using measured values of liquid temperature and pressure.

3. The weighed quantity of fluid is converted to gallons using the density determined in step (2).

4. A pulses/gallon (K) factor is calculated from the data obtained in steps (1), (2), and (3).

5. Steps (1) through (4) are repeated five times successively on each of two different days making a total of ten (10) separate observations.

The K factor reported is the arithmetic mean $\bar{K}$ of the ten observations. Data from many similar calibrations yield a standard deviation (s) of about 0.03 percent for the NBS calibration procedure. The precision index ($s_{\bar{K}}$) for the mean value, is then

$$s_{\bar{K}} = \frac{s}{\sqrt{N_i}} = \frac{0.03\%}{\sqrt{10}} = 0.01\% \qquad \text{(IV-4)}$$

where N_i = the number of observations in the determination of $\bar{K}$. N_i usually is 10; the degrees of freedom is $N_i - 1$ or usually 9. Of course, this is the precision index at just one pulse frequency. The precision indices $s_{\bar{K}_i}$ for M frequencies must be pooled to produce the precision index (s_{NBS}) for the calibration process:

$$s_{NBS} = \pm \sqrt{\frac{\sum_{i=1}^{M} (N_i - 1)\, s_{\bar{K}_i}^2}{\sum_{i=1}^{M} (N_i - 1)}} \qquad \text{(IV-5)}$$

with degrees of freedom $df_{NBS} = \sum_{i=1}^{M} (N_i - 1)$. If the number of tests at each frequency is 10, then these calculations reduce to

$$s_{NBS} = \pm \sqrt{\frac{\sum_{i=1}^{M} s_{\bar{K}_i}^2}{M}} \qquad \text{(IV-6)}$$

and

$$df_{NBS} = M(n-1) = 9M \qquad \text{(IV-7)}$$

Bias limits in the NBS dynamic weight calibrator have been established by repeated comparison calibrations of reference turbine meters on both volumetric (stand pipe) calibrators and gravimetric (weigh) calibrators. These comparison calibrations were performed at several different locations and yielded a bias limit of ±0.1 percent. This then is the bias limit (b_{NBS}) reported by the NBS for turbine meter calibration.

Uncertainty in NBS turbine meter calibrations, is then

$$U = \pm(b_{NBS} + t_{95}s_{NBS}) \tag{IV-8}$$

If, for example, the number of frequency settings is equal to ten, the degrees of freedom are

$$df_{NBS} = 9 \times 10 = 90$$

Since the degree of freedom is greater than thirty,

$$t_{95} = 2.00$$

and

$$U = \pm(0.1 + 2.00 \times 0.01) = 0.12\%$$

4.2.1.1.2 Uncertainty in the Working Standard

The working standard volumetric calibrator generally consists of a standpipe arrangement with liquid level sensors. These mark the top and bottom of a constant volume interval (Fig. IV-4). The interlab standard flowmeter is connected in series with the calibrator.

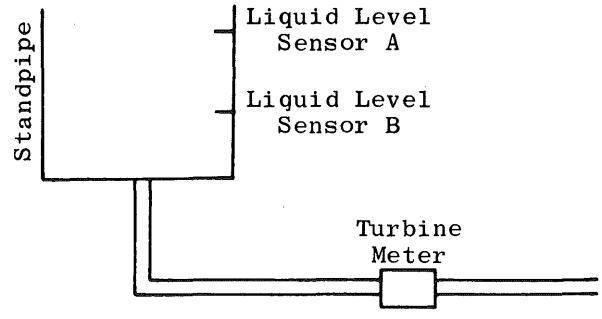

Fig. IV-4 Volumetric Calibrator

To calibrate, liquid is forced out of or into the calibrator at a constant flow rate. The number of pulses generated by the flowmeter are counted while the liquid between sensors A and B is being displaced. The volume (V_i) between A and B is then the quotient of the number of pulses counted (C_i) divided by the turbine meter K factor (K_{NBS}) determined at NBS:

$$V_i = \frac{C_i \text{ pulses}}{K_{NBS} \text{ pulses/gallon}} = \text{gallons} \tag{IV-9}$$

Repeating the calibration process N times improves the estimate of the volume, and the average of the N calibrations is

$$\bar{V} = \frac{\sum_{i=1}^{N} V_i}{N} \tag{IV-10}$$

The precision index estimate for this determination of volume is the precision index for the N determinations divided by the square root of N.

$$s_{\bar{V}} = \frac{s_V}{\sqrt{N}} = \sqrt{\frac{\sum_{i=1}^{N} (V_i - \bar{V})^2}{N\,(N-1)}} \qquad \text{(IV-11)}$$

This is called the standard error of the mean for the N determinations. The associated degrees of freedom is N - 1. Please note in this situation, the precision index of an average value ($\bar{V}$) is of interest rather than the precision index of the individual determinations (V_i). The estimating formula is corrected to provide that estimate by dividing by the square root of N, the number of determinations.

The bias limit ($b_{\bar{V}}$) for this process is the root-sum-square of the bias limit reported by the NBS (b_{NBS}) and the best estimate of any additional bias contributed by the calibration process.

Another way to evaluate the precision error of the calibrator is to determine the standpipe volume by some other means and then compare K factors determined by the calibrator with those produced by the NBS calibrator. The standpipe volume between A and B may be determined by physical measurement of the standpipe dimensions or by measuring the volume of liquid between A and B with fixed volume standards, e.g., 5-, 10-, 50-, 100-gal containers. Then calibrations of the interlab standard turbine meter can be performed with the calibrator by forcing liquid into or out of the standpipe through the turbine meter at a constant flow rate. The total number of pulses generated while flowing the volume of liquid between A and B divided by the measured volume yields the meter K factor:

$$K = \frac{\text{total pulses}}{\text{total gallons}} = \frac{\text{pulses}}{\text{gallon}} \qquad \text{(IV-12)}$$

By repeating this procedure several times and calculating a mean calibration factor ($\bar{K}$) for a constant flow rate as the average of the observed K factors,

$$\bar{K} = \frac{\sum_{i=1}^{N} K_i}{N} \qquad \text{(IV-13)}$$

where N = the number of observations used to determine $\bar{K}$

K_i = K calculated from the i th observation

and the precision index of $\bar{K}$ is estimated from the variation of K_i about $\bar{K}$; it is the precision index for K divided by the square root of the number of observations (N):

$$s_{\bar{K}} = \frac{s_K}{\sqrt{N}} = \sqrt{\frac{\sum_{i=1}^{N} (K_i - \bar{K})^2}{N\,(N-1)}} \qquad \text{(IV-14)}$$

The degrees of freedom associated with $s_{\overline{K}}$ is N - 1.

If an average K factor ($\overline{K}$) is determined at several different flow rates over the range of the meter and corresponding precision index, $S_{\overline{K}}$, is calculated at each flow rate; then pooling the precision indices provides an estimate of overall calibrator precision index:

$$s_{ws} = \pm \sqrt{\frac{\sum_{j=1}^{M} (N_j - 1) s_{K_j}^2}{\sum_{J=1}^{M} (N_j - 1)}} \qquad \text{(IV-15)}$$

The degrees of freedom associated with the pooled precision index (the measurement instrument calibration process) are the sum of the degrees of freedom for each flow rate:

$$df_{ws} = \sum_{j=1}^{M} (N_j - 1) \qquad \text{(IV-16)}$$

where M = the number of pulse frequencies for which a K is determined and N_j = the number of observations made at each frequency setting. The bias in this process can be estimated as follows:

1. Calculate an average calibration factor $\overline{\overline{K}}$ from K_j values calculated from the NBS calibration data

2. Calculate an average calibration factor $\overline{\overline{\overline{K}}}$ from all of the $\overline{K}$'s calculated from volumetric calibrator data

3. Make the correction $\overline{\overline{\overline{K}}} - \overline{\overline{K}}$

4. Estimates of the limits of unknown bias (b_j) for the process should be based on data from interlaboratory or interfacility comparisons and engineering judgment. Then

$$b_{ws} = \pm \sqrt{(b_{NBS})^2 + (b_j)^2} \qquad \text{(IV-17)}$$

Finally, perform the calibration of the measurement turbine meter against the volumetric calibrator in essentially the same manner that the interlab standard turbine meter was calibrated. The precision index (s_j) for this calibration is calculated using Eqs. (IV-15) and (IV-16). The bias limit (b) for the measurement meter calibration process is simply the best estimate based on interlab or interfacility comparison history and engineering experience.

The precision index for the calibration hierarchy is

$$S_1 = \pm \sqrt{\sum_i s_i^2} \qquad \text{(IV-18)}$$

$$S_1 = \pm\sqrt{s_{NBS}^2 + s_{\bar{V}}^2 + s_j^2} \tag{IV-19}$$

or

$$S_1 = \pm\sqrt{s_{NBS}^2 + s_{ws}^2 + s_j^2} \tag{IV-20}$$

Degrees of freedom (df) for the calibration hierarchy are calculated by

$$df_1 = \frac{\left(s_{NBS}^2 + s_{\bar{V}}^2 + s_j^2\right)^2}{\frac{s_{NBS}^4}{df_{NBS}} + \frac{s_{\bar{V}}^4}{df_{\bar{V}}} + \frac{s_j^4}{df_j}} \tag{IV-21}$$

or

$$df_1 = \frac{\left(s_{NBS}^2 + s_{ws}^2 + s_j^2\right)^2}{\frac{S_{NBS}^4}{df_{NBS}} + \frac{S_{ws}^4}{df_{ws}} + \frac{S_j^4}{df_j}} \tag{IV-22}$$

Bias limits for the hierarchy are

$$B_1 = \sqrt{\sum_i b_i^2} \tag{IV-23}$$

$$B_1 = \sqrt{b_{NBS}^2 + b_{\bar{V}}^2 + b_j^2} \tag{IV-24}$$

or

$$B_1 = \sqrt{b_{NBS}^2 + b_{ws}^2 + b_j^2} \tag{IV-25}$$

Uncertainty in the calibration hierarchy is calculated by

$$U_1 = \pm(B_1 + t_{95}S_1) \tag{IV-26}$$

t_{95} is evaluated at df_1 degrees of freedom.

4.2.1.2 Gravimetric Calibrations

The gravimetric flow calibration system has a calibration hierarchy (Fig. IV-5) similar to that for volumetric calibrations. The only difference is that the working standard is a dynamic weigh calibrator rather than a volumetric calibrator.

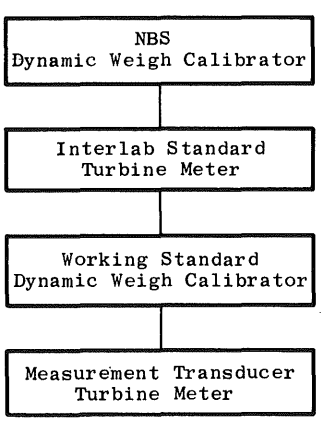

Fig. IV-5 Turbine Meter Gravimetric Calibration Hierarchy

Elemental errors in the gravimetric calibration hierarchy are evaluated in exactly the same way as those for the volumetric hierarchy except for the working standard.

Turbine meter gravimetric calibrations are accomplished by flowing a weighed quantity of liquid through the meter. Liquid temperature and pressure are measured to determine liquid density for conversion of the weighed quantity to gallons. The K factor is calculated by dividing the total number of pulses recorded by the weighed quantity in pounds and multiplying by the density in pounds per gallon:

$$K = \frac{\text{total pulses}}{\text{total pounds}} \times \frac{\text{pounds}}{\text{gallon}} = \frac{\text{pulses}}{\text{gallon}} \tag{IV-27}$$

Figure IV-6 illustrates the basic idea of gravimetric calibration.

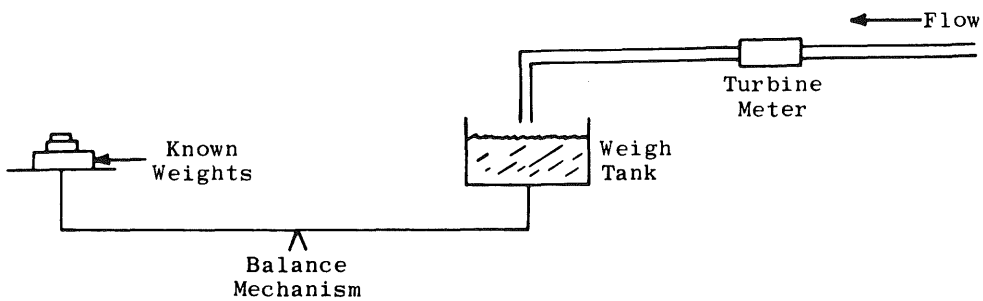

Fig. IV-6 Gravimetric Calibrator

By flowing liquid at a constant flow rate through the turbine meter and into the weigh tank until the weight of the liquid exactly balances the standard weights, the weighed quantity (W) is established in pounds. With the total number of pulses generated (C) and liquid density (ρ) in pounds per gallon, K_i is calculated as follows:

$$K_i = \frac{\text{pulses}}{\text{gallon}} = \frac{C}{W}\rho \tag{IV-28}$$

If N_j observations of K_i are made at one flow rate, average ($\overline{K}$) and precision index ($s_{\overline{K}_j}$) can be calculated:

$$\overline{K} = \frac{\sum_{i=1}^{N_j} K_i}{N_j} \tag{IV-29}$$

$$s_{\overline{K}_j} = \sqrt{\frac{\sum_{i=1}^{N_j} (K_i - \overline{K})^2}{N_j(N_j - 1)}} \tag{IV-30}$$

Then if $\bar{K}$ is established for M different flow rates, the precision index for the calibration process is the pooled precision index (S_{ws}) of the $s_{\bar{K}_j}$ indices:

$$S_{ws} = \pm \sqrt{\frac{\sum_{j=1}^{M} (N_j - 1) s_{\bar{K}_j}^2}{\sum_{j=1}^{M} (N_j - 1)}} \qquad \text{(IV-31)}$$

Degrees of freedom (df_{ws}) for this process are calculated by

$$df_{ws} = \sum_{j=1}^{M} (N_j - 1) \qquad \text{(IV-32)}$$

Bias in this calibration process is estimated by the method described in Section 4.2.1.1.2.

Calibration hierarchy precision index (S_1), degrees of freedom (df_1), bias (B_1), and uncertainty (U_1) are calculated by Eqs. (IV-18) through (IV-26).

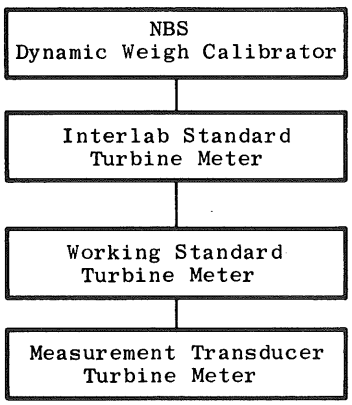

Fig. IV-7 Turbine Meter Comparison Calibration Hierarchy

4.2.1.3 Calibration by Comparison

The third method of calibration is comparison of the measurement meter with a working standard turbine meter. This method substitutes a turbine meter for the volumetric or gravimetric working standards in the calibration hierarchy (Fig. IV-7).

The comparison method has not been widely accepted. However, it does have considerable merit especially in hydrocarbon fuel applications. The NBS has recognized the use of turbine meters as transfer standards because they are very repeatable. The NBS has, in fact, used turbine meters as transfer standards in evaluating bias in the NBS dynamic weigh calibrator.

The precision index and bias limit estimates for the interlab standard are made in the same way as for the volumetric calibration system. The working standard turbine meter is calibrated against the interlab standard turbine meter by installing the two meters in series in a flow system. Figure IV-8 illustrates a typical setup for comparing turbine meter with turbine meter.

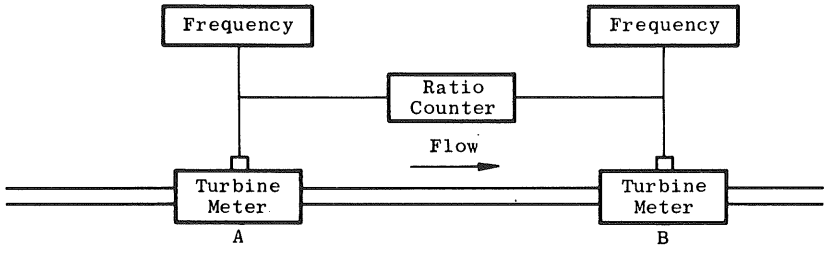

Fig. IV-8 Comparative Calibration

By considering, for example, meter A to be an interlab standard and meter B to be a working standard, a calibration can be performed as follows:

1. Adjust the flow rate by observing the frequency of meter A. From the NBS calibration curve, determine the interlab standard K factor for the particular frequency.

2. With the flow rate adjusted and constant, allow the ratio counter to count the total number of pulses generated by meter A over some predetermined time period. The counter will simultaneously count the total number of pulses generated by meter B over the same time period. The counter will then display digitally the ratio (R):

$$R = \frac{\text{total pulses} - A}{\text{total pulses} - B} \tag{IV-33}$$

then

$$K_B = \frac{K_A}{R} \tag{IV-34}$$

and

$$f_B = \frac{f_A}{R} \tag{IV-35}$$

Thus, calculate K_i for each frequency setting f_A. If N_i observations are made at each frequency setting, an average calibration factor ($\overline{K}$) can be calculated for meter B at f_B by

$$\overline{K} = \frac{\sum_{i=1}^{N_j} K_i}{N_j} \tag{IV-36}$$

The precision index for this average calibration factor is the precision index of the calibration values divided by the square root of the number of observations (N_j):

$$s_{\overline{K}_j} = \frac{s_{\overline{K}}}{\sqrt{N_j}} = \pm\sqrt{\frac{\sum_{i=1}^{N_j} (K_{B_i} - \overline{K})^2}{N_j(N_j - 1)}} \tag{IV-37}$$

If a K is determined at M different frequencies over the range of the meter, the precision index (s_{ws}) for the calibration process is the pooled value for all frequencies:

$$s_{ws} = \pm\sqrt{\frac{\sum_{j=1}^{M} (N_j - 1)\, s_{\overline{K}_j}^2}{\sum_{j=1}^{M} (N_j - 1)}} \tag{IV-38}$$

The degrees of freedom (df_{ws}) for the calibration process are

$$df_{ws} = \sum_{j}^{M} (N_j - 1) \qquad \text{(IV-39)}$$

Bias limits (b_{ws}) for the process are again based on interlab and interfacility comparison history and engineering judgment.

Precision index (S_1), degrees of freedom (df_1), bias limits (B_1), and uncertainty (U_1) for the calibration hierarchy are calculated using Eqs. (IV-18) through (IV-26).

Some important considerations which have not been mentioned heretofore are:

1. At each level in the calibration hierarchy, the flowmeter being calibrated should be accompanied by the plumbing upstream and downstream of the meter in its use condition. Tests have shown that inadequate control of the velocity profile is perhaps the strongest argument against the use of reference turbine meters as standards (see page 184 of "Turbine Flowmeter Performance Model," (AD825354) prepared by Greyrad Corporation).

2. If at all possible, turbine meters should be calibrated with the use liquid at run conditions of temperature and pressure.

These considerations will minimize the errors.

4.2.2 Data Acquisition Errors

The effect of data acquisition errors is determined by applying a known frequency (X) to the data acquisition equipment (Fig. IV-9).

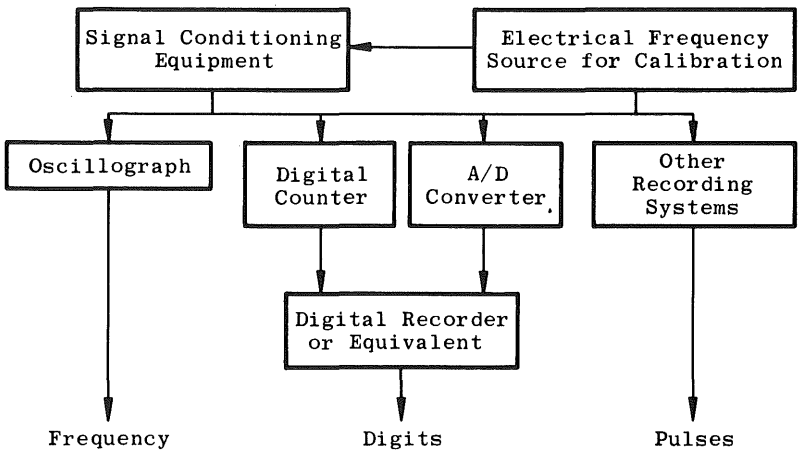

Fig. IV-9 Data Acquisition System Calibration

In the case of digital counters, the total number of input pulses is counted over some preset period of time and the digital indication is recorded. Then the recorded value can be compared with the input. If M recordings on N channels are made, then the average ($\overline{X}_j$) for one channel is

$$\overline{X}_j = \sum_{i=1}^{M} \frac{X_i}{M} \tag{IV-40}$$

where X_i = the recorded value for the ith recording. The grand average ($\overline{X}$) for all channels is

$$\overline{X} = \frac{\sum_{j=1}^{N} \overline{X}_j}{N} \tag{IV-41}$$

The precision index ($s_{\overline{X}}$) for digital counter channels is

$$s_{\overline{X}} = \pm \sqrt{\frac{\sum_{j=1}^{N} (\overline{X}_j - \overline{X})^2}{N - 1}} \tag{IV-42}$$

The degrees of freedom (df_j) are the number of recordings minus one, i.e., N-1.

Bias limits for the data acquisition process are left to the judgment of the most knowledgeable data recording engineers. Errors incurred by frequency-to-analog and analog-to-digital conversions are evaluated by comparing known input frequencies (f) with recorded frequencies. The known frequency (f) is applied to N channels, and M multiple scan recordings are made. A multiple scan average (f_{ij}) is calculated for each channel for each recording. The average ($\overline{f}_j$) for each recording on the jth channel is

$$\overline{f}_j = \frac{\sum_{i=1}^{M} f_{ij}}{M} \tag{IV-43}$$

The grand average ($\overline{f}$) for all channels is

$$\overline{f} = \frac{\sum_{j=1}^{N} \overline{f}_j}{N} \tag{IV-44}$$

The precision index ($s_{\overline{f}}$) is then

$$s_{\overline{f}} = \pm \sqrt{\frac{\sum_{j=1}^{N} (\overline{f}_j - \overline{f})^2}{N - 1}} \tag{IV-45}$$

The degrees of freedom ($df_{\bar{f}}$) in this case are

$$df_{\bar{f}} = N - 1 \tag{IV-46}$$

Bias limits (b_f) for frequency-to-analog and analog-to-digital conversion must be estimated and root-sum-squared with the bias limits (b_{fo}) for the input frequency (f) as determined from the frequency standard calibration hierarchy, i.e.,

$$b_i = \pm\sqrt{b_f^2 + b_{fo}^2}$$

4.2.2.1 Multiple Instruments

Because of the lack of flow rate standards, i.e., gallons per minute or pounds per second standards, multiple instrumentation for flow measurement is highly recommended. Correct application of multiple measurement statistics will never yield an estimate of precision error larger than that obtained with single measurements. The typical multiple instrumentation situation provides a reduction in precision error. The measurement provided by the average of several instruments is more precise than any individual instrument of that set. The reduction of precision error is indicated by the precision index (s_{avg}) of several instruments:

$$s_{avg} = \frac{s_{ind}}{\sqrt{K}} \tag{IV-47}$$

where s_{ind} = the precision index of the individual instrument and K is the number of instruments. The formula for calculating s_{avg} is as follows when the simple average of multiple instruments is used:

$$s_{avg} = \sqrt{\frac{\Sigma s_i^2}{K}}$$

If individual instruments are weighted when combined, the formula for s_{avg} is more complex.

Analysis of flowmeter-to-flowmeter multiple measurements yields

1. Pooled within-run precision index (S_{wr}) and
2. Pooled run-to-run precision index (S_{rr}).

Appendix C gives derivations and formulation for calculating the above precision indices.

Further analysis of multiple measurement data will provide an estimate of flowmeter calibration-to-calibration precision error (S_{cc}) which includes

1. Flowmeter nonrepeatability during calibration,
2. Installation effects between calibration facility and engine test stand, and

3. Calibration facility nonrepeatability, which includes temperature and pressure errors in defining density during calibration.

Derivations and formulation for evaluating S_{cc} are also in Appendix C.

4.2.3 Data Reduction Errors

Data reduction errors are those errors incurred in reducing measured units to units of flow and fall into the following three categories:

1. Density determination errors,
2. Precision errors resulting from test dynamics, and
3. Computer resolution errors.

4.2.3.1 Density Determination Errors

Errors in density determination are a result of errors in the measurement of fuel temperatures and pressures. At this point, these errors may be called s_{de} for the precision index and b_{de} for the bias limits.

The effect of fuel pressure precision errors on fuel density is calculated from

$$S_{de_1} = \pm \frac{1}{\sqrt{K}} \frac{\partial \rho}{\partial P} S_P \qquad \text{(IV-48)}$$

where S_P = Pressure measurement precision index

$\frac{1}{\sqrt{K}}$ = Factor to account for K multiple pressure measurements

$\frac{\partial \rho}{\partial P}$ = The partial derivative of the fuel density versus pressure relationship

The degrees of freedom associated with S_{de} are the same as that for the pressure measurement:

$$df_{de_1} = df_p \qquad \text{(IV-49)}$$

The effect of fuel pressure measurement bias on fuel density is

$$B_{de_1} = \frac{\partial \rho}{\partial P} B_P \qquad \text{(IV-50)}$$

The effect of fuel temperature precision error on fuel density (S_{de_2}) is calculated as follows:

$$S_{de_2} = \pm \frac{1}{\sqrt{K}} \frac{\partial \rho}{\partial T} S_T \qquad \text{(IV-51)}$$

where $\frac{1}{\sqrt{K}}$ = factor to account for K multiple temperature measurements

$\frac{\partial \rho}{\partial T}$ = the partial derivative of the fuel density versus temperature relationship.

The degrees of freedom associated with S_{de_2} are the same as the degrees of freedom for the temperature measurement precision index, i.e.,

$$df_{de_2} = df_T \qquad \text{(IV-52)}$$

The effect of fuel temperature bias on fuel density (B_{de_2}) is calculated from

$$B_{de_2} = \frac{\partial \rho}{\partial T} B_T \qquad \text{(IV-53)}$$

4.2.3.2 Computer Resolution

Computer resolution is the source of a small elemental error. Even the small computers used in experimental test applications have six digit resolution (most have eight or more). The resultant full-scale error would be plus or minus one in 10^6. Even though this error is probably negligible, some consideration should be given to it.

Two types of measurement resolution systems are in use, truncating systems and rounding systems. Consideration will be given the elemental bias and precision errors inherent in each of these.

In multiplying or dividing with six or eight digit numbers, the results may have more digits than the system resolution. The truncating system will eliminate digits on the right until the maximum allowable are left. This results in a bias of 1/2 digit and a uniform distribution of precision errors over the interval ±1/2 digit. The elemental precision index for this type of distribution is derived from the precision index of a uniform distribution (Appendix A):

$$s = \sqrt{\frac{(\text{lower limit - upper limit})^2}{12}} = \sqrt{\frac{1^2}{12}} = \pm 0.3 \qquad \text{(IV-54)}$$

The elemental precision error will be ±3/10 of a digit.

The rounding system will also reduce the number of digits to the resolution of the computer. In doing this it will increase the first digit on the right by one approximately half of the time. The decision to increase the digit is based on the size of the last digit eliminated (and others if necessary).

The bias error of 1/2 digit experienced with the truncating system is eliminated. The precision error, however, is not eliminated. It remains the same, ±3/10 of a digit. For a six-digit computer, the precision error is

$$S_{CR} = \pm 3/10 \times 10^{-6}$$

The conclusion is that the rounding system is superior to the truncating system, and if a choice exists, the rounding system should be used.

4.3 FUEL FLOW MEASUREMENT ERRORS

Fuel flow measurement errors when flowmeter calibrations are performed off site and multiple measurements are made, are then

$$S = \pm \frac{1}{\sqrt{K}} \sqrt{S_1^2 + s_{\bar{X}}^2 + S_{wr}^2 + S_{rr}^2 + S_{cc}^2 + s_{de}^2} \qquad \text{(IV-55)}$$

where S = precision index for the fuel flow measurement and $\frac{1}{\sqrt{K}}$ = the factor to account for K multiple instruments which are averaged to provide the measurement.

$$df = \frac{\left(S_1^2 + s_{\bar{X}}^2 + S_{wr}^2 + S_{rr}^2 + S_{cc}^2 + s_{de}^2\right)^2}{\frac{S_1^4}{df_1} + \frac{s_{\bar{X}}^4}{df_{\bar{X}}} + \frac{S_{wr}^4}{df_{wr}} + \frac{S_{rr}^4}{df_{rr}} + \frac{S_{cc}^4}{df_{cc}} + \frac{s_{de}^4}{df_{de}}} \qquad \text{(IV-56)}$$

where df = degrees of freedom associated with the precision index (S). The bias limit usually is not reduced when multiple instruments are used because they usually have equal biases. Bias errors would be reduced by averaging if the meters were calibrated independently at different facilities. The bias limit would be

$$B = \pm \sqrt{B_1^2 + b_{\bar{X}}^2 + b_{de}^2} \qquad \text{(IV-57)}$$

where B = the bias limits for the measurement process. In Eqs. (IV-55) through (IV-57) if a frequency-to-digital conversion process was employed rather than counters, $s_{\bar{X}}$, $b_{\bar{X}}$, and $df_{\bar{X}}$ may be replaced with $s_{\bar{f}}$, $b_{\bar{f}}$, and $df_{\bar{f}}$. The uncertainty would be

$$U = \pm(B + t_{95}S) \qquad \text{(IV-58)}$$

4.4 END-TO-END CALIBRATION

The best method for determining the errors incurred in the flow measurement process would be to flow a weighed quantity or measured volume of fuel through the turbine meters during an engine run. That is, an in-place, end-to-end calibration would be performed during an engine run. Figure IV-10 illustrates a typical arrangement of components for performing calibrations of this nature.

As an example, suppose a measured quantity (gravimetrically or volumetrically) of fuel was flowed through two flowmeters in series to the gas turbine engine during a run. During the period required to flow the measured quantity, record the following:

1. Total pulses generated by each meter,
2. Fuel temperature and pressure for density determination, and
3. The value for the measured quantity in gallons or pounds.

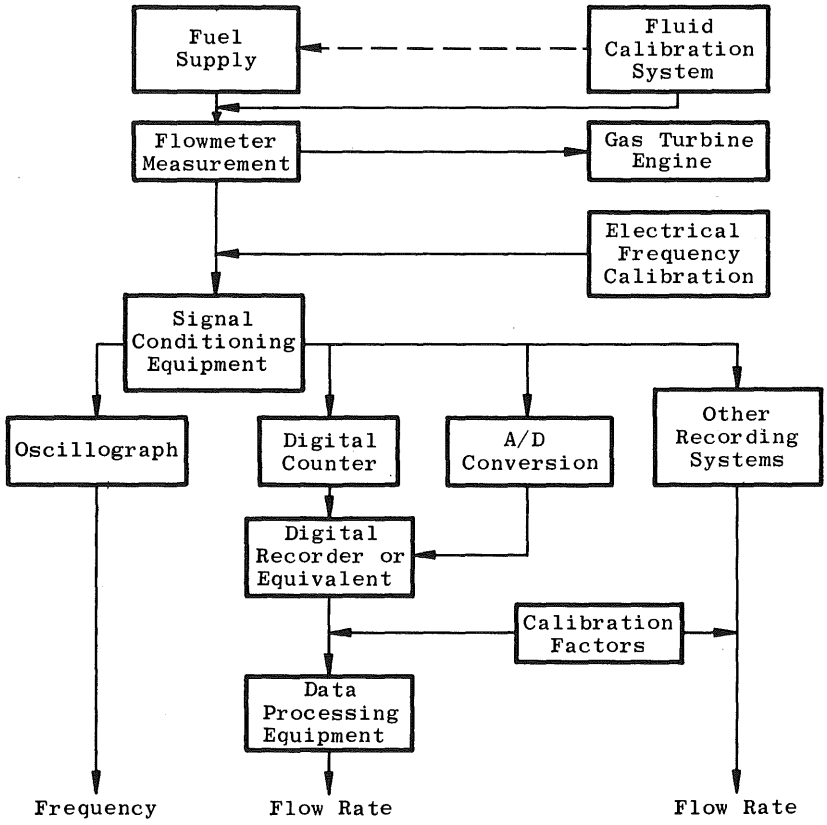

Fig. IV-10 End-to-End Calibration

From these data a meter factor can be calculated.

$$\bar{K}_i = \frac{\text{total pulses}}{\text{total gallons}} \tag{IV-59}$$

for each meter. Then if N runs are made the precision index for data acquisition and reduction for each meter is

$$s_i = \pm\sqrt{\frac{\sum_{i=1}^{N}(K_i - \bar{K})^2}{N-1}} \tag{IV-60}$$

This precision index will include the effects of

1. Meter nonlinearity
2. Electrical calibration
3. Counter or other frequency-to-digital conversion
4. Digital recording
5. Density determination
6. Computer resolution
7. Calibration to calibration precision error

The only precision errors not included in s_i are within-run-precision error (S_{wr}) and the precision error (s_{ws}) of the working standard (calibration system) calibration process. Fuel flow measurement precision index (S) is then

$$S = \pm \frac{1}{\sqrt{K}} \sqrt{s_i^2 + S_{wr}^2 + s_{ws}^2} \tag{IV-61}$$

where $\frac{1}{\sqrt{K}}$ = the factor to account for averaging K multiple instruments. Derivations and formulation for calculating S_{wr} are in Appendix C. The working standard precision error can be determined using Eq. (IV-15) or (IV-30), depending on the type of working standard used.

Degrees of freedom for the flow measurement process are

$$df = \frac{\left(s_i^2 + S_{wr}^2 + s_{ws}^2\right)^2}{\frac{s_i^4}{df_i} + \frac{S_{wr}^4}{df_{wr}} + \frac{s_{ws}^4}{df_{ws}}} \tag{IV-62}$$

where df defines individual degrees of freedom associated with each precision index.

Bias limits (B) in the flow measurement made by this method are the bias in the working standard plus any additional bias based on engineering judgment.

Uncertainty in the measurement is then

$$U = \pm(B + t_{95}S) \tag{IV-63}$$

4.5 SUMMARY

In summary, the elemental errors to be evaluated are listed in Table XIII when off-site calibrations are performed. If end-to-end calibrations are performed while an engine test is in progress, the agony of evaluating all of the above errors is eliminated except those errors determined from multiple measurement statistics which must be evaluated in either case.

Table XIII Elemental Errors

Source	Bias Limit	Precision Index	Degrees of Freedom
Calibration	B_1	S_1	df_1
Data Acquisition	$b_{\bar{x}}$	$s_{\bar{x}}$, S_{wr}, S_{rr}, S_{cc}	$df_{\bar{x}}$, df_{wr}, df_{rr}, df_{cc}
Data Reduction	b_{de}	s_{de}	df_{de}

SECTION V
PRESSURE AND TEMPERATURE MEASUREMENTS

5.1 GENERAL

Pressure and temperature measurements are important in the evaluation of gas turbine engine performance parameters[6], and this section is devoted to the consideration of errors in measurements.

Strain-gage-type pressure transducers are the most common devices used for the measurement of pressures in gas turbine engine testing. Strain-gage pressure transducers are best described as devices which have strain gages fixed directly to a diaphragm or other pressure sensitive surface. The measured strain is calibrated in terms of pressure. Figure V-1 is a simplified diagram illustrating the circuitry for measurement of pressure with a strain-gage-type pressure transducer.

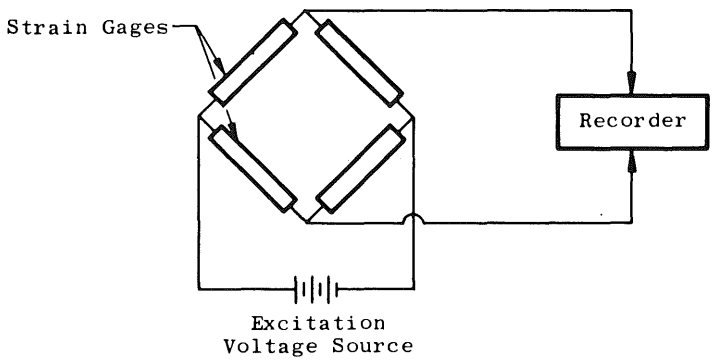

Fig. V-1 Strain-Gage Pressure Transducer Circuitry

There are two different methods for calibrating pressure transducers. One method (Fig. V-2) consists of subjecting the transducer and a pressure standard to the same pressure and recording the outputs. Eleven or more pressure levels over the range of the transducer are recommended. One such pressure standard, which has gained in popularity in recent years, employs a fused quartz helical bourdon tube and optical techniques to produce a digital indication of the applied pressure.

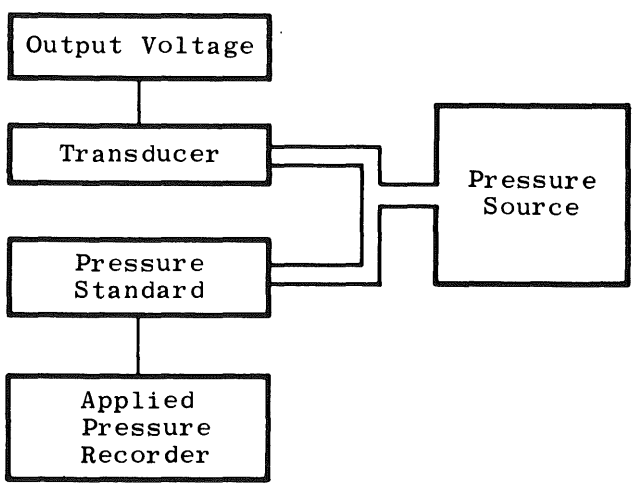

Fig. V-2 Pressure Transducer Calibration with Pressure Standard

[6]For a definition of terms used in this Handbook, see Glossary in Section IX.

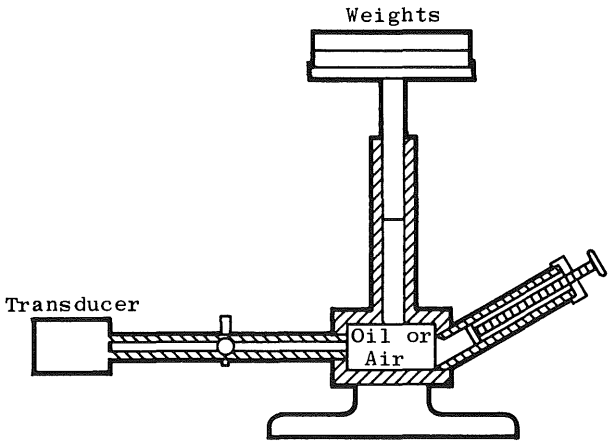

Fig. V-3 Deadweight Piston Gage

The second method (Fig. V-3) consists of applying known pressures to the transducer using an air or liquid deadweight piston gage.

Thermocouples are the most commonly used devices for measuring gas turbine engine temperatures. Resistance thermometers are also used in gas turbine testing. Figure V-4 illustrates typical hook-ups for temperature measurement using resistance thermometers and thermocouples.

There are two methods of calibrating thermocouples and resistance thermometers: (1) by comparison with fixed temperature points and interpolated points as defined by the International Practical Temperature Scale of 1968, and (2) by comparison with platinum-rhodium thermocouples or resistance thermometers used as standards.

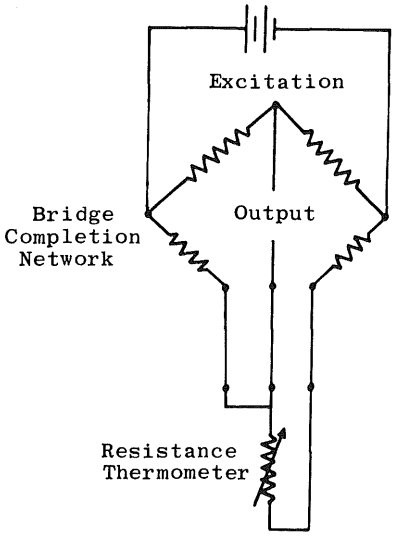

a. Resistance Thermometer Three-Wire System

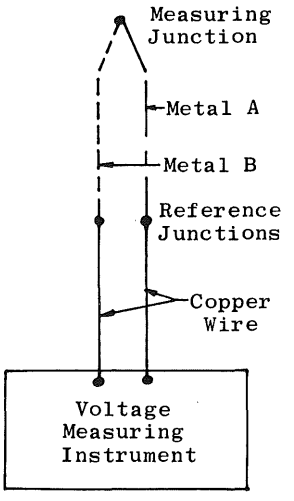

b. Thermocouple System

Fig. V-4 Temperature Measurement

Multiple concurrent measurements of pressure or temperature parameters along the gas path of a gas turbine engine are rarely achieved because of profile effects. Multiple concurrent measurements of pressure or temperature parameters in a turbine engine fuel supply system or airflow measuring system, however, are easily accomplished and should be practiced whenever accuracy requirements dictate.

As an example, multiple measurement of fuel temperature is accomplished by the installation of transducers in adjacent probe bosses in a manner which will allow the two transducers to see the same temperature. Figure V-5 illustrates an accepted method of probe boss arrangement.

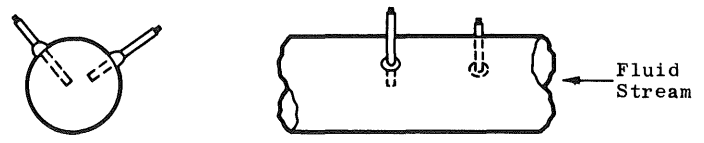

a. Front View b. Side View

Fig. V-5 Probe Boss Arrangement

When the average pressure at a given turbine engine station is required, several individual pressure measurements, each at a unique geometric location, are generally made. If the individual pressure measurements are independent, then the precision index of the average pressure is

$$S_A = \sqrt{\frac{S_p^2 + S_T^2}{N}} \qquad \text{(V-1)}$$

where S_p is the probe precision index, N is the number of independent pressure measurements, and S_T is the transducer precision index.

5.2 PRESSURE MEASUREMENT ERROR SOURCES

5.2.1 Calibration Hierarchy Errors

Figure V-6 illustrates a typical pressure calibration hierarchy.

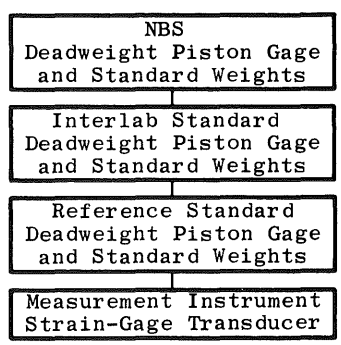

Fig. V-6 Pressure Transducer Calibration Hierarchy

In the typical hierarchy, deadweight piston gages are used as standards at the upper three levels. Calibration of deadweight piston gages is accomplished by comparisons with other deadweight piston gages. Figure V-7 illustrates the setup for this method of calibration.

Weights are applied to the weight table of tester number one until the weights on tester number two are

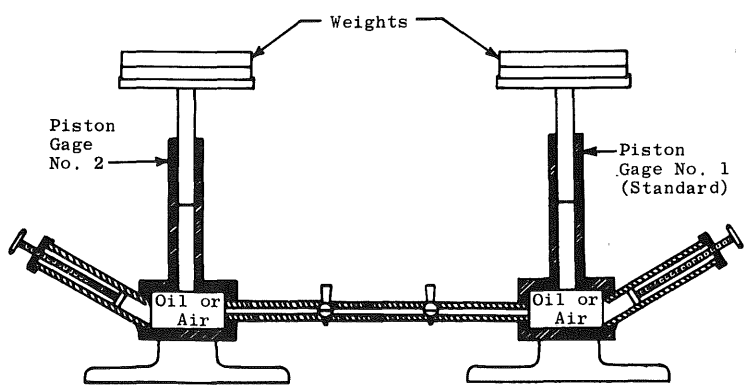

Fig. V-7 Deadweight Piston Gage Calibration

exactly balanced. Knowledge of the effective area of the piston in tester number one and the total mass of the applied weights, weight table, and piston for each tester will allow calculation of the effective area of the piston in tester number two by the relationship

$$\frac{M_1}{A_1} = \frac{M_2}{A_2} \tag{V-2}$$

then,

$$A_2 = \frac{A_1 M_2}{M_1} \tag{V-3}$$

where A_1 = the effective area of the piston in tester number one in square inches

A_2 = the effective area of the piston in tester number two in square inches

M_1 = the total mass of applied weights, weight table, and piston for tester number one in pounds

M_2 = the total mass of applied weights, weight table, and piston for tester number two in pounds

Determination of the piston area at several pressures over the range of the gage and repeatedly at each pressure point will yield a distribution of data. The precision index ($S_{\bar{A}}$) is the standard error of the mean for the calibration process and is estimated from the variation of the individual area determinations about the average ($\bar{A}$). When

$$\bar{A}_i = \frac{\sum_{j=1}^{N} A_j}{N} \tag{V-4}$$

and

$$\bar{A} = \frac{\sum_{i=1}^{K} \bar{A}_i}{K} \tag{V-5}$$

thus,

$$S_{\bar{A}} = \pm \sqrt{\frac{\sum_{j=1}^{N} (A_j - \bar{A}_i)^2}{K\,(N-1)}} \tag{V-6}$$

where N = the total number of observations made at each pressure set point during the calibration

$\bar{A}_i$ = the average piston area at each pressure set point

$\bar{A}$ = the average effective piston area

K = the number of pressure set points

A_j = the area determination at each individual observation at each set point

Degrees of freedom ($df_{\bar{A}}$) associated with the precision index ($S_{\bar{A}}$) are

$$df_{\bar{A}} = K(N - 1) \tag{V-7}$$

Pressure measurements can be made with deadweight piston gages with uncertainties of ±0.01 percent. To do so, a number of parameters of the instrument and its environment must be considered. Consideration of these parameters is primarily for the purpose of minimizing the bias errors incurred by variations in the parameters. Principal instrument parameters are evaluated during calibration, but the user must evaluate those of the environment. For example, the pressure developed by a deadweight piston gage is given by the formula

$$p_p = \frac{\frac{M_m}{A_o}\left(1 - \frac{\rho_a}{\rho_m}\right)kg_L + \frac{V(\rho_{fa} - \rho_a)}{A_o}kg_L + \frac{\gamma C}{A_o}}{[1 + a(t - t_s)][1 + bp_p][1 + d(p_{zo} + S_z p_p - p_j)]} \tag{V-8}$$

where p_p = pressure at the reference level, psi

M_m = mass of the weights, including the piston assembly, lb

A_o = effective area (mean area of the piston and cylinder) in $in.^2$, at atmospheric pressure, temperature t_s, and jacket pressure p_{zo}

ρ_a = mean density of the air displaced by the load, $lb/in.^3$

ρ_m = density of the weights, $lb/in.^3$

k = 1/980.665

g_L = local acceleration due to gravity, cm/sec^2

V = volume of oil in $in.^3$ contributing to the load on the piston

ρ_{fa} = density of the pressure fluid at atmospheric pressure, $lb/in.^3$

γ = surface tension of the pressure fluid, lbf/in.

C = circumference of the piston assembly in inches at the surface of the pressure fluid

a = fractional change in area per °C, and taken as equal to the sum of the thermal coefficients of linear expansion of the piston and cylinder

t = temperature of the piston gage, °C

t_s = reference temperature at which the value for A_o is known

b = fractional change in effective area for 1-psi change in pressure

d = fractional change in effective area for 1-psi change in jacket pressure

p_{zo} = jacket pressure in psi required to reduce the piston-cylinder clearance to zero when $p_p = 0$

S_z = rate of change of zero clearance jacket pressure (p_{zo}) with measured pressure (p_p), psi

p_j = jacket pressure, psi

Obviously, treatment of each of these variables is beyond the scope of this work. They are presented so that the reader will be aware of the considerations that must be made if bias is to be held to a minimum. The NBS will report bias limits for any calibration performed at the Bureau. Bias limits at the lower levels are dependent on the amount of calibration data available and the judgment of the one responsible for calibration data analysis. The bias (b_i) at each level in the hierarchy is at least as large as the bias estimated for the previous level; therefore a conservative estimate is

$$B_i = \pm \sqrt{\sum_{i=1}^{N} b_i^2} \tag{V-9}$$

Upon completion of a strain-gage pressure transducer calibration, a least-squares polynomial curve may be fitted through the data such that

$$X = A_0 + A_1P + A_2P^2 + \cdots + A_MP^K \tag{V-10}$$

where

P = pressure in psia, psid, or psig

A_0, A_1, A_2, and A_M = curve coefficients

X = transducer output voltage

K = degree of the curve fit, i.e., the largest exponent of P

M = the number of curve coefficients

The errors attributed to the calibration process are then the same as those discussed in Section III for laboratory-calibrated force transducers. The precision index (s_i) at any pressure p_i is calculated (Fig. V-8) as

$$s_i = \pm \sqrt{\frac{\sum_{i=1}^{N} (X_i - X)^2}{N - 1}} \tag{V-11}$$

where X_i = measured output voltage corresponding to the applied pressure (P)

X = output voltage from the curve at pressure (P)

N = number of calibration points at pressure (P)

The best procedure is to calculate a precision index for each pressure set point and report the largest as the precision index for the calibration process.

The degrees of freedom (df_i) associated with this precision index are

$$df_i = N - 1 \qquad \text{(V-12)}$$

Bias limits for this calibration process are left to the judgment of the instrumentation engineer.

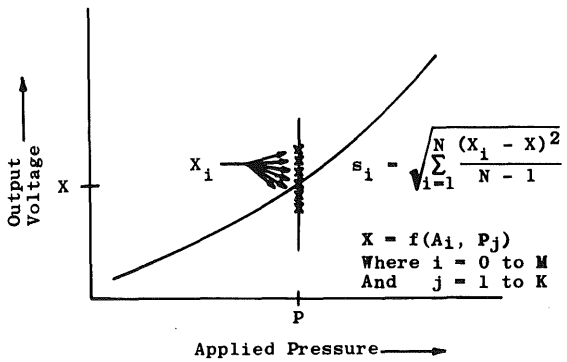

Fig. V-8 Precision Index at Any Applied Pressure (P)

The precision index for the complete hierarchy is calculated by root-sum-squaring the s_i for each level:

$$S_1 = \sqrt{\sum_i s_i^2} \qquad \text{(V-13)}$$

The degrees of freedom for the complete hierarchy are estimated using the Welch-Satterthwaite technique:

$$df_1 = \left[\sum_i s_i^2\right]^2 \Big/ \left[\sum \left(s_i^4 / df_i\right)\right] \qquad \text{(V-14)}$$

The bias limit for the hierarchy would be the root-sum-square of the bias limits for each level:

$$B_1 = \sqrt{\sum_i b_i^2} \qquad \text{(V-15)}$$

5.2.2 Data Acquisition and Reduction Errors

One method of determining the overall effect of the data acquisition and reduction processes is by the periodic performance of special tests. First, select several (four to ten) pressure transducers at random from the pool of calibrated pressure transducers. Connect the transducers to a common manifold (Fig. V-9). Follow the customary recording system pre-run setup procedures. Apply nominal pressure to the manifold, and make a multiple scan (ten or more) recording of transducer outputs. Also, record the level of the applied pressure as defined by a pressure standard (deadweight piston gage or equivalent). Return

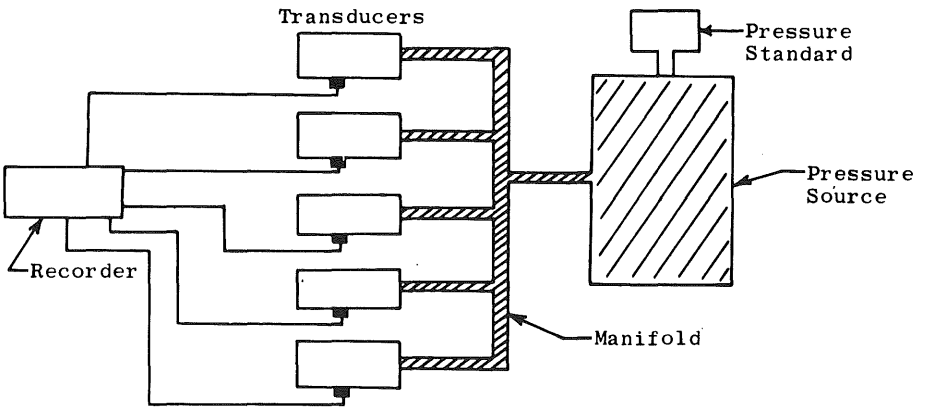

Fig. V-9 Periodic Pressure Tests

the manifold pressure to atmospheric, and then again apply the nominal pressure and record as before. Repeat this procedure at least four times, i.e., make at least four multiple scan recordings of transducer outputs with nominal pressure applied. Reduce the data by means of the normally used gas turbine engine data reduction program. Calculate a multiple scan average ($\bar{X}_{ij}$) for each transducer at each set point:

$$\bar{X}_{ij} = \frac{\sum_{k=1}^{N} X_{ijk}}{N} \tag{V-16}$$

where N = number of scans recorded and X_{ijk} = pressure indicated by the jth transducer on the ith scan of the kth recording. The average ($\bar{X}_j$) for all set points on the jth transducer is

$$\bar{X}_j = \frac{\sum_{i=1}^{M} \bar{X}_{ij}}{M} \tag{V-17}$$

where M = the number of pressure set points.

The precision error for the data acquisition and reduction system is estimated by the variation of the set point recordings ($\bar{X}_{ij}$) about the average ($\bar{X}_j$) for each transducer:

$$s_j = \sqrt{\frac{\sum_{i=1}^{M_j} (\bar{X}_{ij} - \bar{X}_j)^2}{M_j - 1}} \tag{V-18}$$

This estimate is pooled for L transducers to estimate the precision index for the data acquisition and reduction system:

$$S_{\bar{X}} = \sqrt{\frac{\sum_{j=1}^{L} (M_j - 1) s_j^2}{\sum_{j=1}^{L} (M_j - 1)}} = \sqrt{\frac{\sum_{j=1}^{L} \sum_{i=1}^{M_j} (\bar{X}_{ij} - \bar{X}_j)^2}{\sum_{j=1}^{L} (M_j - 1)}} \tag{V-19}$$

The degrees of freedom (df) associated with the precision index are

$$df_{\bar{x}} = \sum_{j=1}^{L} (M_j - 1) \qquad \text{(V-20)}$$

Bias limits for these tests will be based on engineering judgment supported by special test histories.

These statistics include the effects of the following:

1. Pressure standard
2. Pressure transducer
3. Excitation
4. Electrical calibration of the recording system
5. Signal conditioning
6. Recording system
7. Data reduction

but do not include the effects of

1. Probe or tap design and/or coupling configuration
2. Environmental conditions
3. Pressure variations during engine testing

5.2.3 Probe Errors

Treatment of errors from probe or tap design is beyond the scope of this Handbook. The reader is referred to several excellent references which should provide the background required to complete an error analysis:

1. "Aerodynamic Measurements," Robert C. Dean, Jr., MIT Press, 1953, Chapters 3 and 5.

2. "Considerations Entering into the Selection of Probes for Pressure Measurements in Jet Engines," Clarence C. Gettelman and Lloyd N. Krause, ISA Proceedings, Volume 7, Paper No. 52-12-1.

3. "Effect of Interaction among Probes, Supports, Duct Walls, and Jet Boundaries on Pressure Measurements in Ducts and Jets," Clarence C. Gettelman and Lloyd N. Krause, ISA Proceedings, Volume 7, Paper No. 52-12-2.

4. "Review of the Pitot Tube," R. G. Folsom, ASME Transactions, October 1956.

5. "Characteristics of a Wedge with Various Holder Configurations for Static Pressure Measurements in Subsonic Gas Streams," NACA RM E51G09, September 1951.

6. "An Investigation of the Influence of Orifice Geometry on Static Pressure Measurements," R. E. Rayle, Jr., MS Thesis, MIT, 1949.

As an example of the type of error referred to here, suppose an engineer wants to make velocity coefficient corrections to total pressure measurements. Very likely, the correction will be of the form

$$P_T = P_{T_m} + \left(\frac{P_{T_m} - P_T}{q}\right) q \tag{V-21}$$

where

P_T = actual total pressure

P_{T_m} = measured total pressure

$(P_{T_m} - P_T)/q$ = velocity coefficient

q = velocity head = $\frac{1}{2} \rho V^2$

Velocity coefficients for each probe may be determined by calibration. Calibration data will yield the precision index ($S_{P_{T_m}}$) and bias limit ($B_{P_{T_m}}$). Expanding Eq. (V-21) in the Taylor's series gives

$$S_{P_T} = \pm\sqrt{S_{P_{T_m}}^2 + \left[\left(\frac{P_{T_m} - P_T}{q}\right) S_q\right]^2} \tag{V-22}$$

and

$$B_{P_T} = \pm\sqrt{B_{P_{T_m}}^2 + q^2 B^2 \left(\frac{P_{T_m} - P_T}{q}\right)} \tag{V-23}$$

It is to be noted that the term $(P_{T_m} - P_T)/q$ is treated as a constant with bias error only, whereas the term q has only precision error with bias being negligible.

Pressure variations caused by the engine or facility are not errors. The reader is cautioned that time variant data adds additional complexity to the uncertainty analysis (see Section 8.7).

The pooled within-run precision index (S_{wr}) and pooled run-to-run precision index (S_{rr}) may be obtained from multiple measurements. Derivations and formulation for calculating S_{wr} and S_{rr} are in Appendix C.

5.2.4 Pressure Measurement Error Summary

Finally, if precautions are taken to make environmental effects negligible or laboratory tests are performed similar to those suggested in Section III for determining their effects, the measurement precision index may be calculated from

$$S_p = \pm\sqrt{S_1^2 + S_{\bar{x}}^2 + S_{wr}^2 + S_{rr}^2 + s_e^2 + s_b^2 + S_{P_T}^2} \qquad \text{(V-24)}$$

where S_1 = calibration hierarchy precision index

$S_{\bar{x}}$ = data acquisition and reduction precision index

S_{wr} = within-run precision index (multiple measurements only)

S_e = precision error due to environmental effects

S_b = precision error due to the measurement of barometric pressure if transducer zero corrections are in the data reduction process for absolute pressure measurement or if gage pressure measurements are made

S_{rr} = Run-to-run precision index (multiple measurements only)

S_{P_T} = probe velocity coefficient precision index (when applicable)

The degrees of freedom (df) associated with the precision index are,

$$df_p = \frac{\left(S_1^2 + S_{\bar{x}}^2 + S_{wr}^2 + S_{rr}^2 + s_e^2 + s_b^2 + S_{P_T}^2\right)}{\frac{S_1^4}{df_1} + \frac{S_{\bar{x}}^4}{df_{\bar{x}}} + \frac{S_{wr}^4}{df_{wr}} + \frac{S_{rr}^4}{df_{rr}} + \frac{s_e^4}{df_e} + \frac{s_b^4}{df_b} + \frac{S_{P_T}^4}{df_{P_T}}} \qquad \text{(V-25)}$$

Bias limits for the pressure measurement are

$$B_p = \pm\sqrt{B_1^2 + B_{\bar{x}}^2 + B_e^2 + B_b^2 + B_{P_T}^2} \qquad \text{(V-26)}$$

If special tests are not performed to determine the overall effect of the data acquisition and reduction processes, then each of the elemental errors must be evaluated as in Section III. The precision index for the pressure measurement would, therefore, be calculated as follows:

$$S_p = \pm\sqrt{S_1^2 + S_2^2 + S_3^2 + S_{wr}^2 + S_{rr}^2 + s_e^2 + s_b^2 + S_{P_T}^2} \qquad \text{(V-27)}$$

where S_1 = the root-sum-square of the elemental precision errors in the calibration hierarchy

S_2 = the root-sum-square of the elemental precision errors in the data acquisition process

S_3 = the root-sum-square of the elemental precision errors in the data reduction process

The degrees of freedom for the pressure measurement are

$$df_p = \frac{\left(S_1^2 + S_2^2 + S_3^2 + S_{wr}^2 + S_{rr}^2 + s_e^2 + s_b^2\right)^2}{\frac{S_1^4}{df_1} + \frac{S_2^4}{df_2} + \frac{S_3^4}{df_3} + \frac{S_{wr}^4}{df_{wr}} + \frac{S_{rr}^4}{df_{rr}} + \frac{s_e^4}{df_e} + \frac{s_b^4}{df_b}} \qquad \text{(V-28)}$$

Bias limits for the pressure measurement are calculated as the root-sum-square of the elemental bias limits

$$B_p = \sqrt{B_1^2 + B_2^2 + B_3^2 + b_e^2 + b_b^2} \qquad \text{(V-29)}$$

5.3 TEMPERATURE MEASUREMENT ERROR SOURCES

5.3.1 Calibration Hierarchy Errors

The apex of the calibration hierarchy is, of course, the NBS as indicated in Fig. V-10.

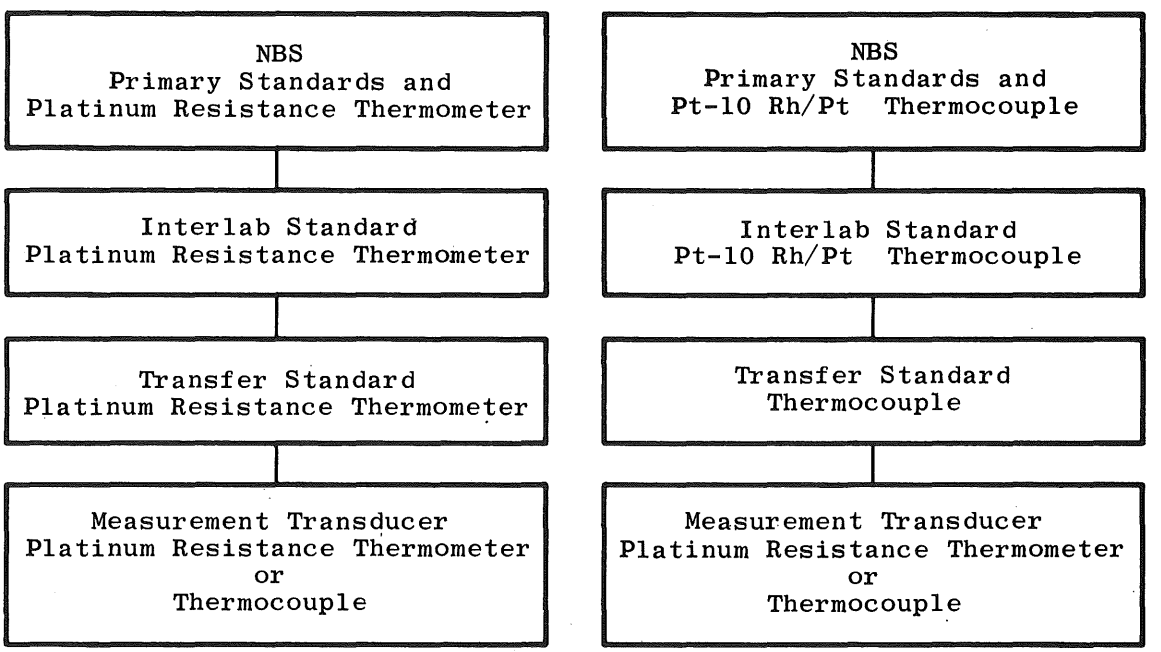

Fig. V-10 Temperature Transducer Calibration Hierarchy

The NBS certifies platinum resistance thermometers by the International Practical Temperature Scale of 1968 (IPTS-68). The International Practical Temperature Scale is based on a number of fixed and reproducible equilibrium temperatures and on internationally agreed-upon measuring instruments and interpolation formulas. The eleven primary equilibrium temperatures and a few secondary temperatures are listed in Table XIV.

Table XIV International Practical Temperature Scale of 1968

Reference	Temperature			
	°C	°K	°F	°R
Freezing Point Gold*	1064.43	1337.58	1947.97	2407.64
Freezing Point Silver*	961.93	1235.08	1763.47	2223.14
Freezing Point Aluminum	660.37	933.52	1220.67	1680.34
Freezing Point Antimony	630.74	903.89	1167.33	1627.00
Boiling Point Sulfur	444.674	717.824	832.413	1292.083
Freezing Point Zinc*	419.58	692.73	787.24	1246.91
Freezing Point Lead	327.502	600.652	621.504	1081.174
Freezing Point Tin	231.9681	505.1181	449.5426	909.2126
Boiling Point Water*	100.	373.15	212.	671.67
Triple Point Water*	+0.01	273.16	32.02	491.69
Boiling Point Oxygen*	-182.962	90.188	-297.332	162.338
Triple Point Oxygen*	-218.789	54.361	-361.820	97.850
Boiling Point Neon*	-246.048	27.102	-410.886	48.784
Boiling Point Hydrogen*	-252.87	20.28	-423.166	36.50
Boiling Point Hydrogen, 25/76 atm*	-256.108	17.042	-428.994	30.676
Triple Point Hydrogen*	-259.34	13.81	-434.812	24.86

*Indicates IPTS-68 Defining Temperature

A typical calibration report from the NBS reads as follows:

Temperatures between 0°C and 630.74°C on the new International Practical Temperature Scale of 1968 (IPTS-68) are defined by the indications (resistance values) of standard platinum resistance thermometers and the following expressions:

$$t = t' + M(t') \tag{1}$$

$$t' = \frac{1}{\alpha}\left(\frac{R_t}{R_o} - 1\right) + \delta\left(\frac{t'}{100} - 1\right)\frac{t'}{100} \tag{2}$$

$$M(t') = 0.045\left(\frac{t'}{100}\right)\left(\frac{t'}{100} - 1\right)\left(\frac{t'}{419.58} - 1\right)\left(\frac{t'}{630.74} - 1\right) \tag{3}$$

where t is the temperature, at the outside of the tube protecting the platinum resistor, in °C on the International Practical Temperature Scale of 1968 and R_t and R_o are the resistances of the platinum resistor at t°C and 0°C, respectively, measured with a continuous current through the platinum resistor. The value of M(t'), given by expression (3), is the same for all thermometers and is a function only of the quantity t'. The addition of the small value represented by (3) serves to make the IPTS-68 conform more closely to the thermodynamic scale than can be done with only the simple quadratic of expression (2).

An alternate form which is completely equivalent to expression (2) is

$$R_t = R_o(1 + At' + Bt'^2) \tag{4}$$

In some instances expression (4) is less difficult to calculate than (2). The constants A and B used in (4) are related directly to α and δ.

$$A = \alpha(1 + \delta/100) \tag{5}$$

$$B = -\alpha\delta/10^4 \tag{6}$$

CAUTION: The values of A, B, and δ on the new 1968 scale are distinctly different from the corresponding values on the old 1948 or 1927 scale. The values of α and R_0 are also different but only trivially so.

Temperatures below 0°C on the new 1968 scale are calculated using a standard reference table which gives values of R_t/R_0 for a fictitious "mean" standard thermometer. This reference table and a specified deviation equation are combined to give the values for a particular thermometer. The standard reference table used for IPTS-68 is referred to as the "CCT-68" table. It is convenient to use the symbol W_t in place of R_t/R_0. For the special reference values of R_t/R_0 tabulated in CCT-68, the special symbol W_t^* is used. The table giving values of W_t for a particular thermometer from 0°C down to -182.962°C may be calculated from the following expressions:

$$W_t = W_t^* + W_t \tag{7}$$

$$W_t = A_4 t + C_4 t^3 (t - 100) \tag{8}$$

Expression (8) is the specified deviation equation in the range 0°C to -182.962°C. ...

A table calculated from the constants for this thermometer is on the following pages. If no value for C_4 is given, the table below 0°C was calculated with an assumed value of this constant. The first column of the table gives values of temperature. Unless a different function is requested, the second column gives R_t/R_0 (i.e. the ratio of the resistance at the stated temperature to the resistance at the ice point). The third column gives the inverse (reciprocal) of the difference between successive values in the second column. These reciprocal first differences are included to facilitate interpolation. The error introduced by using linear interpolation will be less than 0.0001°C.

The range of this table does not imply that this thermometer is necessarily a satisfactory instrument over exactly the same range. The range was selected to cover an interval believed to include the needs of the majority of users of this type of thermometer.

Temperature transducers certified by this procedure by the NBS exhibit negligibly small errors when compared with errors associated with calibration processes below the NBS level.

Calibrations of transfer standard temperature transducers are accomplished by placing the transfer standard in a calibration medium along with the interlab standard which defines the temperature of the medium. If comparisons are made between the interlab standard and transfer standard at K temperatures and the process is repeated at specified time intervals, a calibration data bank will be established from which calibration precision indices and bias limits may be established, i.e.,

$$S_j = \pm\sqrt{\frac{\sum_{i=1}^{N}(X_{ij} - \bar{X}_j)}{N-1}} \tag{V-30}$$

where S_j = calibration process precision index at temperature j

X_{ij} = individual temperatures indicated by the transfer standard at temperature j

$\bar{X}_j$ = the average indication by the transfer standard at temperature j

N = number of indications at temperature j

$$S_{TS} = \pm\sqrt{\frac{\sum_{j=1}^{K} S_j^2}{K}} \tag{V-31}$$

where S_{TS} is the calibration process precision index for the transfer standard. The degrees of freedom (df_{TS}) are

$$df_{TS} = K(N-1) \tag{V-32}$$

Bias limits for the transfer standard calibration process should be estimated on the basis of interlab and interfacility comparisons and engineering judgment.

Temperature transducers used in jet engine testing are usually calibrated against a transfer standard transducer. The same techniques described for transfer standards are used in these calibrations. Comparisons are made at a minimum of three different temperatures over the test transducer range to establish conformance with the manufacturer's specifications. If the manufacturer specifies limits for precision error and bias, the precision index for the transducer is the precision error limit divided by t = 2.0, i,e., if

$$t_{95}s_i = \pm 0.36 \tag{V-33}$$

then

$$s_i = \pm 0.18 \tag{V-33}$$

where $t_{95}s_i$ is the specified precision error limit and s_i is the transducer precision index.

The degrees of freedom (df_i) associated with the precision index are assumed to be greater than 30.

Bias limits (B_i) for the transducer are equal to the limits specified by the manufacturer.

If extensive calibration histories have been accrued, it may be advantageous to calculate the precision index directly from calibration data rather than accept the values

provided by the manufacturer. The manufacturer's specified limits will likely be conservative. This being the case, the precision index is calculated from

$$S_{T_j} = \pm\sqrt{\frac{\sum_{i=1}^{N}(X_{ij} - \bar{X}_j)^2}{N - 1}} \tag{V-34}$$

where S_{T_j} = the precision index for N transducers at temperature j

X_{ij} = individual indication at temperature j by the ith transducer

$\bar{X}_j$ = the average indication at temperature j by all transducers

N = the number of transducers calibrated

$$S_T = \pm\sqrt{\frac{\sum_{j=1}^{M} S_{T_j}^2}{M}} \tag{V-35}$$

where S_T = measurement transducer precision index

M = number of temperatures at which comparisons are made

The degrees of freedom for this calibration process are

$$df_T = M(N - 1) \tag{V-36}$$

Bias limit estimates are left to the judgment of the instrumentation engineer.

The precision index for the calibration hierarchy is

$$S_1 = \pm\sqrt{S_{TS}^2 + S_T^2} \tag{V-37}$$

The degrees of freedom for S_1 are

$$df_1 = \frac{\left(S_{TS}^2 + S_T^2\right)^2}{\frac{S_{TS}^4}{df_{TS}} + \frac{S_T^4}{df_T}} \tag{V-38}$$

The bias limit for the calibration hierarchy is

$$B_1 = \pm\sqrt{B_{TS}^2 + B_T^2} \tag{V-39}$$

5.3.2 Data Acquisition and Reduction Errors

Evaluation of the overall effect of data acquisition and reduction errors is best accomplished by monitoring systems or special tests specifically designed for this purpose.

5.3.2.1 Thermocouples

A reference temperature monitoring system will provide an excellent source of data for evaluating errors due to the recording apparatus and data reduction process.

Figure V-11 depicts a typical setup for measuring gas turbine engine gas path temperatures with Chromel®-Alumel® thermocouples.

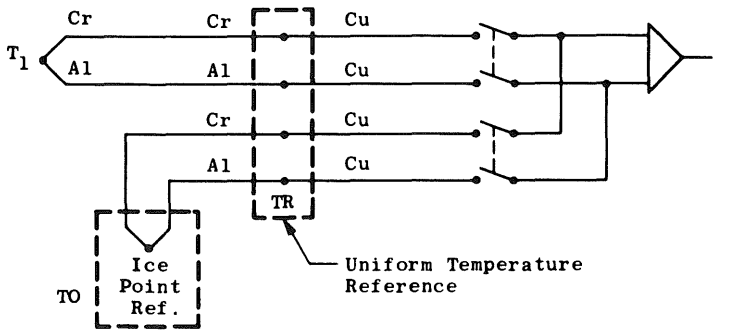

Fig. V-11 Typical Thermocouple Channel

If several calibrated thermocouples are utilized to monitor the temperature of the reference junction block, statistically useful data can be recorded each time test data are recorded. Assuming that those thermocouple data are recorded and reduced to engineering units by processes identical to those employed for engine temperature measurements, a stockpile of data will be gathered, from which data acquisition and reduction errors may be estimated.

For the purpose of illustration, suppose N calibrated Chromel-Alumel thermocouples are employed to monitor the reference block temperature of a temperature measuring system similar to that depicted by Fig. V-11. If each time a test data point is recorded, multiple scan recordings are made for each of the thermocouples and if a multiple scan average (X_{ij}) is calculated for each thermocouple, then the average ($\overline{X}_j$) for all recordings of the jth thermocouple is

$$\overline{X}_j = \frac{\sum_{i=1}^{K} X_{ij}}{K} \tag{V-40}$$

where K is the number of multiple scan recordings for the jth thermocouple.

The grand average ($\overline{X}$) is computed for all monitor thermocouples as

$$\overline{X} = \frac{\sum_{j=1}^{N} \overline{X}_j}{N} \tag{V-41}$$

The precision index ($S_{\overline{X}}$) for the data acquisition and reduction processes is then

$$S_{\overline{X}} = \pm \sqrt{\frac{\sum_{j=1}^{N} \sum_{i=1}^{K} (X_{ij} - \overline{X}_j)^2}{\sum_{j=1}^{N} (K - 1)}} \tag{V-42}$$

The degrees of freedom associated with $S_{\bar{X}}$ are

$$df_{\bar{X}} = \sum_{i=1}^{N} (K - 1) \tag{V-43}$$

Bias limits for the data acquisition process will be estimated by the instrumentation engineer.

Error sources accounted for by this method are:

1. Ice point reference precision error
2. Reference block temperature precision error
3. Recording system resolution error
4. Recording system electrical noise
5. Analog-to-digital conversion error
6. Chromel-Alumel thermocouple millivolt output versus temperature curve-fit error
7. Computer resolution error

Several errors which are not included in the monitoring system statistics are

1. Conduction error (B_C)
2. Radiation error (B_R)
3. Recovery error (B_Y)
4. Calibration error (B_1)

These errors are a function of probe design and environmental conditions. Detailed treatment of these error sources is beyond the scope of this work. Several good references which should provide the background required to complete an error analysis are listed below:

1. "A Design Procedure for Thermocouple Probes," Laurence B. Haig, General Motor Corp., SAE Preprint 158C, SAE National Aeronautics Meeting, April 1960.

2. "Experimental Determination of Time Constants and Nusselt Numbers for Bare-Wire Thermocouples in High-Velocity Air Streams and Analytic Approximation of Conduction and Radiation Errors," Marvin D. Scadron and Isidore Warshawsky, NACA TN 2599, January 1952.

3. "Recovery Corrections for Butt-Welded, Straight-Wire Thermocouples in High-Velocity, High-Temperature Gas Streams," Fredrick S. Simmons, NACA RM E54G22a, September 1954.

4. "Radiation and Recovery Corrections and Time Constants of Several Chromel-Alumel Thermocouple Probes in High-Temperature, High-Velocity Gas Streams," George E. Glawe, Fredrick S. Simmons, and Truman M. Stickner, NACA TN 3766, October 1956.

5. "Performance of Three High-Recovery-Factor Thermocouple Probes for Room-Temperature Operation," Marvin D. Scadron, Clarence C. Gettelman, and George J. Pock, NACA RM E50I29, December 1950.

6. "Recovery Characteristics of a Single-Shielded Self-Aspirating Thermocouple Probe at Low Pressure Levels and Subsonic Speeds," C. E. Willbanks, AEDC-TR-71-68, April 1971.

5.3.2.2 Resistance Thermometers

One tried and proved procedure for evaluating the data acquisition and reduction errors associated with resistance thermometer temperature measurements is as follows:

1. Wirewound resistors, matched to ±0.01 percent of the desired value, are substituted in place of resistance thermometers.

2. With the exception of the substitution resistors, the temperature measurement system should be identical to that used during engine testing. Components of the system (Fig. V-12) are

   a. Bridge completion network (BCN)
   b. Power supply
   c. Recording system electrical calibration
   d. Switching components
   e. Signal conditioning equipment
   f. Analog-to-digital converter
   g. Magnetic tape recorder.

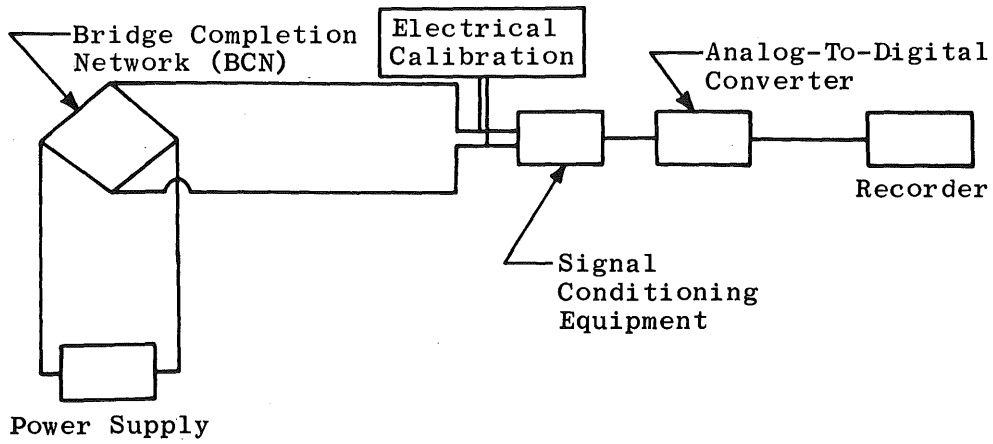

Fig. V-12 Temperature Data Recording Calibration

3. Select at least four resistance thermometer channels.

4. Follow normal pre-run procedures for setting up the recording system.

5. Make several (ten or more) multiple scan (ten or more) recordings.

6. Reduce the data by means of the normally used gas turbine engine data reduction program and calculate a multiple scan average (X_{ij}) for each recording of each channel. The average ($\bar{X}_j$) for all recordings on the jth channel is

$$\bar{X}_j = \frac{\sum_{i=1}^{M_j} X_{ij}}{M_j} \tag{V-44}$$

where M_j = the number of recordings on the jth channel. The grand average ($\bar{\bar{X}}$) is computed for all channels:

$$\bar{\bar{X}} = \frac{\sum_{j=1}^{N} \bar{X}_j}{N} \tag{V-45}$$

where N = number of channels tested.

The precision index ($S_{\bar{\bar{X}}}$) for the data acquisition and reduction processes is then

$$S_{\bar{\bar{X}}} = \sqrt{\frac{\sum_{j=1}^{N} \sum_{i=1}^{M_j} (X_{ij} - \bar{X}_j)^2}{\sum_{j=1}^{N} (M_j - 1)}} \tag{V-46}$$

The degrees of freedom associated with the precision index are

$$df_{\bar{\bar{X}}} = \sum_{j=1}^{N} (M_j - 1) \tag{V-47}$$

Bias limit estimates are left to the judgment of the instrumentation engineer.

The only error sources not accounted for are bridge completion network (BCN) environmental effects and errors resulting from the dynamics of an engine test. The first will be accounted for if the BCN environment is at engine test conditions. If not, then laboratory tests are required to determine the effects of BCN temperature variations on temperature measurements. Errors resulting from the dynamics of an engine test are accounted for by means of multiple measurement statistics. From multiple measurements, the pooled within-run precision error (S_{wr}) and the pooled run-to-run precision error (S_{rr}) for each resistance thermometer may be obtained. Derivations and formulation for

calculating S_{wr} and S_{rr} are in Appendix C. If thermometer and BCN are not calibrated as a unit (interchangeable BCN's) then a third multiple measurement statistic (S_{cc}) must be calculated. This statistic is referred to as the pooled calibration-to-calibration precision error. Derivations and formulation for this statistic are also in Appendix C.

5.3.3 Temperature Measurement Error Summary

5.3.3.1 Thermocouples

The precision index for temperature measurements made with thermocouples is

$$S_T = \pm\sqrt{S_1^2 + S_{\bar{X}}^2 + S_{wr}^2 + S_{rr}^2} \tag{V-48}$$

where S_1 = calibration hierarchy precision index

$S_{\bar{X}}$ = data acquisition and reduction precision index

S_{wr} = within-run precision index (multiple measurements only)

S_{rr} = run-to-run precision index (multiple measurements only)

The degrees of freedom associated with S_T are

$$df_T = \frac{\left(S_1^2 + S_{\bar{X}}^2 + S_{wr}^2 + S_{rr}^2\right)^2}{\frac{S_1^4}{df_1} + \frac{S_2^4}{df_2} + \frac{S_{wr}^4}{df_{wr}} + \frac{S_{rr}^4}{df_{rr}}} \tag{V-49}$$

Bias limits for the measurements are

$$B_T = \pm\sqrt{B_1^2 + B_{\bar{X}}^2 + B_C^2 + B_R^2 + B_Y^2} \tag{V-50}$$

where B_1 = calibration hierarchy bias limits

$B_{\bar{X}}$ = data acquisition and reduction bias limits

B_C = conduction error bias limits

B_R = radiation error bias limits

B_Y = recovery factor bias limits

5.3.3.2 Resistance Thermometers

The precision index for temperature measurements made with resistance thermometers is

$$S_T = \pm\sqrt{S_1^2 + S_{\bar{X}}^2 + S_{wr}^2 + S_{rr}^2 + S_{cc}^2 + s_e^2} \tag{V-51}$$

where S_1 = calibration hierarchy precision index

$S_{\bar{X}}$ = data acquisition and reduction precision index

S_{wr} = within-run precision index (multiple measurements only)

S_{rr} = run-to-run precision index (multiple measurements only)

S_{cc} = calibration-to-calibration precision index (multiple measurements only)

s_e = BCN environmental effects not included in $S_{\bar{X}}$

The degrees of freedom df associated with this precision index are

$$df_T = \frac{\left(S_1^2 + S_{\bar{X}}^2 + S_{wr}^2 + S_{rr}^2 + S_{cc}^2 + s_e^2\right)^2}{\frac{S_1^4}{df_1} + \frac{S_{\bar{X}}^4}{df_{\bar{X}}} + \frac{S_{wr}^4}{df_{wr}} + \frac{S_{rr}^4}{df_{rr}} + \frac{S_{cc}^4}{df_{cc}} + \frac{s_e^4}{df_e}} \tag{V-52}$$

Bias in the temperature measurement is estimated by

$$B_T = \pm \sqrt{B_1^2 + B_{\bar{X}}^2 + b_e^2} \tag{V-53}$$

where b_e is the bias resulting from BCN environmental effects.

If special tests are not performed to determine the overall effects of data acquisition and reduction processes, each of the elemental errors must be evaluated as in Section III. The precision index for the temperature measurement is then

$$S_T = \sqrt{S_1^2 + S_2^2 + S_3^2 + S_{wr}^2 + S_{rr}^2 + S_{cc}^2 + s_e^2} \tag{V-54}$$

where S_1, S_2, and S_3 are the root-sum-square of the elemental precision errors in the calibration hierarchy, data acquisition process, and data reduction process, respectively.

The degrees of freedom for the temperature measurement are

$$df_T = \frac{\left(S_1^2 + S_2^2 + S_3^2 + S_{wr}^2 + S_{rr}^2 + S_{cc}^2 + s_e^2\right)^2}{\frac{S_1^4}{df_1} + \frac{S_2^4}{df_2} + \frac{S_3^4}{df_3} + \frac{S_{wr}^4}{df_{wr}} + \frac{S_{rr}^4}{df_{rr}} + \frac{S_{cc}^4}{df_{cc}} + \frac{s_e^4}{df_e}} \tag{V-55}$$

Bias limits for the temperature measurement are calculated by root-sum-squaring the elemental biases.

$$B_T = \pm \sqrt{\sum_i b_i^2} \tag{V-56}$$

SECTION VI
AIRFLOW

6.1 GENERAL

Airflow rate measurements in gas turbine engine systems are generally made with one of three types of flowmeters: venturis, nozzles, and orifices. Selection of the specific type of flowmeter to use for a given application is contingent upon a trade-off between measurement accuracy[7] of requirements, allowable pressure drop, and fabrication complexity/cost.

Flowmeters may be further classified into two categories: subsonic flow and critical flow. With a critical flowmeter, in which sonic velocity is maintained in the flowmeter, mass flow rate is a function only of the upstream gas properties. With a subsonic flowmeter, where the throat Mach number is less than sonic, mass flow rate is a function of both upstream and downstream gas properties.

Equations for the indicated mass flow rate through nozzles, venturis, and orifices are derived from the continuity equation;

$$W = \rho AV \tag{VI-1}$$

where W = mass flow rate, lb/sec

ρ = density of the gas at the meter throat, lb/ft^3

A = cross-sectional area of the throat, ft^2

V = gas velocity at the throat, ft/sec

In using the continuity equation as a basis for indicated flow equation derivations, it is normal practice to assume conservation of mass and energy and one-dimensional isentropic flow. Expressions for indicated flow will not yield the actual flow since actual conditions always deviate from ideal. An empirically determined correction factor, the discharge coefficient (C_d), is used to adjust indicated to actual flow:

$$C_d = \frac{W_{actual}}{W_{indicated}} \tag{VI-2}$$

Gas flow through venturis and nozzles closely follows the contour of the constriction, which results in geometric control of the flow area; in an orifice, the flow stream is contracted downstream of the constriction at the vena contracta. Location and size of the vena contracta (minimum flow area) vary with flow rate. As a result, flow through venturis and nozzles can be better described analytically, and therefore, flow measurements made with venturis and nozzles are potentially more accurate than flow measurements made with orifices.

---

[7]For a definition of terms used in this Handbook, see the Glossary in Section IX.

Since, in the evaluation of turbine engine performance, engine inlet total airflow is one of the three most important measurement parameters, the requirement for high measurement accuracy generally outweighs all other considerations. Hence, it is recommended that a venturi system, operating at critical flow conditions, be used.

In the sections to follow, airflow measurement techniques will be discussed on the basis of the two basic systems: subsonic flowmeters and critical flowmeters.

6.2 AIRFLOW RATE MEASUREMENT TECHNIQUES

6.2.1 Subsonic Flowmeters

6.2.1.1 Venturis and Nozzles

Figure VI-1 schematically depicts a representative venturi and nozzle design.

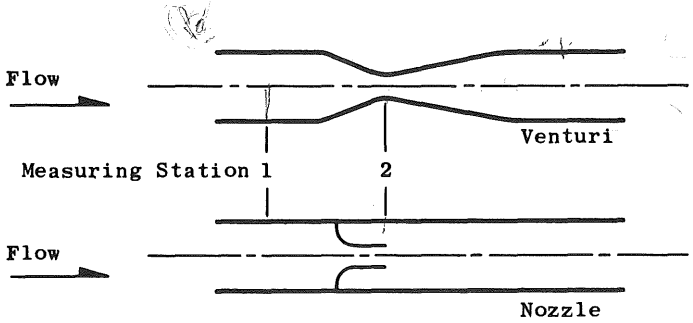

Fig. VI-1 Schematic of Typical Venturi and Nozzle with Measuring Stations

Flow rates through subsonic venturis and nozzles may be calculated by means of Eq. (VI-3) which is derived from the continuity equation.

$$W = \frac{\pi d^2}{4} C_d F_a \frac{P_1 \left(\frac{P_2}{P_1}\right)^{\frac{1}{K}}}{\sqrt{T_1}} \sqrt{\frac{K}{K-1}\left[1 - \left(\frac{P_2}{P_1}\right)^{\frac{K-1}{K}}\right]\frac{2gM}{ZR}} \qquad \text{(VI-3)}$$

where

W = airflow rate, lbm/sec

d = meter throat diameter, in.

C_d = meter discharge coefficient (unitless)

F_a = meter thermal expansion correction factor (unitless) (evaluated at meter skin temperature)

P_1 = upstream total pressure, lbf/in.^{2}

T_1 = upstream total temperature, °R

p_2 = throat static pressure, lbf/in.^{2}

K = ratio of specific heats at T_1 (unitless)

M = molecular weight of the flowing gas, lbm/lbm-mol

Z = compressibility factor (unitless)

R = universal gas constant, 1545 ft lbf/lbm-mol-°R

g = dimensional constant, 32.174 lbm-ft/lbf-sec^2

Equation (VI-3) is a general expression for the case where meter upstream total pressure and temperature are measured. A typical example of this type of measurement system is the airflow measurement at the compressor inlet station of a gas turbine engine in the flow channel (nozzle) formed by the engine inlet ducting and the engine inlet centerbody or spinner.

It should be noted that derivation of Eq. (VI-3) from the continuity Eq. (VI-1) requires the assumption of a calorically perfect gas, in which case Z = 1. It is further assumed that the upstream total temperature (T_1) has been corrected for conduction, convection and radiation losses and for probe recovery factor, as specified in Section 5.3.2.1. For real gases, values of the specific heat ratio (K), the molecular weight (M), and the compressibility factor (Z) are a function of the gas composition, pressure, and temperature. The equation is suitable for gases normally encountered in turbine engine work; the value of K should be evaluated at the upstream stagnation conditions, whereas the value of Z should be evaluated at the meter throat static conditions. The meter discharge coefficient (C_d) is a function of the meter construction, the measurement and calculation techniques, and the gas properties at the meter throat station.

Taylor's series expansion of Eq. (VI-3) results in Eq. (VI-4) for calculation of the precision index (S_w) and Eq. (VI-5) for the bias limit (B_w). Errors associated with values of π, F_a, K, g, μ, Z, and R in Eq. (VI-3) are assumed negligible in the following calculations.

$$S_w = \pm W \sqrt{\left(\frac{1}{C_d} S_{C_d}\right)^2 + \left(\frac{2}{d} S_d\right)^2 + \left(\frac{-1}{2T_1} S_{T_1}\right)^2 + \left\{\frac{K-1}{KP_1} + \frac{\left(\frac{K-1}{K}\right)\left(\frac{P_2}{P_1}\right)^{-\frac{1}{K}}\left(\frac{P_2}{P_1^2}\right)}{2\left[1-\left(\frac{P_2}{P_1}\right)^{\frac{K-1}{K}}\right]}\right\}^2 S_{P_1}^2 + \left\{\frac{1}{KP_2} - \frac{\left(\frac{K-1}{K}\right)\left(\frac{P_2}{P_1}\right)^{-\frac{1}{K}}\left(\frac{1}{P_1}\right)}{2\left[1-\left(\frac{P_2}{P_1}\right)^{\frac{K-1}{K}}\right]}\right\}^2 S_{P_2}^2} \quad \text{(VI-4)}$$

$$B_w = \pm W \sqrt{\left(\frac{1}{C_d} B_{C_d}\right)^2 + \left(\frac{2}{d} B_d\right)^2 + \left(\frac{-1}{2T_1} B_{T_1}\right)^2 + \left\{\frac{K-1}{KP_1} + \frac{\left(\frac{K-1}{K}\right)\left(\frac{P_2}{P_1}\right)^{-\frac{1}{K}}\left(\frac{P_2}{P_1^2}\right)}{2\left[1-\left(\frac{P_2}{P_1}\right)^{\frac{K-1}{K}}\right]}\right\}^2 B_{P_1}^2 + \left\{\frac{1}{KP_2} - \frac{\left(\frac{K-1}{K}\right)\left(\frac{P_2}{P_1}\right)^{-\frac{1}{K}}\left(\frac{1}{P_1}\right)}{2\left[1-\left(\frac{P_2}{P_1}\right)^{\frac{K-1}{K}}\right]}\right\}^2 B_{P_2}^2} \quad \text{(VI-5)}$$

Note that each term in Eqs. (VI-4) and (VI-5) has been divided by W to simplify the equations. The following list of partial derivatives is given as an aid for the analyst:

$$\frac{\partial W}{\partial d} = \frac{\pi}{2} d C_d F_a \left(\frac{P_1}{\sqrt{T_2}}\right)\left(\frac{P_2}{P_1}\right)^{\frac{1}{K}} \sqrt{\frac{K}{K-1}\left[1-\left(\frac{P_2}{P_1}\right)^{\frac{K-1}{K}}\right]\frac{2gM}{ZR}}$$

$$\frac{\frac{\partial W}{\partial d}}{W} = \frac{2}{d}$$

$$\frac{\partial W}{\partial C_d} = \frac{\pi}{4} d^2 F_a \left(\frac{P_1}{\sqrt{T_1}}\right)\left(\frac{P_2}{P_1}\right)^{\frac{1}{K}} \sqrt{\frac{K}{K-1}\left[1-\left(\frac{P_2}{P_1}\right)^{\frac{K-1}{K}}\right]\frac{2gM}{ZR}}$$

$$\frac{\frac{\partial W}{\partial C_d}}{W} = \frac{1}{C_d}$$

$$\frac{\partial W}{\partial T_1} = -\frac{\pi}{8} d^2 F_a \left(\frac{P_1}{T_1\sqrt{T_1}}\right)\left(\frac{P_2}{P_1}\right)^{\frac{1}{K}} \sqrt{\frac{K}{K-1}\left[1-\left(\frac{P_2}{P_1}\right)^{\frac{K-1}{K}}\right]\frac{2gM}{ZR}}$$

$$\frac{\frac{\partial W}{\partial T_1}}{W} = -\frac{1}{2T_1}$$

$$\frac{\partial W}{\partial P_2} = \frac{\pi}{4} d^2 C_d F_a \sqrt{\frac{2gM}{T_1 ZR}}\left[\frac{-1}{2\sqrt{\frac{K}{K-1}\left[1-\left(\frac{P_2}{P_1}\right)^{\frac{K-1}{K}}\right]}} + \frac{1}{K}\left(\frac{P_2}{P_1}\right)^{\frac{1-K}{K}} \sqrt{\frac{K}{K-1}\left(1-\left(\frac{P_2}{P_1}\right)^{\frac{K-1}{K}}\right)}\right]$$

$$\frac{\frac{\partial W}{\partial P_2}}{W} = \frac{1}{KP_2} - \frac{\frac{K-1}{K}\left(\frac{P_2}{P_1}\right)^{\frac{-1}{K}}\frac{1}{P_1}}{2\left[1-\left(\frac{P_2}{P_1}\right)^{\frac{K-1}{K}}\right]}$$

$$\frac{\partial W}{\partial P_2} = \frac{\pi}{4} d^2 C_d F_a \sqrt{\frac{2gM}{T_1 ZR}}\left[\frac{P}{2P_1\sqrt{\frac{K}{K-1}\left[1-\left(\frac{P_2}{P_1}\right)^{\frac{K-1}{K}}\right]}} + \left(\frac{K-1}{K}\right)\left(\frac{P_2}{P_1}\right)^{\frac{1}{K}} \sqrt{\frac{K}{K-1}\left(1-\left(\frac{P_2}{P_1}\right)^{\frac{K-1}{K}}\right)}\right]$$

$$\frac{\frac{\partial W}{\partial P_1}}{W} = \frac{K-1}{KP_1} + \frac{\left(\frac{K-1}{K}\right)\left(\frac{P_2}{P_1}\right)^{\frac{-1}{K}}\left(\frac{P_2}{P_1^2}\right)}{2\left[1-\left(\frac{P_2}{P_1}\right)^{\frac{K-1}{K}}\right]}$$

In Eqs. (VI-4) and (VI-5), it is assumed that P_1 and p_2 are independent measurements on two different pressure transducers. If P_1 is measured and a ΔP equal to $(P_1 - p_2)$ is measured, Eqs. (VI-4) and (VI-5) reduce to

$$S_w = \pm W \sqrt{\left(\frac{1}{C_d} S_{C_d}\right)^2 + \left(\frac{2}{d} S_d\right)^2 + \left(\frac{-1}{2T_1} S_{T_1}\right)^2 + \left(\frac{\partial W/\partial P_1}{W} S_{p_1}\right)^2 + \left(\frac{\partial W/\partial \Delta P}{W} S_{\Delta P}\right)^2} \tag{VI-6}$$

$$B_w = \pm W \sqrt{\left(\frac{1}{C_d} B_{C_d}\right)^2 + \left(\frac{2}{d} B_d\right)^2 + \left(\frac{-1}{2T_1} B_{T_1}\right)^2 + \left(\frac{\partial W/\partial P_1}{W} B_{p_1}\right)^2 + \left(\frac{\partial W/\partial \Delta P}{W} B_{\Delta P}\right)^2} \tag{VI-7}$$

where

$$\frac{\partial W/\partial P_1}{W} = \frac{\Delta P}{K P_1^2 \left(1 - \frac{\Delta P}{P_1}\right)} - \frac{\left(\frac{K-1}{K}\right)\Delta P}{2P_1^2 \left(1 - \frac{\Delta P}{P_1}\right)^{\frac{1}{K}} \left[1 - \left(1 - \frac{\Delta P}{P_1}\right)^{\frac{K-1}{K}}\right]} \tag{VI-8}$$

$$\frac{\partial W/\partial \Delta P}{W} = \frac{-1}{K P_1 \left(1 - \frac{\Delta P}{P_1}\right)} + \frac{\frac{K-1}{K}}{2P_1 \left(1 - \frac{\Delta P}{P_1}\right)^{\frac{1}{K}} \left[1 - \left(1 - \frac{\Delta P}{P_1}\right)^{\frac{K-1}{K}}\right]} \tag{VI-9}$$

Several recommended practices are available for designs of subsonic venturis and flow nozzles. In this document, the ASME recommended practice contained in "Fluid Meters, Their Theory and Applications," (6th Edition, 1971) will be used. When using a specific design practice, extreme care must be exercised to ensure that not only the meter design, but also the measuring systems, meet the recommended practice, since the tabulated values of meter constants apply only to a specific combination of meter design plus measurement technique.

The adiabatic isentropic equation for flow of an ideal-compressible fluid through a venturi or flow nozzle is (from the cited ASME reference)

$$W_t = a \left[2g \frac{(p_1 - p_2)\gamma_1 \, r^{\frac{2}{k}} \left(\frac{k}{k-1}\right) \left(\frac{1-r^{\frac{k-1}{k}}}{1-r}\right)}{1 - \beta^4 r^{\frac{2}{k}}} \right]^{\frac{1}{2}} \tag{VI-10}$$

where W_t = theoretical weight rate of flow

a = meter throat area

p_1 = upstream static pressure

p_2 = downstream static pressure

γ_1 = specific weight of gas at station 1

r = pressure ratio, p_2/p_1

k = ratio of specific heats, c_p/c_v

β = ratio of throat diameter to pipe diameter

g = dimensional constant

For simplification, an adiabatic expansion factor (Ya) is defined as

$$Ya = \left[r^{\frac{2}{k}} \left(\frac{k}{k-1} \right) \left(\frac{1-r^{\frac{k-1}{k}}}{1-r} \right) \left(\frac{1-\beta^4}{1-\beta^4 r^{\frac{2}{k}}} \right) \right]^{\frac{1}{2}} \tag{VI-11}$$

Values of Ya are graphically presented in the ASME reference. Substituting Eq. (VI-11) into Eq. (VI-10) results in

$$W_t = a(Ya) \sqrt{\frac{2g\gamma_1(p_1-p_2)}{1-\beta^4}} \tag{VI-12}$$

Applying the meter discharge coefficient (C) to correct indicated flow to actual flow and the area factor (F_a) to account for thermal expansion of the meter throat area and rearranging the terms of Eq. (VI-12) result in the following expression:

$$W_t = \frac{\pi d^2}{4} \frac{C}{\sqrt{1-\beta^4}} Ya\, F_a \sqrt{2g\gamma_1(p_1-p_2)} \tag{VI-13}$$

where d = meter throat diameter.

Values of venturi and flow nozzle discharge coefficient are graphically presented in the ASME reference.

Expressing the gas specific weight (γ) in terms of measurable parameters of pressure and temperature, accounting for gas composition, and utilizing the gas compressibility factor (Z) to account for deviations of real gases from an ideal gas give

$$\gamma_1 = \frac{p_1 M}{ZRT_1} \tag{VI-14}$$

where p_1 = upstream static pressure

M = gas molecular weight

Z = gas compressibility factor

R = universal gas constant

T_1 = gas temperature, corrected for losses and probe recovery factor

Substituting into Eq. (VI-13) and utilizing nomenclature consistent with that used in Eq. (VI-3) result in

$$W = \frac{\pi d^2}{4} \frac{C_d}{\sqrt{1-\beta^4}} Y a F_a \left[(p_1-p_2) \frac{p_1}{T_1} \frac{2gM}{ZR}\right]^{\frac{1}{2}} \qquad \text{(VI-15)}$$

6.2.1.2 Orifices

As with venturis and nozzles, several recommended practices exist for orifice designs. A typical orifice, with measuring stations, is shown schematically in Fig. VI-2.

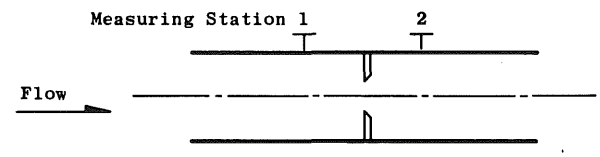

Fig. VI-2 Schematic of Typical Orifice with Measuring Stations

The ASME recommended practive for thin-plate orifice design contained in "Fluid Meters, Their Theory and Applications," (6th Edition, 1971) will be utilized in this section. Care must again be exercised to ensure that not only the orifice design requirements are met, but also the recommended practice for pressure and temperature measurements are followed, since, for thin-plate, square-edged orifices, values for both the meter expansion factor and the discharge coefficient have been empirically determined for the specified meter design and pressure measurement system.

Flow through an orifice may be calculated by use of Eq. (VI-15), using appropriate values of discharge coefficient (C_d) and expansion factor (Y). When metering gases with venturi tubes or flow nozzles, the expansion which accompanies the change in pressure takes place in an axial direction only, because of the confining walls of these meters, and the adiabatic expansion factor (Ya) compensates for this unidirectional expansion. With a thin-plate orifice, there are no confining walls, and the expansion takes place both radially and axially. To account for this multidirectional expansion, an empirical expansion factor (Y_1) is used. Values of Y_1 are graphically presented in the ASME reference. For all the referenced pressure tap locations except pipe taps, the empirical expression for the orifice expansion factor is

$$Y_1 = 1 - \left(0.41 + 0.35\beta^4\right)\left(\frac{p_1-p_2}{p_1}\right)\frac{1}{K} \qquad \text{(VI-16)}$$

where β = ratio of orifice diameter to pipe diameter

p_1 = upstream static pressure

p_2 = downstream static pressure

k = ratio of gas specific heats

Error equations for orifices when upstream static pressure is measured on an absolute transducer and ΔP is measured on a differential transducer are as follows (Errors associated with values of π, β, Ya, F_a, g, μ, Z, and R in Eq. (VI-15) are assumed negligible in the following calculations.):

$$S_W = W\sqrt{\left(\frac{2S_d}{d}\right)^2 + \left(\frac{S_{C_d}}{C_d}\right)^2 + \left(\frac{-S_{T_1}}{2T_1}\right)^2 + \left(\frac{3S_{\Delta p}}{2\Delta p}\right)^2 + \left(\frac{-S_{p_1}}{2p_1}\right)^2} \qquad \text{(VI-17)}$$

$$B_W = W\sqrt{\left(\frac{2B_d}{d}\right)^2 + \left(\frac{B_{C_d}}{C_d}\right)^2 + \left(\frac{-B_{T_1}}{2T_1}\right)^2 + \left(\frac{3B_{\Delta p}}{2\Delta p}\right)^2 + \left(\frac{-B_{p_1}}{2p_1}\right)^2} \qquad \text{(VI-18)}$$

The Welch-Satterthwaite formula must be used to determine overall degrees of freedom associated with S_W. If the degrees of freedom are greater than 30 for each term in the flow error equation, the overall df will be greater than 30, and $t_{95} = 2$ is used in the determination of flow uncertainty:

$$U_W = \pm(B_W + 2S_W)$$

6.2.2 Critical Venturi Flowmeters

Figure VI-3 schematically depicts a representative critical venturi flowmeter installed in the inlet ducting upstream of a turbine engine. Measuring station designations used in this section represent AEDC standard practice.

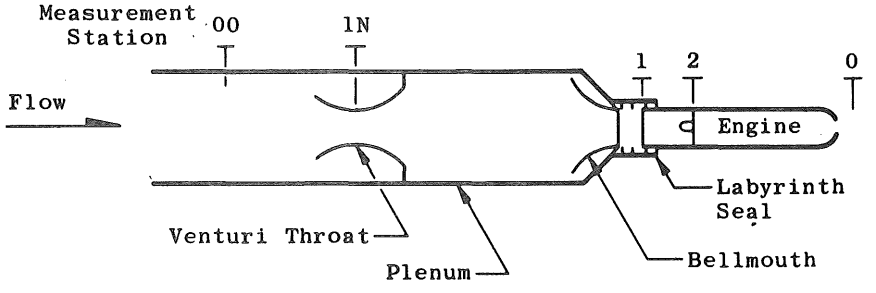

Fig. VI-3 Schematic of Critical Venturi Flowmeter Installation Upstream of a Turbine Engine

When a venturi flowmeter is operated at critical pressure ratios, i.e., p_{1N}/P_{oo} is a minimum, the flow rate through the venturi is a function of the upstream conditions only and may be calculated from

$$W_{1N} = \frac{\pi d^2}{4} C_d F_a C^* \frac{P_{oo}}{\sqrt{T_{oo}}} \tag{VI-19}$$

where

W_{1N} = airflow rate through venturi, lbm/sec

d = venturi throat diameter, in.

C_d = meter discharge coefficient

F_a = meter thermal expansion correction factor

P_{oo} = upstream total pressure, lbf/in.^{2}

T_{oo} = upstream total temperature, °R

C^* = critical flow factor,

$$= \left[\left(\frac{2}{K+1}\right)^{\frac{K+1}{K-1}} \left(\frac{KgM}{ZR}\right)\right]^{\frac{1}{2}}, \frac{\text{lbm}-\sqrt{°R}}{\text{lbf}-\text{sec}} \tag{VI-20}$$

K = ratio of specific heats evaluated at T_{oo} (unitless)

g = dimensional constant, 32.174 lbm-ft/lbf-sec^2

R = universal gas constant, 1545 ft-lbf/lbm-mol °R

Z = compressibility factor (unitless)

M = molecular weight of flowing gas, lbm/lbm-mol

The indicated upstream total temperature measurement must be corrected for thermal losses and probe recovery factor as discussed in Section 5.3.2.1.

For a venturi designed according to the specifications set forth in ASME Paper No. 61-WA-211, the value of C_d may be theoretically determined as described in the referenced paper.

Equations for determination of precision index (S) and bias limit (B) are as follows (Errors associated with values of π, F_a, and C^* in Eq. (VI-19) are assumed negligible in the following calculations.):

$$S_{W_{1N}} = \pm W_{1N} \sqrt{\left(\frac{1}{C_d} S_{C_d}\right)^2 + \left(\frac{2}{d^2} S_d\right)^2 + \left(\frac{-1}{2T_{oo}} S_{T_{oo}}\right)^2 + \left(\frac{1}{P_{oo}} S_{P_{oo}}\right)^2} \tag{VI-21}$$

and

$$B_{W_{1N}} = \pm W_{1N} \sqrt{\left(\frac{1}{C_d} B_{C_d}\right)^2 + \left(\frac{2}{d^2} B_d\right)^2 + \left(\frac{-1}{2T_{oo}} B_{T_{oo}}\right)^2 + \left(\frac{1}{P_{oo}} B_{P_{oo}}\right)^2} \tag{VI-22}$$

Again the degrees of freedom will be determined by the Welch-Satterthwaite formula. If the degrees of freedom are greater than 30 for each error term, then t_{95} can be assumed equal to 2.

The reader is cautioned about two pitfalls common to gas flow measurement with critical flowmeters.

1. Mass flow rate is a function of upstream total pressure. Therefore, approach velocity corrections must be made if wall static pressure measurements are used. As a rule, if the velocity is maintained at 50 ft/sec or less, use of the isentropic flow relations to obtain total pressure from the measurement of wall static pressure will result in negligible errors in flow rate determination.

2. It is essential that the choked condition be maintained if Eq. (VI-19) is used to calculate airflow. A critical flowmeter can, however, be operated subcritically; in this event, the flow rate calculation method is identical to that shown by Eq. (VI-3) using the venturi throat static pressure (p_{1N}) (Fig. VI-3) for the p_2 term of Eq. (VI-3). However, the uncertainty of the airflow measurement will be slightly greater than for the case of critical operation of the venturi.

6.2.3 Calibration Techniques

Venturi, nozzle, and orifice calibrations are performed to determine the discharge coefficient.

6.2.3.1 Calibration by Calculation

Discharge coefficients for critical flow venturis and nozzles can be calculated with an accuracy greater than that for the experimentally determined C_d provided that the design criteria and considerations discussed in Section 6.3.1.1 are adhered to. In many instances, determination of C_d by calculation is so accurate that critical venturis are considered primary standards when associated pressure and temperature measurements are traceable to the NBS.

6.2.3.2 Experimental Calibration

Flowmeters for which the discharge coefficient cannot be accurately calculated may be calibrated experimentally by one of three ways:

1. Flow in series with a critical venturi for which the C_d can be accurately calculated.

2. Flow a known volume of liquid through the meter at fixed temperature and pressure and appeal to dynamic similarity to translate the results to compressible flow.

3. Traverse the meter with a pitot static probe to define the flow profile. The results of a complete traverse, including boundary layer measurements, constitute a flow profile which will yield total flow when integration beneath the profile is performed. Definition of the relationship between total flow and measured pressures and temperature constitutes a calibration.

6.2.3.3 Calibration by Fabrication

The ASME has determined the discharge coefficients for a variety of flowmeters including venturis, nozzles, and orifices. The ASME discharge coefficients have been published along with C_d error tolerances in the ASME publication "Fluid Meters, Their Theory and Applications," (6th Edition, 1971). Care must be taken to ensure that meter design and measurement systems conform to those specified by the ASME.

If a flowmeter does not comply with ASME design tolerances, ASME discharge coefficient error tolerances do not apply, and calibration is required for flow measurement uncertainty analysis.

6.3 ELEMENTAL ERROR SOURCES

6.3.1 Discharge Coefficient

Discharge coefficient (C_d) errors of concern are primarily biases, and the sign is unknown, i.e., the error is just as likely to be in one direction as the other. The error distribution will probably be near normal (Fig. VI-4).

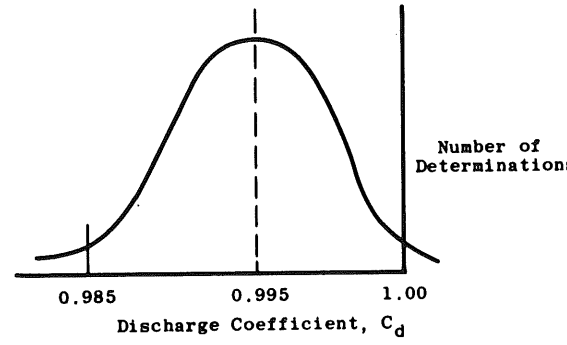

Fig. VI-4 Discharge Coefficient Error Distribution

The values of C_d may exceed one because of the combination of measurement error and calculation technique and the assumptions utilized in determining the value of discharge coefficient. The best value of C_d to use for data reduction is:

$$\bar{C}_d = \frac{\sum_{i=1}^{N} C_{d_i}}{N} \qquad \text{(VI-23)}$$

and

$$S_{C_d} = \pm \sqrt{\frac{\sum_{i=1}^{N} (C_{d_i} - \bar{C}_d)^2}{N-1}} \qquad \text{(VI-24)}$$

6.3.1.1 Calculated C_d

Discharge coefficients for critical flow venturis may be calculated provided the venturi design conforms to criteria set forth in "A Theoretical Method of Determining Discharge Coefficients for Venturis Operating at Critical Flow Conditions," by Robert E. Smith, Jr., and Roy J. Matz, Journal of Basic Engineering, December 1962, page 434, ASME Paper No. 61-WA-211. Venturi design considerations for inlet contour, inlet to throat area ratio, and throat Reynolds number are given in the above paper. Errors of less than ±0.1 percent will

result from assumptions made in the calculation. This error is considered an unknown bias and is relatively small as compared with errors common to other sources.

6.3.1.2 Experimentally Determined C_d

Critical flowmeters which do not fulfill the conditions set forth in Section 6.3.1.1 must be calibrated experimentally to ensure maximum accuracy in C_d determination.

Three common methods of experimental calibration are:

1. Comparison with a critical flow standard.
2. Calibration by traversing the flowmeter.
3. Liquid calibration.

6.3.1.2.1 Comparison with a Standard Flowmeter

Venturis, nozzles, and orifices, sonic or subsonic, may be calibrated in series with a critical flow venturi of known C_d.

For the purpose of illustration, assume two choked venturis in series (Fig. VI-5) and further assume that the inlet flow to both venturis satisfies the criteria set forth in the ASME paper referenced in Section 6.3.1.1.

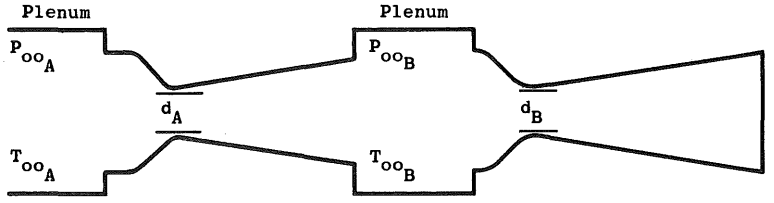

Fig. VI-5 Calibration by Comparison

Assume that the C_d for venturi A has been calculated with a bias no greater than ±0.1 percent.

The mass flow rate through venturi A is

$$W_A = \left(\frac{\pi d_A^2}{4}\right) C_{d_A} F_{a_A} C^* \left(\frac{P_{oo_A}}{\sqrt{T_{oo_A}}}\right) \qquad \text{(VI-25)}$$

The mass flow rate through venturi B is

$$W_B = \left(\frac{\pi d_B^2}{4}\right) C_{d_B} F_{a_B} C^* \left(\frac{P_{oo_B}}{\sqrt{T_{oo_B}}}\right) \qquad \text{(VI-26)}$$

In series, $W_A = W_B$; therefore, the two equations may be set equal to each other and solved for the product $d_B{}^2 C_{d_B}$. Simplification results from the assumption that the critical flow factor (C*) is equal within the range of conditions to be encountered for each venturi. However, if d_B is much greater than d_A, significant real gas effects may be experienced in venturi A. Monitoring the temperature of each meter will allow thermal expansion corrections, and

$$d_B{}^2 C_{d_B} = d_A{}^2 C_{d_A} \left(\frac{F_{a_A}}{F_{a_B}}\right)\left(\frac{P_{oo_A}}{P_{oo_B}}\right)\sqrt{\frac{T_{oo_B}}{T_{oo_A}}} \qquad \text{(VI-27)}$$

Expanding Eq. (VI-27) in a Taylor's series results in Eqs. (VI-28) and (VI-29) for the precision index and bias limit, respectively. Errors associated with values of F_{a_A} and F_{a_B} are assumed negligible in the following calculations:

$$S_{d_B{}^2 C_{d_B}} = \pm d_B{}^2 C_{d_B} \sqrt{\left(\frac{1}{C_{d_A}} S_{C_{d_A}}\right)^2 + \left(\frac{2}{d_A} S_{d_A}\right)^2 + \left(\frac{1}{P_{oo_A}} S_{P_{oo_A}}\right)^2 + \left(\frac{1}{P_{oo_B}} S_{P_{oo_B}}\right)^2 + \left(\frac{-1}{2T_{oo_A}} S_{T_{oo_A}}\right)^2 + \left(\frac{-1}{2T_{oo_B}} S_{T_{oo_B}}\right)^2} \qquad \text{(VI-28)}$$

$$B_{d_B{}^2 C_{d_B}} = \pm d_B{}^2 C_{d_B} \sqrt{\left(\frac{1}{C_{d_A}} B_{C_{d_A}}\right)^2 + \left(\frac{2}{d_A} B_{d_A}\right)^2 + \left(\frac{1}{P_{oo_A}} B_{P_{oo_A}}\right)^2 + \left(\frac{1}{P_{oo_B}} B_{P_{oo_B}}\right)^2 + \left(\frac{-1}{2T_{oo_A}} B_{T_{oo_A}}\right)^2 + \left(\frac{-1}{2T_{oo_B}} B_{T_{oo_B}}\right)^2} \qquad \text{(VI-29)}$$

The following example will indicate the effect of typical errors on discharge coefficient determination by comparison. Table XV lists the elemental errors assumed for this example.

Table XV Elemental Errors for Calibration by Comparison

Error Source	Nominal	Precision Error, percent	Bias Error, percent	Degrees of Freedom
C_{d_A}	0.995	0	±0.1	> 30
d_A	10.0 in.	±0.01	±0.01	
P_{oo_A}	100. psi	±0.1	±0.15	
P_{oo_B}	100. psi	±0.1	±0.15	
T_{oo_A}	600. °R	±0.16	±0.08	
T_{oo_B}	600. °R	±0.16	±0.08	

Substituting these values into Eq. (VI-28) for precision index and Eq. (VI-29) for bias limit gives

$$\frac{S_{d_B{}^2 C_{d_B}}}{d_B{}^2 C_{d_B}} = \pm\sqrt{(0.00)^2 + 4(0.01)^2 + (0.1)^2 + (0.1)^2 + \tfrac{1}{4}(0.16)^2 + \tfrac{1}{4}(0.16)^2}$$

$$= \pm 0.18 \text{ percent}$$

$$\frac{B_{d_B{}^2 C_{d_B}}}{d_B{}^2 C_{d_B}} = \pm\sqrt{(0.1)^2 + 4(0.01)^2 + (0.15)^2 + (0.15)^2 + \tfrac{1}{4}(0.08)^2 + \tfrac{1}{4}(0.08)^2}$$

$$= \pm 0.24 \text{ percent}$$

Since each of the elemental degrees of freedom is greater than 30, the overall degrees of freedom are also greater than 30; $t_{95} = 2.0$, and

$$U = \pm[0.24 + 2(0.18)]$$

$$= \pm 0.60 \text{ percent}$$

Obviously, determination of discharge coefficients by this method is less accurate than the same C_d if evaluated by calculation.

Note that the error in discharge coefficient evaluation is but one of several elemental sources of error in the calculation of airflow.

6.3.1.2.2 Calibration by Traverse

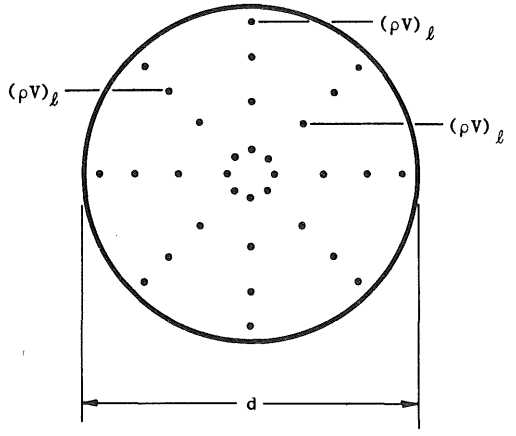

Fig. VI-6 Flowmeter Throat Traverse

Flowmeter discharge coefficients may also be determined by traversing the meter throat with a pitot static probe to define the meter throat mass-velocity profile. It is recommended to traverse several meter throat diameters, equally spaced circumferentially, to better define the mass-velocity profile. The result of a typical four-diameter traverse is an array of gas stream measurements as shown in Fig. VI-6. For convenience the measurement points on each diameter should be located at the centers of equal area annuli.

For the general case of airflow measurement, the local mass-velocity is a function of both radial and circumferential position:

$$(\rho V)_\ell = f(r,\theta) \tag{VI-30}$$

and

$$W_a = \int_0^{2\pi} \int_0^r (\rho V)_\ell \, r\,dr\,d\theta \tag{VI-31}$$

where W_a = total mass flow rate through meter throat

$(\rho V)_\ell$ = local value of mass-velocity

r = radial location of local measurement

θ = circumferential location of local measurement

The $(\rho V)_\ell$ term may be obtained from the traverse data by solving Eq. (VI-3) for flow rate per unit area and using the local values of throat total and static pressure and total temperature:

$$(\rho V)_\ell = \left(\frac{W}{A}\right)_\ell = \left(\frac{p}{\sqrt{T}}\right)_\ell \left(\frac{p}{P}\right)_\ell^{\frac{1}{K}} \sqrt{\left(\frac{K}{K-1}\right)\left[1 - \left(\frac{p}{P}\right)_\ell^{\frac{K-1}{K}}\right]\frac{2gM}{ZR}} \qquad \text{(VI-32)}$$

The effect of a variation of $(\rho V)_\ell$ with circumferential position in the nozzle throat may be approximated by averaging the local mass-velocity measurements at particular radial positions (r) common to each diameter traversed. An average mass-velocity profile can then be developed as shown in Fig. VI-7. Care should be exercised to ensure that boundary layer profiles are sufficiently defined.

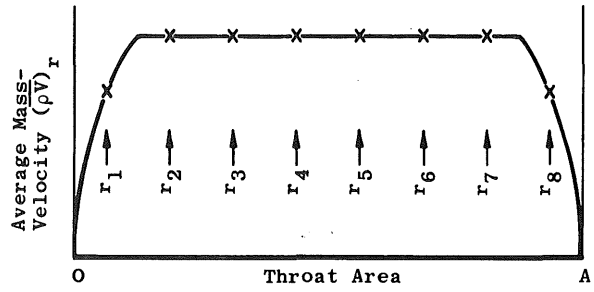

Fig. VI-7 Flat Mass-Velocity Profile

Integration beneath the profile defined by the average mass-velocities provides a measure of total mass flow rate:

$$W_t = \int_o^A (\overline{\rho V})_r \, dA \qquad \text{(VI-33)}$$

where

$$(\overline{\rho V})_r = \frac{\sum_{\theta=1}^{\theta=N} \left[(\rho V)_\ell\right]_{\theta,r}}{N} \qquad \text{(VI-34)}$$

N = number of equally spaced circumferential measurements taken at each radial position

dA = incremental flow area over which each average mass-velocity $(\overline{\rho V})_r$ is effective

Mass-velocity profile errors are dominated by two sources: profile distortion and instrumentation errors. If the profile is distorted (Fig. VI-8) the cause of distortion should be diagnosed and corrected, if possible. With a distorted profile, a larger number of diameter traverses and a greater number of points along each diameter are recommended to precisely define the existing profile.

Whether the profile is distorted or undistorted, a valid approximation to the total flow given by Eq. (VI-33) may be obtained by summing the flows calculated for each incremental ring area (A_R) as shown below:

$$W_t = \sum_{R=1}^{R=i} W_R = \sum_{R=1}^{R=i} (\overline{\rho V})_r A_R \qquad \text{(VI-35)}$$

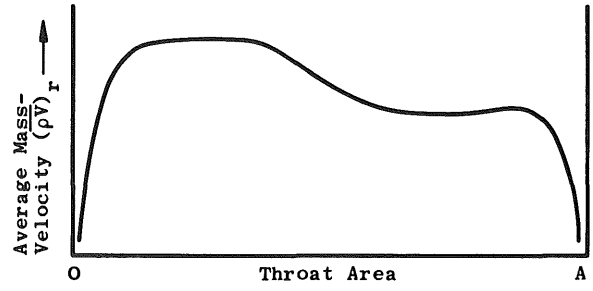

Fig. VI-8 Distorted Mass-Velocity Profile

where

W_t = total mass flow rate through meter throat

W_R = mass flow rate through each incremental ring

$(\overline{\rho V})_r$ = average mass-velocity in each incremental ring

A_R = area of each incremental ring

i = number of incremental rings

The precision index for each incremental flow is evaluated by expansion of Eq. (VI-32) in the Taylor's series:

$$S_{W_R} = \pm \sqrt{\left[(\overline{\rho V})_r S_{A_R}\right]^2 + \left[A_R S_{(\overline{\rho V})_r}\right]^2} \qquad \text{(VI-36)}$$

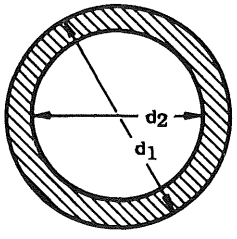

Fig VI-9 Shaded Area Calculated as a Function of d_1 and d_2

The precision index $S_{(\overline{\rho V})_r}$ may be obtained as previously shown in Eq. (VI-4) with elimination of the meter throat area terms (S_{C_d} and S_d).

The precision index S_{A_R} is dependent on the repeatability of the traverse probe radial position indication d_1 and d_2. Figure VI-9 illustrates this dependence.

$$A = \frac{\pi d_1^2}{4} - \frac{\pi d_2^2}{4} = \pi \frac{(d_1^2 - d_2^2)}{4} \qquad \text{(VI-37)}$$

Taking the partials with respect to the probe radial locations gives

$$\frac{\partial A}{\partial d_1} = \frac{\pi d_1}{2} \quad \text{and} \quad \frac{\partial A}{\partial d_2} = \frac{-\pi d_2}{2}$$

$$S_{A_R} = \sqrt{\left(\frac{\partial A}{\partial A_1} S_{d_1}\right)^2 + \left(\frac{\partial A}{\partial d_2} S_{d_2}\right)^2} = \sqrt{\left(\frac{\pi d_1}{2} S_{d_1}\right)^2 + \left(\frac{-\pi d_2}{2} S_{d_2}\right)^2} \qquad \text{(VI-38)}$$

where S_{d_1} and S_{d_2} are the precision indices for the respective probe radial locations.

The precision index for the total mass flow rate determination is then

$$S_W = \pm \sqrt{\sum_{R=1}^{R=i} S_{W_R}^2} \qquad \text{(VI-39)}$$

The airflow bias limit B_{W_R} cannot be calculated directly from the traverse data. This error is due entirely to elemental bias errors imposed by the instrumentation and may be estimated by the use of Eq. (VI-5) and dropping the terms for diameter (d) and discharge coefficient (C_d).

Solving Eq. (VI-19) for C_d in the case of a critical venturi results in

$$C_d = \frac{4 W_{1N} \sqrt{T_{oo}}}{\pi d^2 F_a C^* P_{oo}} \tag{VI-40}$$

Expanding Eq. (VI-40) in the Taylor's series results in Eq. (VI-41) and (VI-42) for the precision index and bias limit, respectively. Errors associated with values of π, F_a, and C^* are assumed negligible in the following calculations:

$$S_{C_d} = \pm C_d \sqrt{\left(\frac{\partial C_d}{\partial W_{1N}} S_{W_{1N}}\right)^2 + \left(\frac{\partial C_d}{\partial d} S_d\right)^2 + \left(\frac{\partial C_d}{\partial T_{oo}} S_{T_{oo}}\right)^2 + \left(\frac{\partial C_d}{\partial P_{oo}} S_{P_{oo}}\right)^2} \tag{VI-41}$$

$$B_{C_d} = \pm C_d \sqrt{\frac{\left(\frac{\partial C_d}{\partial W_{1N}} B_{W_{1N}}\right)^2 + \left(\frac{\partial C_d}{\partial d} B_d\right)^2 + \left(\frac{\partial C_d}{\partial T_{oo}} B_{T_{oo}}\right)^2 + \left(\frac{\partial C_d}{\partial P_{oo}} B_{P_{oo}}\right)^2}{C_d^2}} \tag{VI-42}$$

where

$$\frac{\frac{\partial C_d}{\partial W_{1N}}}{C_d} = \frac{1}{W_{1N}}; \quad \frac{\frac{\partial C_d}{\partial P_{oo}}}{C_d} = -\frac{1}{P_{oo}}; \quad \frac{\frac{\partial C_d}{\partial T_{oo}}}{C_d} = \frac{1}{2T_{oo}}; \quad \frac{\frac{\partial C_d}{\partial d}}{C_d} = -\frac{2}{d}$$

The degrees of freedom (df) associated with S_{C_d} will probably be greater than thirty so that t_{95} will equal 2.0. If this is not obvious then df must be calculated using the Welch-Satterthwaite formula.

Equation (VI-3) may be solved in similar fashion for the C_d of subsonic meters. Expansion in the Taylor's series will result in equations for the precision index and bias limits for subsonic flowmeters.

6.3.1.2.3 Calibration by Liquid

Venturi, nozzle, and orifice discharge coefficients may be evaluated by liquid calibration. Methods used are fully analogous to those detailed in Section IV. For this reason, the treatment of errors involved with this calibration technique will not be discussed here. However, the reader is warned that, when this method of calibration is employed, published data on expansion factors must be used with the associated errors which will be reflected in the discharge coefficient. Further, an appeal to dynamic similarity through the Reynolds analogy is required, and quantitative assessment of the uncertainty of the similarity is unavoidable.

6.3.1.2.4 Calibration by Fabrication

The ASME has cataloged discharge coefficients for a variety of venturis, nozzles, and orifices. The cataloged values are the result of an extremely large number of actual calibrations over a period of many years. The results of this experimental work is documented in the ASME publication, "Fluid Meters, Their Theory and Applications," (6th Edition, 1971). Discharge coefficients cataloged in this ASME reference are applicable to all flowmeters which conform to this specification. Detailed engineering comparisons must be exercised to ensure that the flowmeter conforms to one of the groups tested before using the tabulated values for discharge coefficients and error tolerances.

A later ASME publication, "A Statistical Approach to the Prediction of Discharge Coefficients for Concentric Orifice Plates," by R. B. Dowdell and Yu-Lin Chen, Paper No. 69-WA/FM-6, may be useful in determining which C_d to use and in evaluating errors associated with it.

When an independent flowmeter is used to determine flow rates during a calibration for C_d, dimensional errors are effectively calibrated out. However, when C_d is calculated or taken from the ASME reference, errors in the measurement of pipe and throat diameters will be reflected as bias errors in the flow measurement.

Dimensional errors in large venturis, nozzles, and orifices are generally negligible. For example, an error of 0.001 in. in the throat diameter of a 5-in. nozzle will result in a 0.04 percent bias in airflow.

6.3.2 Non-Ideal Gas Behavior and Variation in Gas Compositions

The equations given in preceding sections for calculation of gas flow rate (Eqs. (VI-3), (VI-15), (VI-19)) are specifically valid for any calorically perfect gas. Non-ideal gas behavior and changes in gas composition are accounted for by selection of the proper values for compressibility factor (Z), molecular weight (M), and ratio of specific heats (K) for the specific gas flow being measured.

For the specific case of airflow measurement, the main factor contributing to variation of composition is the moisture content of the air. Though small, the effect of a change in air density due to water vapor on airflow measurement should be evaluated in every measurement process.

6.3.3 Thermal Expansion Correction Factor

The thermal expansion correction factor (F_a) corrects for changes in throat area caused by changes in flowmeter temperature.

For steels, a 30°F flowmeter temperature difference, between the time of a test and the time of calibration, will introduce an airflow error of 0.06 percent if no correction is made. If flowmeter skin temperature is determined to within ±5°F and the correction factor applied, the resulting error in airflow will be negligible.

6.3.4 Ratio of Specific Heats and Compressibility Factor

The ratio of specific heat (K) at constant pressure to specific heat at constant volume (cp/cv = K) and the compressibility factor (Z) are functions of gas stream composition, pressure, and temperature and may be obtained from gas tables. When used in the equations provided for calculation of flow rate, the value of K should be evaluated at upstream stagnation conditions, whereas the value of Z must be evaluated at the throat static conditions.

When values of K and Z are obtained at the stated pressure and temperature conditions, airflow errors resulting from errors in K and Z will be negligible.

6.3.5 Measurement Systems

Errors associated with pressure and temperature measurements and their respective probe recovery factors are described in Section V.

6.4 PROPAGATION OF ERROR TO AIRFLOW

6.4.1 Critical-Flow Venturi

For an example of propagation of errors in airflow measurement using a critical-flow venturi, consider a venturi (designed according to criteria presented in ASME Paper No. 61-WA-211) having a throat diameter of 21.81 in. operating with dry air at an upstream total pressure of 12.78 psia and an upstream total temperature of 478.7°R. Equation (VI-19), repeated below, is the flow equation to be analyzed:

$$W_{1N} = \frac{\pi d^2}{4} C_d F_a \sqrt{\left(\frac{2}{K+1}\right)^{\frac{K+1}{K-1}} \left(\frac{KgM}{ZR}\right)} \frac{P_{oo}}{\sqrt{T_{oo}}}$$

Assume, for this example, that the theoretical discharge coefficient (C_d) has been determined, using the procedures outlined in ASME Paper No. 61-WA-211, to be 0.995. Further assume that the thermal expansion correction factor (F_a) and the compressibility factor (Z) are equal to 1.0. Table XVI lists nominal values, bias limits, precision indices, and degrees of freedom for each error source in the above equation.

Note that, in the following table, airflow errors resulting from errors in F_a, Z, K, g, M, and R are considered negligible.

From Eq. (VI-19), airflow is calculated as

$$W_{1N} = \frac{3.142}{4} (21.81)^2 \times 0.995 \times 1.0 \sqrt{\left(\frac{2}{2.401}\right)^{\frac{2.401}{0.401}} \left(\frac{1.401 \times 28.95 \times 32.174}{1545}\right)} \times \frac{12.78}{\sqrt{478.7}}$$

$$= 115.5 \text{ lbm/sec}$$

Table XVI Airflow Measurement Error Source

Error Source	Nominal Value	Bias Limit	Precision Index	df	Uncertainty
P_{oo}	12.78 psia	±0.04 psia	±0.02 psia	15	±0.08 psia
T_{oo}	478.7°R	±1.8°R	±0.20°R	100	±2.2°R
d	21.81 in.	±0.001 in.	±0.001 in.	100	±0.003 in.
C_d	0.995	±0.003	---	---	±0.003 in.
F_a	1.0	---	---	---	---
Z	1.0	---	---	---	---
K	1.401	---	---	---	---
g	32.174 lbm-ft/ lbf-sec^2	---	---	---	---
M	28.95 lbm/lbm-mol	---	---	---	---
R	1545 lbf-ft/ lbm-mol-°R	---	---	---	---

Equations for determination of precision index (S) and bias limit (B) were given by Eqs. (VI-21) and (VI-22):

$$\frac{S_{W_{1N}}}{W_{1N}} = \pm\sqrt{\left(\frac{S_{P_{oo}}}{P_{oo}}\right)^2 + \left(\frac{-S_{T_{oo}}}{2T_{oo}}\right)^2 + \left(\frac{S_{C_d}}{C_d}\right)^2 + \left(\frac{2S_d}{d}\right)^2}$$

$$= \pm\sqrt{\left(\frac{0.02}{12.78}\right)^2 + \left(\frac{-0.20}{2 \times 478.7}\right)^2 + \left(\frac{0}{0.995}\right)^2 + \left(\frac{2 \times 0.001}{21.8^2}\right)^2}$$

$$= \pm\sqrt{(0.0012)^2 + (-0.0002)^2 + (9) + (0.000004)^2}$$

$$= \pm 0.0012 = \pm 0.12 \text{ percent}$$

$$S_{W_{1N}} = \pm 0.12 \text{ percent} \times 115.5 \text{ lbm/sec} = \pm 0.139 \text{ lbm/sec}$$

$$\frac{B_{W_{1N}}}{W_{1N}} = \pm\sqrt{\left(\frac{B_{P_{oo}}}{P_{oo}}\right)^2 + \left(\frac{-B_{T_{oo}}}{2T_{oo}}\right)^2 + \left(\frac{B_{C_d}}{C_d}\right)^2 + \left(\frac{2B_d}{d}\right)^2}$$

$$= \pm\sqrt{\left(\frac{0.04}{12.78}\right)^2 + \left(\frac{-1.8}{2 \times 478.7}\right)^2 + \left(\frac{0.003}{0.995}\right)^2 + \left(\frac{2 \times 0.001}{21.8^2}\right)^2}$$

$$= \pm\sqrt{(0.0024)^2 + (-0.0018)^2 + (0.003015)^2 + (0.000004)^2}$$

$$= \pm 0.0046 = \pm 0.46 \text{ percent}$$

$$B_{W_{1N}} = \pm 0.46 \text{ percent} \times 115.5 \text{ lbm/sec} = \pm 0.531 \text{ lbm/sec}$$

By using the Welch-Satterthwaite formula, Eq. (I-11), the degrees of freedom for the combined precision index is determined from

$$df = \frac{\left(S_{P_{oo}}^2 + S_{T_{oo}}^2 + S_d^2\right)^2}{\frac{S_{P_{oo}}^4}{df_{P_{oo}}} + \frac{S_{T_{oo}}^4}{df_{T_{oo}}} + \frac{S_d^4}{df_d}}$$

which results in an overall degrees of freedom > 30, and therefore a value for t_{95} of 2.0.

Total airflow uncertainty is then,

$$\frac{U_{W_{1N}}}{W_{1N}} = \pm\left(\frac{B_{W_{1N}}}{W_{1N}} + 2\frac{S_{W_{1N}}}{W_{1N}}\right)$$

$$= \pm[0.0046 + 2(0.0012)]$$

$$= \pm 0.007 = \pm 0.7 \text{ percent}$$

$$U_{W_{1N}} = \pm 0.7 \text{ percent} \times 115.5 \text{ lbm/sec} = \pm 0.81 \text{ lbm/sec}$$

6.4.2 Subsonic Orifice

Consider a 2-in. orifice installed in a 4-in. pipe and used for airflow measurement. The meter is a square-edged orifice with flange taps, and the value for C_d has been taken from the ASME references.

Equation (VI-15) is the flow equation to be analyzed. The variables to be considered are d, C_d, Δp, p_1, and T_1. Indicated total temperature (T_1) should be corrected for losses and probe recovery factor.

From the ASME references, $C_d = 0.6025 \pm 0.58\%$ (2 sigma). Table XVII lists nominals, precision indices and bias limits for each error source.

Table XVII Airflow Error Source

Error Source	Nominal Value	Bias Limit	Precision Index (S)
d	2.0 in.	±0.001 in.	---
C_d	0.6025	±0.0017	---
Δ_p	5.00 psid	±0.005 psid	±0.010 psid
p_1	20.00 psia	±0.02 psia	±0.04 psia
T_1	520.00 °R	±1.00 °R	±0.25 °R

From Eqs. (VI-17) and (VI-18), with S_d and $S_{Cd} = 0$,

$$\frac{S_W}{W} = \sqrt{\left(\frac{-0.25}{2(520)}\right)^2 + \left(\frac{3 \times 0.01}{2 \times 5.0}\right)^2 + \left(\frac{-0.04}{2 \times 20.0}\right)^2}$$

$$= 0.0031714 = 0.32 \text{ percent}$$

$$\frac{B_W}{W} = \sqrt{\left(\frac{2 \times 0.001}{2.0}\right)^2 + \left(\frac{0.0017}{0.6025}\right)^2 + \left(\frac{-1.0}{2 \times 520}\right)^2 + \left(\frac{3 \times 0.005}{2 \times 5.0}\right)^2 + \left(\frac{-0.02}{2 \times 20.0}\right)^2}$$

$$= 0.0035194 = 0.35 \text{ percent}$$

If the overall degrees of freedom are assumed to be greater than thirty, then

$$\frac{U_W}{W} = \pm\left(\frac{B_W}{W} + \frac{2S_W}{W}\right)$$

$$= \pm(0.35 + 2 \times 0.32) = \pm 0.99 \text{ percent}$$

SECTION VII
NET THRUST AND NET THRUST SPECIFIC FUEL CONSUMPTION

7.1 GENERAL

This section details an error analysis for net thrust and net thrust specific fuel consumption at an altitude test facility. In order to calculate net thrust, engine gross (jet) thrust must first be determined. Two independent techniques for the determination of gross thrust can be used: (1) external forces, or scale force method and (2) internal forces, or momentum balance method. Both techniques are utilized for most gas turbine engine performance programs when the determination of net thrust and thrust specific fuel consumption is a primary requirement. Performance determined by each method can be compared for agreement in order to improve the confidence in thrust data. Error analysis is presented only for the external forces or scale force method. The relationship between gross thrust and net thrust will be shown in Section 7.3.

The measurements associated with the determination of net thrust and net thrust specific fuel consumption include pressure, temperature, force, fuel flow, and airflow measurements. Error analysis of measurement systems have been presented in prior sections as follows: temperature and pressure measurements (Section V), force measurement (Section III), fuel flow measurement (Section IV), and airflow measurement (Section VI).

7.2 GROSS THRUST MEASUREMENT TECHNIQUES

7.2.1 Scale Force Method

The engine assembly and engine support mount are installed on a thrust stand which is flexure mounted on a model support cart. The engine inlet duct system contains a zero-leakage, labyrinth-type air seal. Resultant axial forces are measured by a strain-gage load cell. This installation permits the defining of a control volume (Fig. VII-1) which allows the calculation of gross (jet) thrust (F_G) from easily measurable parameters.[8]

The freebody diagram associated with the scale force method of thrust determination is shown in Fig. VII-1.

The derivation of gross thrust (F_G) from Fig. VII-1 is

$$\Sigma F_X = 0 = \frac{W_{A1} V_1}{g} + A_1 p_1 + F_S - p_o \int_{A_J}^{A_1} dA - \frac{W_J V_J}{g} - A_J p_J$$

Rearranging and combining terms give

$$\frac{W_J V_J}{g} + A_J(p_J - p_o) = \frac{W_{A1} V_1}{g} + A_1(p_1 - p_o) + F_S$$

[8]For a definition of terms used in this Handbook, see Glossary in Section IX.

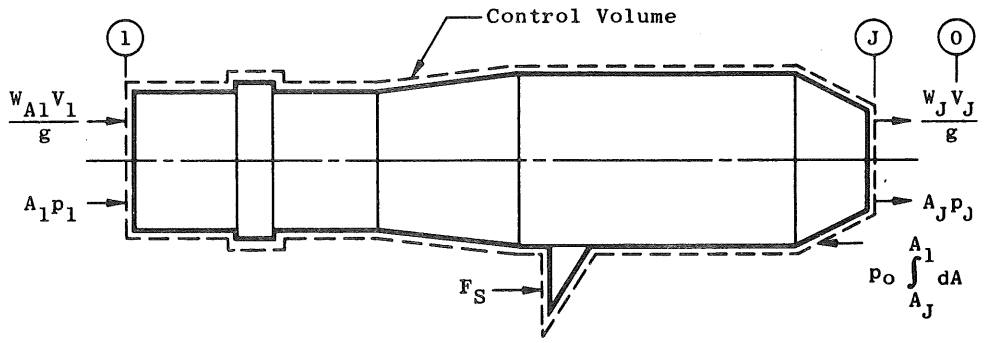

W_{A1} = engine inlet airflow rate, lbm/sec

V_1 = engine inlet airflow velocity, ft/sec

g = dimensional constant, 32.174 lbm-ft/lbf-sec^2

A_1 = engine inlet duct cross-sectional area (OD), in.^{2}

p_1 = engine inlet duct static pressure, lbf/in.^{2}

F_S = force measuring transducer output (scale force), lbf

W_J = engine exhaust nozzle exit gas flow rate, lbm/sec

V_J = engine exhaust nozzle exit gas flow velocity, ft/sec

A_J = engine exhaust nozzle exit area, in.^{2}

p_J = engine exhaust nozzle exit static pressure, lbf/in.^{2}

p_o = free-stream (ambient) static pressure, lbf/in.^{2}

Fig. VII-1 Freebody Diagram for External Forces (Scale Force) Method of Determining Engine Gross (Jet) Thrust

Engine gross (jet) thrust in pounds force is, by definition,

$$F_G = \frac{W_J V_J}{g} + A_J(p_J - p_o)$$

therefore,

$$F_G = \frac{W_{A1} V_1}{g} + A_1(p_1 - p_o) + F_S \qquad \text{(VII-1)}$$

7.2.2 Momentum Balance Method

The momentum balance method of thrust determination utilizes the nozzle throat total pressure and temperature profiles obtained with a traversing probe and a mathematical flow field integration to determine the nozzle stream thrust.

Theoretical calculations utilized in the momentum balance method assume the fluid to be inviscid, thermally perfect, and non-heat-conducting. The method of calculation consists of direct numerical integration of the equations for continuity, momentum, and

energy to define the gas state at the nozzle throat. The gas properties at the nozzle throat are then used to determine the exit momentum and pressure-area forces required to obtain the nozzle stream thrust.

The freebody diagram associated with the momentum balance method of thrust determination is shown in Fig. VII-2.

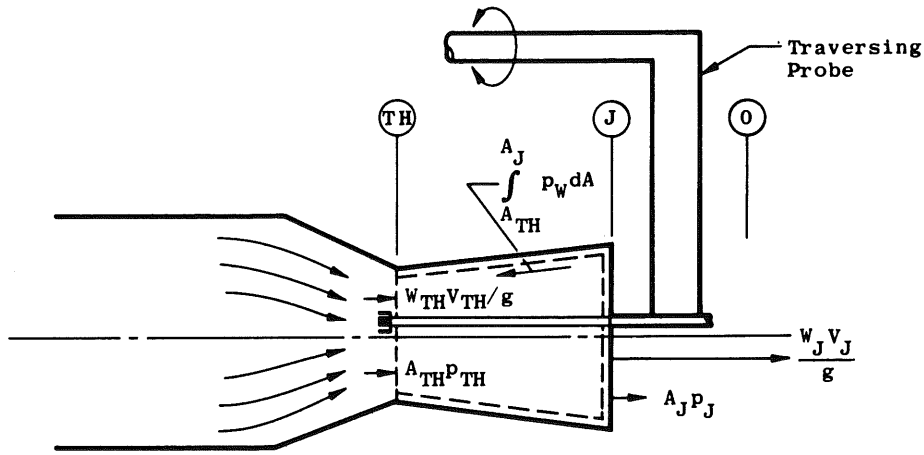

W_{TH} = gas flow rate at nozzle throat, lbm/sec

V_{TH} = gas flow velocity at nozzle throat, ft/sec

g = dimensional constant, 32.174 lbm-ft/lbf-sec^2

A_{TH} = nozzle throat area, in.^{2}

p_{TH} = nozzle throat static pressure, lbf/in.^{2}

W_J = gas flow rate at nozzle exit, lbm/sec

V_J = gas flow velocity at nozzle exit, ft/sec

A_J = nozzle exit area, in.^{2}

p_J = nozzle exit static pressure, lbf/in.^{2}

p_W = nozzle wall static pressure, lbf/in.^{2}

p_o = free-stream (ambient) static pressure, lbf/in.^{2}

Fig. VII-2 Freebody Diagram for Internal Forces (Momentum Balance) Method of Determining Engine Gross (Jet) Thrust

The derivation of gross thrust from Fig. VII-2 is

$$\Sigma F_X = 0 = \int_o^{A_{TH}} \frac{W_{TH}V_{TH}/g}{A}\,dA + \int_o^{A_{TH}} p_{TH}\,dA + \int_{A_{TH}}^{A_J} p_W\,dA - \int_o^{A_J} \frac{W_JV_J/g}{A}\,dA - \int_o^{A_J} p_J\,dA$$

Engine gross (jet) thrust in pounds force is, by definition,

$$F_G = \int_o^{A_J} \frac{W_J V_J / g}{A} dA + \int_o^{A_J} p_J \, dA - A_J P_o$$

therefore,

$$F_G = \int_o^{A_{TH}} \frac{W_{TH} V_{TH} / g}{A} dA + \int_o^{A_{TH}} p_{TH} \, dA + \int_o^{A_J} p_W \, dA - A_J P_o \qquad \text{(VII-2)}$$

7.3 PROPAGATION OF ERRORS TO NET THRUST

When F_G has been obtained by either the scale force or the momentum balance method, or both, identical equations are used to obtain net thrust. The external force (scale force) method for measuring net thrust is used as the example, and the derivation of this method is shown in Section 7.2.1. The Taylor's series method (Appendix B) of propagating error to net thrust is used.

The relationship of net thrust (F_N) to gross thrust (F_G) is

$$F_N = F_G - F_R \qquad \text{(VII-3)}$$

where

$$F_R = \frac{W_{A1} V_o}{g} \qquad \text{(VII-4)}$$

and V_o is the aircraft free-stream velocity in ft/sec, W_{A1} is the engine inlet airflow rate in lbm/sec, and g is a dimensional constant. Combining Eqs. (VII-1), (VII-3), and (VII-4) then results in the following equation for engine net thrust:

$$F_N = \frac{W_{A1}}{g}(V_1 - V_o) + A_1(p_1 - p_o) + F_S \qquad \text{(VII-5)}$$

where

$$V_1 = \sqrt{\frac{2KgRT_1}{K-1}\left[1 - \left(\frac{p_1}{P_1}\right)^{\frac{K-1}{K}}\right]} \qquad \text{(VII-6)}$$

$$V_o = \sqrt{\frac{2KgRT_1}{K-1}\left[1 - \left(\frac{p_o}{P_1}\right)^{\frac{K-1}{K}}\right]} \qquad \text{(VII-7)}$$

P_1 = engine inlet duct total pressure, lbf/in.^{2}

K = ratio of specific heats at T_1

R = gas constant for air at T_1, ft-lbf/lbm-°R

All other parameters are as designated in Fig. VII-1.

Net thrust in terms of pressure, temperature, area, airflow, a gas constant, a ratio of specific heats, a dimensional constant, and force measurement now becomes

$$F_N = \frac{W_{A1}}{g}\left(\frac{2KgRT_1}{K-1}\right)^{\frac{1}{2}}\left[\sqrt{1-\left(\frac{P_1}{P_1}\right)^{\frac{K-1}{K}}} - \sqrt{1-\left(\frac{P_o}{P_1}\right)^{\frac{K-1}{K}}}\right] + A_1(p_1 - p_o) + F_S \quad \text{(VII-8)}$$

The propagation formulas for the bias limit and precision index are derived from Eq. (VII-8) for F_N.

The bias limit propagation formula is the weighted root-sum-square of the bias limits for W_{A1}, g, R, K, T_1, P_1, p_1, p_o, A_1, and F_S:

$$B_{F_N}^2 = \pm\left\{\left(\frac{\partial F_N}{\partial W_{A1}} B_{W_{A1}}\right)^2 + \left(\frac{\partial F_N}{\partial g} B_g\right)^2 + \left(\frac{\partial F_N}{\partial K} B_K\right)^2 + \left(\frac{\partial F_N}{\partial T_1} B_{T_1}\right)^2 + \left(\frac{\partial F_N}{\partial R} B_R\right)^2\right.$$

$$\left. + \left(\frac{\partial F_N}{\partial P_1} B_{P_1}\right)^2 + \left(\frac{\partial F_N}{\partial p_1} B_{p_1}\right)^2 + \left(\frac{\partial F_N}{\partial p_o} B_{p_o}\right)^2 + \left(\frac{\partial F_N}{\partial A_1} B_{A_1}\right)^2 + \left(\frac{\partial F_N}{\partial F_S} B_{F_S}\right)^2\right\} \quad \text{(VII-9)}$$

In the same way, the precision index propagation formula is the weighted root-sum-square of the precision indices of W_{A1}, g, K, R, T_1, P_1, p_1, p_o, A_1, and F_S:

$$S_{F_N}^2 = \pm\left\{\left(\frac{\partial F_N}{\partial W_{A1}} S_{W_{A1}}\right)^2 + \left(\frac{\partial F_N}{\partial g} S_g\right)^2 + \left(\frac{\partial F_N}{\partial K} S_K\right)^2 + \left(\frac{\partial F_N}{\partial T_1} S_{T_1}\right)^2 + \left(\frac{\partial F_N}{\partial R} S_R\right)^2\right.$$

$$\left. + \left(\frac{\partial F_N}{\partial P_1} S_{P_1}\right)^2 + \left(\frac{\partial F_N}{\partial p_1} S_{p_1}\right)^2 + \left(\frac{\partial F_N}{\partial p_o} S_{p_o}\right)^2 + \left(\frac{\partial F_N}{\partial A_1} S_{A_1}\right)^2 + \left(\frac{\partial F_N}{\partial F_S} S_{F_S}\right)^2\right\} \quad \text{(VII-10)}$$

Errors associated with values of g, K, and R are generally assumed negligible.

The uncertainty for net thrust (F_N) is calculated using the uncertainty formula:

$$U = \pm(B + t_{95}S) \quad \text{(VII-11)}$$

The following list of partial derivatives is given as an aid to the analyst:

$$\frac{\partial F_N}{\partial W_{A1}} = \frac{1}{g}\left[\frac{2KgRT_1}{K-1}\right]^{\frac{1}{2}}\left[B_1^{\frac{1}{2}} - B_2^{\frac{1}{2}}\right]$$

$$\frac{\partial F_N}{\partial T_1} = \frac{W_{A1}}{g}\left[\frac{KgR}{(K-1)T_1}\right]^{\frac{1}{2}}\left[B_1^{\frac{1}{2}} - B_2^{\frac{1}{2}}\right]$$

$$\frac{\partial F_N}{\partial A_1} = P_1 - P_0$$

$$\frac{\partial F_N}{\partial F_S} = 1.0$$

$$\frac{\partial F_N}{\partial P_0} = W_{A1}\left(\frac{1}{P_0}\right)^{\frac{1}{K}}\left(\frac{1}{P_1}\right)^{\frac{K-1}{K}}\left(\frac{(K-1)RT_1}{2gKB_2}\right)^{\frac{1}{2}} - A_1$$

$$\frac{\partial F_N}{\partial P_1} = W_{A1}\left(\frac{1}{P_1}\right)^{\frac{1}{K}}\left(\frac{1}{P_1}\right)^{\frac{K-1}{K}}\left(\frac{(K-1)RT_1}{2gKB_1}\right)^{\frac{1}{2}} + A_1$$

$$\frac{\partial F_N}{\partial P_1} = W_{A1}\left(\frac{(K-1)RT_1}{2gK}\right)^{\frac{1}{2}}(P_1)^{\frac{1-2K}{K}}\left[\left((P_1)^{\frac{K-1}{K}}B_1^{-\frac{1}{2}}\right) - \left((P_0)^{\frac{K-1}{K}}B_2^{-\frac{1}{2}}\right)\right]$$

where

$$B_1 = 1 - \left(\frac{P_1}{P_1}\right)^{\frac{K-1}{K}} \quad \text{and} \quad B_2 = 1 - \left(\frac{P_0}{P_1}\right)^{\frac{K-1}{K}}$$

By using Eqs. (VII-9) and (VII-10), the partial derivative equations above, and the example values listed in Table XVIII, the propagation of error to net thrust can be determined.

In this example, values for the partial derivative terms above were approximated through the basic net thrust equation. First, the thrust level is determined from the measured values using performance Eq. (VII-8). Then each measured value in Eq. (VII-8) is changed, independently, by the amount of its precision index, and the resulting change in F_N is obtained. This process, repeated for each measured value, provides good approximate numerical values for each term in Eq. (VII-10). For example to obtain the approximate value for the term $[(\partial F_N/\partial W_{A1})S_{W_{A1}}]$ of Eq. (VII-10), determine F_N (Eq. (VII-8)) with the measured values. Then, determine the change in $F_N(\Delta F_N)$ by changing airflow (W_{A1}) by the amount of its precision index. The change in F_N resulting from the change in W_{A1} is approximately equal to the term $[(\partial F_N/\partial W_{A1})S_{W_{A1}}]$. The identical process is repeated for bias limits to obtain numerical values for the terms in Eq. (VII-9).

Table XVIII
Typical Measurement and Uncertainty Values Used in Net Thrust for Supersonic Afterburning Turbofan Engine

Flight Condition: 30,000-ft Altitude, Mach Number 0.9, Military Power

Component	Nominal Value	Bias Limit	Precision Index	Uncertainty, U	Degrees of Freedom**
F_S, Scale Force, lbf	4,388	7.90	3.95	15.80	105
g, Dimensional Constant, $\frac{lbm - ft}{lbf - sec^2}$	32.174	*	*	*	*
A_1, Inlet Duct Area (OD), in.^{2}	984	0.050	0.050	0.160	12
p_1, Inlet Duct Static Pressure, psia	6.50	0.0065	0.0065	0.0202	15
p_o, Free-Stream Static Pressure, psia	4.31	0.0099	0.0099	0.0310	15
R, Gas Constant for Air at T_1, $\frac{ft - lbf}{lbm - °R}$	53.329	*	*	*	*
T_1, Inlet Duct Total Temperature, °R	477	±2.48	±0.19	±2.86	100
K, Ratio of Specific Heats at T_1	1.4034	*	*	*	*
P_1, Inlet Duct Total Pressure, psia	7.43	±0.0074	±0.0111	±0.0312	15
W_f, Total Fuel Flow, lbm/hr	4662	±6.06	±5.13	±16.32	35

*Bias, precision, and uncertainty considered as negligible in thrust uncertainty.
**Degrees of freedom determined by the Welch-Satterthwaite formula (Eq. I-11).

By using Eqs. (VII-6), (VII-7), and (VII-8) and the measurement values and their uncertainty components listed in Table XVIII, the propagation of error to V_o, V_1, F_R, F_N, and TSFC are shown in Table XIX. Wa_1 of Table XIX was obtained from Section VI.

Table XIX
Derived Measurement Uncertainty Values

Parameter	Nominal	Bias Limit	Precision Index	Uncertainty	Degrees of Freedom
V_o, Free-Stream Velocity, ft/sec	908.4	±3.049	±2.119	±7.414	26
V_1, Inlet Duct Velocity, ft/sec	463.4	±2.684	±3.057	±8.981	26
Wa_1, Inlet Duct Airflow, lbm/sec	115.5	±0.531	±0.139	±0.825	16
F_R, Ram Drag, lbf	3261.	±18.563	±8.559	±35.681	38
F_N, Net Thrust, lbf	4945	±12.498	±7.471	±27.440	59
TSFC, Net Thrust Specific Fuel Consumption, lbm/lbf-hr	0.943	±0.0027	±0.0018	±0.0063	94

7.4 PROPAGATION OF ERROR TO NET THRUST SPECIFIC FUEL CONSUMPTION

$$TSFC = \frac{W_F}{F_N}, \frac{lbm/hr}{lbf} \tag{VII-12}$$

where W_F is total engine fuel flow (lbm/hr), and F_N is net thrust (lbf).

The error analysis for fuel flow is shown in Section IV, and the error analysis for net thrust is shown in Section 7.3.

The bias limit propagation formula is the root-sum-square of the bias limits for W_F and F_N weighted by the partial derivatives (Appendix B):

$$B_{TSFC}^2 = \pm\left[\left(\frac{\partial TSFC}{\partial W_F} B_{W_F}\right)^2 + \left(\frac{\partial TSFC}{\partial F_N} B_{F_N}\right)^2\right] \tag{VII-13}$$

In the same way, the precision index is calculated as the root-sum-square of the precision indices for W_F and F_N:

$$S_{TSFC}^2 = \pm\left[\left(\frac{\partial TSFC}{\partial W_F} S_{W_F}\right)^2 + \left(\frac{\partial TSFC}{\partial F_N} S_{F_N}\right)^2\right] \tag{VII-14}$$

The partial derivatives for the terms in Eqs. (VII-13) and (VII-14) are

$$\frac{\partial TSFC}{\partial W_F} = \frac{1}{F_N} \quad \text{and} \quad \frac{\partial TSFC}{\partial F_N} = -\frac{W_F}{F_N^2}$$

Equations (VII-13) and (VII-14) are now evaluated using the above partials and the measurement values and uncertaintv components from Tables XVIII and XIX for W_F and F_N, respectively.

$$B_{TSFC} = \pm\sqrt{[(0.0002022)(6.06)]^2 + [(0.0001906)(12.498)]^2}$$
$$= \pm 0.0027 \text{ lbm/hr/lbf}$$

$$S_{TSFC} = \pm\sqrt{[(0.0002022)(5.13)]^2 + [(0.0001906)(7.471)]^2}$$
$$= \pm 0.0018 \text{ lbm/hr/lbf}$$

The uncertainty for TSFC is calculated using the uncertainty formula:

$$U = \pm(B + t_{95}S)$$

Here t_{95} is = 2.0 since the degrees ot freedom are greater than 30.

$$U = \pm[0.0027 + 2(0.0018)]$$
$$= \pm 0.0063 \text{ lbm/hr/lbf}$$

SECTION VIII
SPECIAL METHODS

8.1 GENERAL

This section treats several methods for special situations or conditions:

1. Measurement uncertainty[9] for multi-engine installation (similar engines).
2. Measurement uncertainty for the single stand, single engine process in comparison with the many stand, many engine process.
3. Confidence interval for uncertainty when biases are negligible.
4. Compressor efficiency error analysis.
5. How to interpret uncertainty.
6. Dynamic measurement uncertainty.

8.2 MEASUREMENT UNCERTAINTY FOR MULTI-ENGINE INSTALLATIONS (SIMILAR ENGINES)

8.2.1 General

The uncertainty in performance parameters for the multi-engine aircraft for similar engines is a function of bias limits and precision indices of the individual engines for those performance parameters. If, for example, the parameter of interest is thrust, the total thrust (F_T) for the aircraft is the sum of the thrust values for the individual engines. The precision index (S_{F_T}) for total thrust is the root-sum-square of the precision indices (S_i) for the individuals (assuming that the engine run-to-run variance is negligible) and where S_i is the same for all engines:

$$S_{F_T}^2 = \sum_{i=1}^{K} S_i^2 = KS_i^2$$

or

$$S_{F_T} = S_i\sqrt{K} \qquad \text{(VIII-1)}$$

where K is the number of engines. The degrees of freedom (df) associated with a production engine facility would exceed 30 in almost every case. The df is calculated from the degrees of freedom (df_i) for each engine.

$$df = \frac{\left(\sum_{i=1}^{K} S_i^2\right)^2}{\sum_{i=1}^{K} \frac{S_i^4}{df_i}} \equiv \frac{\left(KS_i^2\right)^2}{\left(\frac{1}{df_i}\right)KS_i^4} = Kdf_i > 30 \qquad \text{(VIII-2)}$$

[9]For a definition of terms used in this Handbook, see the Glossary in Section IX.

The bias limit (B) for the installation is the sum of the bias limits (B_i) for each of the engines:

$$B = \sum_{i=1}^{K} B_i = KB_i \qquad \text{(VIII-3)}$$

The bias limits are added rather than root-sum-squared because the bias errors for similar engines are not usually independent. (If the bias errors are independent, the bias limits may be root-sum-squared.) Therefore, these errors do not tend to cancel, and the limit is best estimated as the sum of the limits. This is consistent with the philosophy that independent bias limits are combined by root-sum-squaring. Finally, the uncertainty for the installation can be calculated:

$$U = \pm\left[KB_i + (t_{95})\, S_i\sqrt{K}\right] \qquad \text{(VIII-4)}$$

where t_{95} is the student's "t" value for 95 percent (two-tailed) confidence and df_i times K are the degrees of freedom.

8.2.2 Example of a Four-Engine Installation

Suppose an aircraft installation consists of four, 20,000-lb-thrust engines, each with the following reported measurement uncertainty:

Bias limit	±36 lb	df	27.8
Precision limit	±75 lb	Uncertainty	±190 lb

The precision index for the installation is calculated from Eq. (VIII-1):

$$S_{F_T} = \pm(75)\sqrt{4} = \pm(75)(2) = \pm 150.0$$

The degrees of freedom (Eq. (VIII-2)) for the precision index are 27.8 x 4 = 111.2. The bias limit (Eq. (VIII-3)) for the installation is 4 times (±36) = ±144. The uncertainty limit (Eq. (VIII-4)) for the cluster is

$$U = \pm(144 + t_{95} \times 150) = \pm[144 + 2(150)] = \pm 444 \text{ lb}$$

Since the degrees of freedom exceed 30, $t_{95} = 2.0$ is used.

8.3 MEASUREMENT PROCESSES

The measurement uncertainty estimate is a function of a specific measurement process. In this section, two different but related processes are discussed. The models illustrate extremes: many tests over a long period of time versus two tests over a short time interval. In the paragraphs that follow, the general model for many engines and many test stands is contrasted with the model for back-to-back development testing of a single engine on a single stand.

Note that in the following examples the engine hardware, instrumentation, and test stand might be identical but that the uncertainties are different because the measurement of interest is different.

8.3.1 Many Stand, Many Engine Model

The general process, which was defined in Section 1.7 and discussed throughout this Handbook, pertains to the measurement process defined for many sets of measurement instruments, many test stands, many calibrations, and many months of operation. An example is the measurement of TSFC at an engine production facility. The problem is to determine the absolute level of performance.

Table XX A Measurement System with Six Error Sources

Source	Bias Limit	Precision Index	Uncertainty
NBS, Interlab Standard	±0.1	±0.1	±0.3
Interlab, Transfer Standard	±0.1	±0.1	±0.3
Transfer, Working Standard	±0.5	±0.5	±1.5
Working, End Instrument	±0.5	±0.5	±1.5
Calibration Hierarchy Error	±0.72	±0.72	±2.16
Data Acquisition	±0.5	±0.5	±1.5
Data Reduction	±0.2	±0.2	±0.6
Combined Error	±0.9	±0.9	±2.7

The uncertainty for this measurement process is $U = \pm(B + t_{95} S)$, where B is the root-sum-square of all elemental bias limits and S is the root-sum-square of all elemental precision indices for the process. For example, Table XX lists the elemental errors for a measurement system with six error sources. The root-sum-square of the bias limits is ±0.9. The root-sum-square of the precision indices is also ±0.9. The uncertainty of the general process is ±2.7.

8.3.2 Single Stand, Single Engine Model

During a gas turbine development program, many tests are devoted to evaluating new component designs. The objective is to obtain the most accurate determination of the incremental change in performance between the baseline and the new configuration.

The engine (or rig) is installed on a test stand, and a baseline calibration is performed. Then, an engine design change is made without modification to the stand or instrumentation. Typically, these changes may be made without removing the engine from the test stand. For example, the inlet guide vanes might be replaced or compressor stator vane angles adjusted. Then, the engine is tested again, and performance is measured for comparison with the baseline calibration. The measurement is the difference between corresponding performance values for the two tests. The difference should be due to only three causes: instrumentation precision error, engine repeatability (which has been assumed to be negligible), and the design change. Since the repetitive tests are confined to a single set of instruments and a single engine, the measurement uncertainty is reduced; bias errors are not considered because they will be the same for each test and will not affect the comparison. The only errors which need to be considered are the

run-to-run precision errors of the measurement system for each of the runs. For the data in Table XX, the precision index of the data acquisition is 0.5 and reduction processes is 0.2 for each run. The uncertainty must be calculated for the difference in the two runs. It is the root-sum-square of the run-to-run precision error of the data acquisition and reduction precision error for each run:

$$U = t_{95}\sqrt{S_{\text{run one}}^2 + S_{\text{run two}}^2} = t_{95}\sqrt{S_{\text{data acq}}^2 + S_{\text{data red}}^2 + S_{\text{data acq}}^2 + S_{\text{data red}}^2}$$

$$= t_{95}\sqrt{2(0.5^2 + 0.2^2)} = 2\sqrt{2}\sqrt{0.29} = 1.523$$

where $t_{95} = 2.0$.

8.4 CONFIDENCE INTERVAL WHEN BIASES ARE NEGLIGIBLE OR CAN BE IGNORED

When the bias is very small (negligible) or can be ignored, i.e., as in a back-to-back development test, the uncertainty parameter (U) becomes a statistical confidence interval.

The interpretation and the use of the uncertainty parameter are not changed. However, it is now defined with known exact characteristics. An uncertainty limit of six pounds force means that it would be "reasonable to expect" that the true value would be within six pounds force of the measured value. For 95 percent confidence intervals, 95 percent of the intervals will contain the true value. The qualitative concept "reasonable to expect" is quantified by the confidence concept. It is not necessary to distinguish between uncertainty intervals with and without bias errors. The same simple interpretation of uncertainty applies.

As an example of a confidence interval, take the following measurement data for specific fuel consumption for a 10,000-lbf gas turbine engine:

Specific Fuel Consumption	= 0.88
Bias Limit	= 0.0
Precision Index (S)	= 0.02
Degrees of Freedom	= 25.2

The point estimate or unbiased estimate of specific fuel consumption is 0.88. The uncertainty (U) is a 95 percent confidence interval estimate:

$$U = \pm t_{95} \times 0.02 = \pm 0.041$$

That is the 95-percent confidence interval is 0.88 ± 0.041 or 0.839 to 0.921. In repeated sampling, such an interval will contain the true value with 95-percent frequency.

8.5 COMPRESSOR EFFICIENCY ERROR ANALYSIS

8.5.1 General

Consider a compressor efficiency uncertainty analysis for the many stand, many compressor model and the single stand, single compressor model. For each analysis, Eq. (VIII-5) is used for the calculation of adiabatic efficiency (η) of a compressor as a function of the pressure and temperature ratios across the compressor:

$$\eta = \left[\left(\frac{P_1}{P_o}\right)^{\frac{K-1}{K}} - 1.0\right] \Bigg/ \left[\left(\frac{T_1}{T_o}\right) - 1.0\right] \qquad \text{(VIII-5)}$$

where

P_o = inlet pressure

P_1 = exit pressure

T_o = inlet temperature

T_1 = exit temperature

K = ratio of specific heats

The nominal values and elemental bias limits and precision indices are listed in Table XXI. These data imply a pressure ratio of 6.5, inlet and exhaust temperatures of 530 and 960°R, and efficiency of 85 percent.

8.5.2 The General Process

Many compressors are tested in many rigs with many instrumentation setups over a period of years.

The measurement uncertainty for this process is the uncertainty associated with the absolute level of performance for a compressor. The interval includes all the bias errors and precision measurement errors associated with compressor efficiency calculation. All of the error estimates listed in Table XXI contribute to the uncertainty.

Table XXI Tabulation of the Elemental Errors

Source	Bias Limit	Precision Index
T_o Nominal, 530°R		
Thermocouples at 530°R	0.0°F to +0.10°F	0.20°F
Reference	-0.10°F to +0.10°F	0.10°F
Signal Conditioning	-0.10°F to +0.10°F	0.50°F
Data Reduction	Negligible	Negligible
Combining	-0.14°F to +0.17°F	0.55°F
T_1 Nominal, 960°R		
Thermocouples	0.0°F to +1.00°F	0.50°F
Reference	-0.10°F to +0.10°F	0.10°F
Signal Conditioning	-0.10°F to +0.10°F	0.50°F
Data Reduction	Negligible	Negligible
Combining	-0.14°F to +1.01°F	0.714°F
P_o Nominal 14.696 psia		
Transducers	±0.1% ~0.015 psia	0.15% ~0.022 psia
Recovery Factor	Negligible	Negligible
Signal Conditioning	±0.1% ~0.015 psia	0.10% ~0.015 psia
Data Reduction	Negligible	Negligible
Combining	±0.14% ~0.021 psia	0.18% ~0.027 psia
P_1 Nominal 95.524 psia		
Transducers	±0.10% ~0.10 psia	0.15% ~0.14 psia
Recovery Factor	±0.10% ~0.10 psia	Negligible
Signal Conditioning	±0.10% ~0.10 psia	0.10% ~0.10 psia
Data Reduction	Negligible	Negligible
Combining	±0.17% ~0.173 psia	0.18% ~0.17 psia

Degree of freedom is assumed >30.
K is ratio of specific heats, Nominal, 1.39, errors negligible.

For each of the four values T_o, T_1, P_o, and P_1, the elemental bias limits are root-sum-squared and the elemental precision indices are root-sum-squared. Table XXII presents a summary of the combined bias limits and precision indices from Table XXI.

Table XXII Summary of Errors

Source	Bias Limits	Precision Index
T_o	$B_{T_o}^- = -0.14°F$ $B_{T_o}^+ = 0.17°F$	$S_{T_o} = 0.55°F$
T_1	$B_{T_1}^- = -0.14°F$ $B_{T_o}^+ = 1.01°F$	$S_{T_1} = 0.714°F$
P_o	$B_{P_o} = \pm 0.14\%$ or 0.021 psia	$S_{p_o} = 0.18\%$ or 0.027 psia
P_1	$B_{p_1} = \pm 0.17\%$ or 0.173 psia	$S_{p_1} = 0.18\%$ or 0.17 psia

The errors in T_o, T_1, P_o, and P_1 are propagated to efficiency using the Taylor's series method described in Appendix B. The appropriate calculations for the propagation are

$$S_\eta^2 = \left(\frac{\partial \eta}{\partial T_o} S_{T_o}\right)^2 + \left(\frac{\partial \eta}{\partial T_1} S_{T_1}\right)^2 + \left(\frac{\partial \eta}{\partial P_o} S_{P_o}\right)^2 + \left(\frac{\partial \eta}{\partial P_1} S_{P_1}\right)^2 \qquad \text{(VIII-6)}$$

$$B_\eta^2 = \left(\frac{\partial \eta}{\partial T_o} B_{T_o}\right)^2 + \left(\frac{\partial \eta}{\partial T_1} B_{T_1}\right)^2 + \left(\frac{\partial \eta}{\partial P_o} B_{P_o}\right)^2 + \left(\frac{\partial \eta}{\partial P_1} B_{P_1}\right)^2 \qquad \text{(VIII-7)}$$

where

$$\frac{\partial \eta}{\partial T_o} = \frac{T_1\left[\left(P_1/P_o\right)^{\frac{K-1}{K}} - 1\right]}{(T_1 - T_o)^2}$$

the rate of change of η with respect to T_o

$$\frac{\partial \eta}{\partial T_1} = \frac{-T_o\left[\left(P_1/P_o\right)^{\frac{K-1}{K}} - 1\right]}{(T_1 - T_o)^2}$$

the rate of change of η with respect to T_1

$$\frac{\partial \eta}{\partial P_o} = \frac{-\left(\frac{K-1}{K}\right)\left(P_1/P_o\right)^{\frac{-1}{K}}\left(P_1/P_o^2\right)}{(T_1/T_o) - 1}$$

the rate of change of η with respect to P_o

$$\frac{\partial \eta}{\partial P_1} = \frac{\left(\frac{K-1}{K}\right)\left(\frac{1}{P_o}\right)\left(P_1/P_o\right)^{\frac{-1}{K}}}{(T_1/T_o) - 1}$$

the rate of change of η with respect to P_1

By substituting into Eqs. (VIII-6) and (VIII-7), the precision index and the upper and lower bias limits are calculated.

$$S_\eta^2 = [(0.0036)(0.55)]^2 + [(-0.00198)(0.714)]^2 + [(-0.0398)(0.027)]^2 + [(0.0061)(0.17)]^2$$

$$= 0.00000815$$

$$S_\eta = 0.002854$$

$$(B_\eta^-)^2 = [(0.0036)(-0.14)]^2 + [(-0.0020)(-0.14)]^2 + [(-0.0398)(0.021)]^2 + [(0.0061)(0.173)]^2$$

$$= 0.00000214$$

$$B_\eta^- = 0.00146$$

$$(B_\eta^+)^2 = [(0.0036)(0.17)]^2 + [(-0.0020)(1.01)]^2 + [(0.0398)(0.021)]^2 + [(0.0061)(0.173)]^2$$

$$= 0.00000626$$

$$B_\eta^+ = 0.0025$$

$B_{\bar{\eta}}$ is assigned a negative value since the lower limits in Table XXI are all negative.

The propagated values to efficiency are S = 0.0029 for the precision index, and B^- = -0.0015 and B^+ = 0.0025 for the bias limits. The error in specific heat parameters (K) is considered negligible.

The uncertainty for the general model is the interval contained between U^- and U^+ where:

$$U^- = +B_\eta^- - t_{95}S_\eta \quad \text{(VIII-8)}$$

$$U^+ = +B_\eta^+ + t_{95}S_\eta \quad \text{(VIII-9)}$$

In this case, t_{95} = 2.0 since all the degrees of freedom are greater than 30.

$$U^- = -0.0015 - 2(0.0029) = -0.0073$$

$$U^+ = +0.0025 + 2(0.0029) = 0.0083$$

For the nominal values of Table XXI, the uncertainty interval would be 85% - 0.0073 to 85% + 0.0083 or 84.27% to 85.83%.

8.5.3 Single Stand, Single Compressor Process

For a back-to-back development process, two tests are performed on a single stand with a single compressor. No changes are allowed to the stand system or data recording equipment. The process would involve testing the compressor to establish a baseline efficiency value, changing the compressor configuration and retesting to determine a new efficiency value and to determine the delta from the baseline efficiency value.

The uncertainty interval for these tests is a function of the precision error only of the measurement system. The original table of elemental errors (Table XXI) is now reduced to Table XXIII.

Table XXIII Elemental Errors

Parameter	T_o, °F	T_1, °F	P_o, psia	P_1, psia
Signal Conditioning	0.5	0.5	0.015	0.1
Precision Index Reference	0.1	0.1	---	---
Root-Sum-Square	0.51	0.51	0.015	0.1

The root-sum-square errors are propagated to efficiency using Taylor's series methods described above and in Appendix B. The measurement of concern is the delta between two tests. Therefore, the uncertainty must be propagated to the delta value:

$$\Delta\eta = \eta_2 - \eta_1$$

where η_2 is the efficiency for the second run and η_1 is the efficiency for the first run. The propagation for the precision term $S_{\Delta\eta}$ is:

$$S_{\Delta\eta} = \pm\sqrt{S_{\eta_2}^{\,2} + (-1)^2 S_{\eta_1}^{\,2}} = \pm\sqrt{2\,S_{\eta}^{\,2}} = \pm S_{\eta}\sqrt{2} \qquad \text{(VIII-10)}$$

The uncertainty resulting from the values of Table XXIII is 0.0065.

8.6 HOW TO INTERPRET UNCERTAINTY

Uncertainty is a function of the measurement process as discussed in Section 8.3. A different definition of the process would significantly change the uncertainty. Table XXIV lists the uncertainty values for the many stand, many engine model and for the single stand, single engine model. These values are significantly different, yet both are based on the elemental errors listed in Table XXI.

Table XXIV Uncertainty Values for Two Processes

Measurement Process	Uncertainty Interval
General Measurement Process (for Intercompany Comparisons)	+ 3.7
Back-to-Back Testing Measurement Process	+ 2.0

Uncertainty, then, is a function of the measurement process. It provides an estimate of the largest error that may reasonably be expected for that measurement process (Fig. VIII-1).

Errors larger than the uncertainty should rarely occur. On repeated runs within a given measurement process, the parameter values should be within the uncertainty interval. These differences might look like Fig. VIII-2. Run-to-run differences between corresponding values of Parameter A should be less than the uncertainty for A.

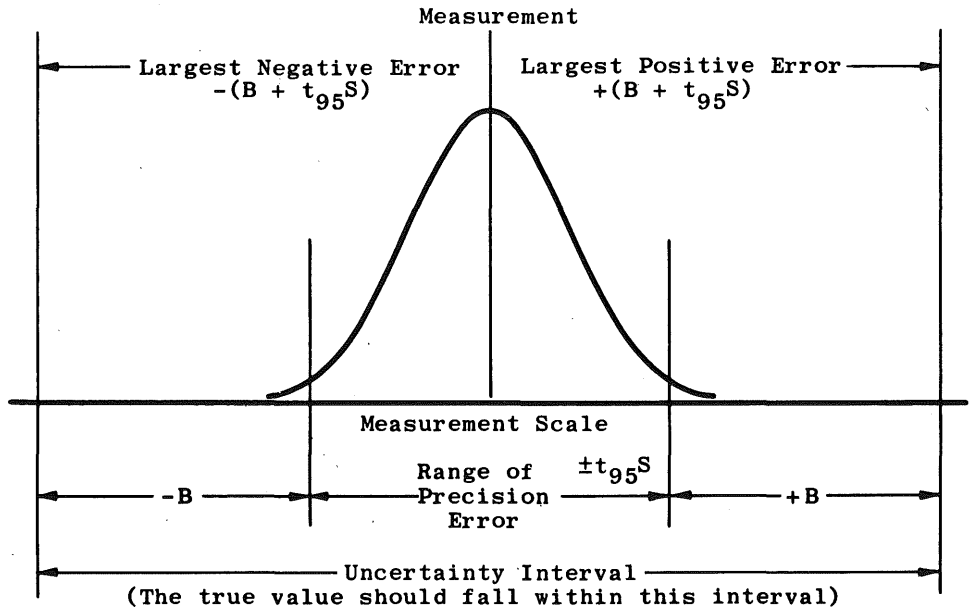

Fig. VIII-1 Measurement Uncertainty

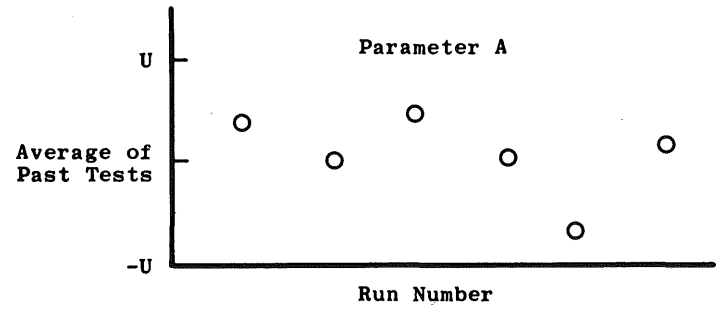

Fig. VIII-2 Run-to-Run Differences

If the difference to be detected in an experiment is of the same size or smaller than the projected uncertainty, corrective action should be taken to reduce the uncertainty. Therefore, measurement uncertainty analysis should always be done before the test or experiment. The corrective action to reduce the uncertainty may involve (1) improvements or additions to the instrumentation, (2) selection of a different function to obtain the parameter of interest, and/or (3) repeated testing. Cost and time will dictate the choice. If corrective action cannot be taken, the test should be cancelled as there is a high risk that the real differences will be lost in the uncertainty interval (undetected). If the measurement uncertainty analysis is made after the test, the opportunity for corrective action is lost, and the test may be wasted.

8.7 DYNAMIC MEASUREMENT UNCERTAINTY

The same basic measurement uncertainty model may be applied to time-varying data. However, there are added complex problems to solve, and the services of a statistician are recommended. Some of these problems are

1. Time Lags
   Different instrumentation will have different time lags which cause serious problems in determining time-variant parameters. For example, thrust specific fuel consumption (TSFC) is based on fuel flow and on thrust determinations. During a transient, if the measured value for one lags behind the other, the ratio, TSFC, will be in error.

2. Uncertainty Varies with Parameter Level
   The uncertainty of the measurements will probably change as the level of the parameter changes. This will be hard to predict because some instruments have errors which are constant, independent of level (error is a constant percentage of full scale, for example); other instrument precision errors and biases vary as the level of the measured parameter varies (error as a percentage of point). Therefore, the uncertainty will be a combination of these two types of error and will neither remain a constant percentage nor change as a constant percentage of point.

3. Shifting Flow Profiles
   Flow profiles are usually considered fixed at steady-state points. During transients, the profile will often shift or change. The uncertainty is increased by this added variation.

4. Autocorrelation between Measurements
   Time-variant measurements on gas turbines will usually be highly related in time (autocorrelated). The degree of autocorrelation will have a significant effect on the uncertainty of the performance parameter.

5. Number of Probes, Location of Probes, Sampling Rate
   If the parameter to be measured involves extreme values like inlet distortion and burner temperature pattern factor, the uncertainty will be highly dependent on the number and the location of the probes. If the parameter involves frequency, the time rate of sampling will be significant and the uncertainty will vary as a function of both sampling rate and frequency.

6. Outliers
   Outliers in time-variant data are much more difficult to detect and flag because of the variation in the level of the parameter. This could result in more outliers being included as good data because they appear to be variations in the parameter. Therefore, for time-variant data, an outlier detection technique should be used very carefully.

SECTION IX
GLOSSARY

1. Accuracy – The closeness or agreement between a measured value and a standard or true value; uncertainty as used herein, is the maximum inaccuracy or error that may reasonably be expected (see measurement error).

2. Average Value – The arithmetic mean of N readings. The average value is calculated as:

$$\bar{X} = \text{average value} = \frac{\sum_{i=1}^{N} X_i}{N}$$

3. Bias (B) – The difference between the average of all possible measured values and the true value. The systematic error or fixed error which characterizes every member of a set of measurements (Fig. IX-1).

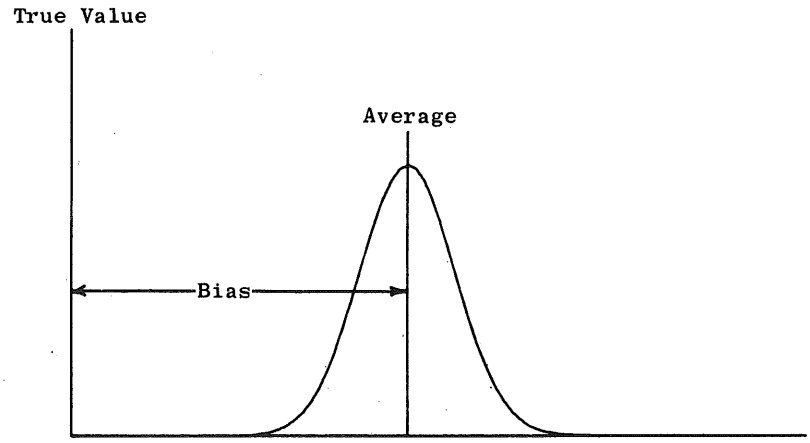

Fig. IX-1 Bias in a Random Process

4. Calibration – The process of comparing and correcting the response of an instrument to agree with a standard instrument over the measurement range.

5. Calibration Hierarchy – The chain of calibrations which link or trace a measuring instrument to the National Bureau of Standards.

6. Correlation Coefficient – A measure of the linear interdependence between two variables. It varies between -1 and +1 with the intermediate value of zero indicating the absence of correlation. The limiting values indicate perfect negative (inverse) or positive correlation (Fig. IX-2).

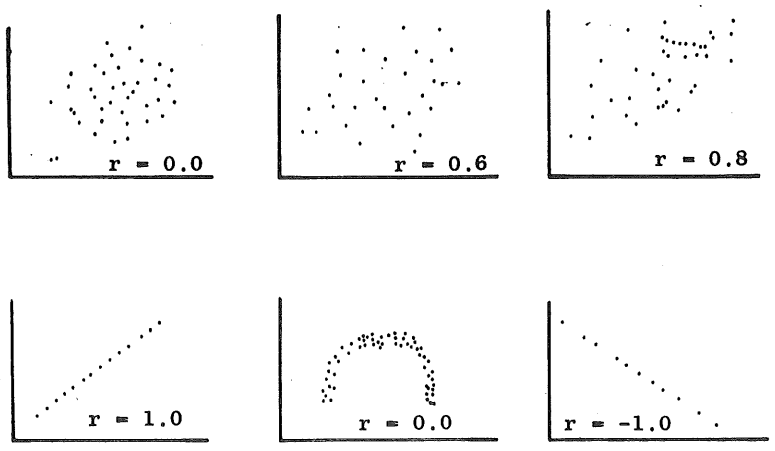

Fig. IX-2 Correlation Coefficients

7. Coverage - A property of confidence intervals with the connotation of including or containing within the interval with a specified relative frequency. Ninety-five-percent confidence intervals provide 95-percent coverage of the true value. That is, in repeated sampling when a 95-percent confidence interval is constructed for each sample, over the long run the intervals will contain the true value 95 percent of the time.

8. Degrees of Freedom (df) – A sample of N values is said to have N degrees of freedom, and a statistic calculated from it is also said to have N degrees of freedom. But if k functions of the sample values are held constant, the number of degrees of freedom is reduced by k. For example, the statistic $\sum_{i=1}^{N} (X_i - \bar{X})^2$, where $\bar{X}$ is the sample mean, is said to have N - 1 degrees of freedom. The justification for this is that (a) the sample mean is regarded as fixed or (b) in normal variation the N quantities $(X_i - \bar{X})$ are distributed independently of $\bar{X}$ and hence may be regarded as N - 1 independent variates or N variates connected by the linear relation $\Sigma(X_i - \bar{X}) = 0$.

9. Elemental Error – The bias and/or precision error associated with a single component or process in a chain of components or processes.

10. Estimate – A value calculated from a sample of data as a substitute for an unknown population constant. For example, the sample standard deviation (S) is the estimate which describes the population standard deviation (σ).

11. Joint Distribution Function – A function describing the simultaneous distribution of two variables. The cumulative probability distribution for 2 variables.

12. Laboratory Standard – An instrument which is calibrated periodically at the NBS. The laboratory standard may also be called an interlab standard.

13. Mathematical Model – A mathematical description of a system. It may be a formula, a computer program, or a statistical model.

14. Measurement Error – The collective term meaning the difference between the true value and the measured value. Includes both bias and precision error; see accuracy and uncertainty. Accuracy implies small measurement error and small uncertainty.

15. Multiple Measurement – More than a single concurrent measurement of the same parameter.

16. NBS – National Bureau of Standards. The reference or source of the true value for all measurements in the United States of America.

17. Parameter – An unknown quantity which may vary over a certain set of values. In statistics, it occurs in expressions defining frequency distributions (population parameters). Examples: the mean of a normal distribution, the expected value of a Poisson variable.

18. Precision Error – The random error observed in a set of repeated measurements. This error is the result of a large number of small effects, each of which is negligible alone.

19. Precision Index – The precision index is defined herein as the computed standard deviation of the measurements.

$$s = \sqrt{\frac{\sum_{i=1} (X_i - \bar{X})^2}{N-1}} \quad \text{usually, but sometimes } S = \sqrt{\sum_i s^2}$$

20. Proving Ring – Laboratory standard for force measurements.

21. Sample Size (N) – The number of sampling units which are to be included in the sample.

22. Standard Deviation (σ) – The most widely used measure of dispersion of a frequency distribution. It is the precision index and is the square root of the variance: S is an estimate of σ calculated from a sample of data.

23. Standard Error of Estimate – The measure of dispersion of the dependent variable (output) about the least-squares line in curve fitting or regression analysis. It is the precision index of the output for any fixed level of the independent variable input. The formula for calculating this is

$$S_{EE} = \sqrt{\frac{\sum_{i=1}^{N} \left(Y_{OBS} - Y_{CAL}\right)^2}{N-K}}$$

for a curve fit for N data points in which K constants are estimated for the curve.

24. Standard Error of the Mean – An estimate of the scatter in a set of sample means based on a given sample of size N. The sample standard deviation (S) is estimated as

$$S = \sqrt{(X_i - \bar{X})^2/(N-1)}$$

Then the standard error of the mean is $S/\sqrt{N}$. In the limit, as N becomes large, the estimated standard error of the mean converges to zero, while the standard deviation converges to a fixed non-zero value.

25. Statistic – A parameter value based on data. $\bar{X}$ and S are statistics. The bias limit, a judgment, is not a statistic.

26. Statistical Confidence Interval – An interval estimate of a population parameter based on data. The confidence level establishes the coverage of the interval. That is, a 95-percent confidence interval would cover or include the true value of the parameter 95 percent of the time in repeated sampling.

27. Statistical Quality Control Charts – A plot of the results of repeated sampling versus time. The central tendency and upper and lower limits are marked. Points outside the limits and trends and sequences in the points indicate non-random conditions.

28. Student's "t" Distribution (t) – The ratio of the difference between the population mean and the sample mean to a sample standard deviation (multiplied by a constant) in samples from a normal population. It is used to set confidence limits for the population mean.

29. Taylor's Series – A power series to calculate the value of a function at a point in the neighborhood of some reference point. The series expresses the difference or differential between the new point and the reference point in terms of the successive derivatives of the function.

Its form is $f(X) - f(a) = \sum_{r=1}^{r=n-1} \frac{(X-a)^r}{r!} f^{(r)}(a) + R_n$

where $f^{(r)}(a)$ denotes the value of the rth derivative of f(x) at the reference point $X = a$. Commonly, if the series converges, the remainder R_n is made infinitesimal by selecting an arbitary number of terms.

30. Traceability – The ability to trace the calibration of a measuring device through a chain of calibrations to the National Bureau of Standards.

31. Transducer – A device for converting mechanical stimulation into an electrical signal. It is used to measure quantities like pressure, temperature, and force.

32. Transfer Standard – A laboratory instrument which is used to calibrate working standards and which is periodically calibrated against the laboratory standard.

33. True Value – The reference value defined by the National Bureau of Standards which is assumed to be the true value of any measured quantity.

34. Uncertainty (U) – The maximum error reasonably expected for the defined measurement process: $U = \pm(B + t_{95} S)$.

35. Variance (σ^2) – A measure of scatter or spread of a distribution. It is estimated by $S^2 = \frac{\Sigma(X_i - \bar{X})^2}{N-1}$ from a sample of data. The variance is the square of the standard deviation.

36. Working Standard – An instrument which is calibrated in a laboratory against an interlab or transfer standard and is used as a standard in calibrating measuring instruments.

APPENDIXES

A. PRECISION INDEX FOR UNIFORM DISTRIBUTION OF ERROR
B. PROPAGATION OF ERRORS BY TAYLOR'S SERIES
C. ESTIMATES OF THE PRECISION INDEX FROM MULTIPLE MEASUREMENTS
D. OUTLIER DETECTION
E. TABLES

APPENDIX A
PRECISION INDEX FOR UNIFORM DISTRIBUTION OF ERROR

The precision index for a uniform distribution of error is easily calculated by considering the definition of the variance:

$$\sigma^2 = \int_a^b (x - \mu)^2 \, p(x) \, dx \qquad \text{(the general formula for the variance).}$$

For a uniform distribution (Fig. A-1) between the limits of a and b, the formula is

$$\sigma^2 = \int_a^b \left(x - \frac{a + b}{2}\right)^2 \frac{1}{(b - a)} \, dx$$

where (a + b)/2 is the mean (μ) of the uniform distribution.

$$\sigma^2 = \int_a^b \left(x^2 - (a + b)\, x + \frac{a^2 + 2ab + b^2}{4}\right) \frac{1}{(b - a)} \, dx$$

$$\sigma^2 = \frac{1}{(b - a)} \left(\int_a^b x^2 \, dx - \frac{(a + b)}{1} \int_a^b x \, dx + \frac{a^2 + 2ab + b^2}{4} \int_a^b dx \right)$$

$$\sigma^2 = \frac{1}{(b - a)} \left[\frac{b^3 - a^3}{3}\right] - \frac{(a + b)}{(b - a)} \left[\frac{b^2 - a^2}{2}\right] + \frac{a^2 + 2ab + b^2}{4(b - a)} \left[b - a\right]$$

$$\sigma^2 = \frac{(b - a)^2}{12} \quad \text{or} \quad \sigma = \sqrt{\frac{(b - a)^2}{12}}$$

When a = -1 and b = +1, $\sigma = \sqrt{\frac{[1.0 - (-1.0)]^2}{12}} = \sqrt{\frac{1}{3}} \approx 0.577$

when a = -1/2 and b = +1/2, $\sigma = \sqrt{\frac{\left(\frac{1}{2} - \left(-\frac{1}{2}\right)\right)^2}{12}} = \sqrt{1/12} \approx 0.3$

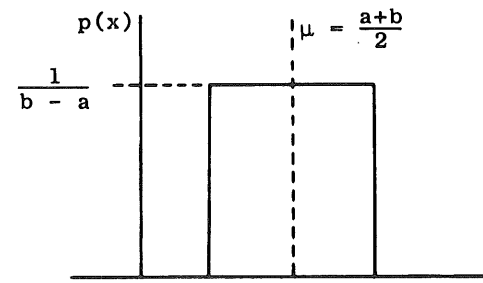

Fig. A-1 Uniform Distribution of Error

APPENDIX B
PROPAGATION OF ERRORS BY TAYLOR'S SERIES

GENERAL

The proofs in this section are shown for two- and three-variable functions. These proofs can be easily extended to functions with more variables, although, because of its length, the general case is not shown here.

TWO INDEPENDENT VARIABLES

If it is assumed that response Z is defined as a function of measured variables (x and y), the two restrictions that must be considered are

1. Z is continuous in the neighborhood of the point (μ_x, μ_y). Both x and y will have error distributions about this point and the notation (μ_x and μ_y) indicates the mean values of these distributions.

2. Z has continuous partial derivatives in a neighborhood of the point (μ_x, μ_y).

These conditions are satisfied if the functions to be considered are restricted to smooth curves in a neighborhood of the point with no discontinuities (jumps or breaks in the curve). The Taylor's series expansion for Z is

$$Z = Z_{\mu_x, \mu_y} + \frac{\partial Z}{\partial x}(x - \mu_x) + \frac{\partial Z}{\partial y}(y - \mu_y) + R_2 \tag{B-1}$$

where $\frac{\partial Z}{\partial x}$ and $\frac{\partial Z}{\partial y}$ are evaluated at the point (μ_x, μ_y).

$$R_2 \leq \frac{1}{2}\left[\frac{\partial^2 Z}{\partial x^2}(x - \mu_x)^2 + \frac{\partial^2 Z}{\partial y^2}(y - \mu_y)^2\right] \tag{B-2}$$

where $\frac{\partial^2 Z}{\partial x^2}$ and $\frac{\partial^2 Z}{\partial y^2}$ are evaluated at (θ_1, θ_2) with θ_1 between x and μ_x, and θ_2 between y and μ_y.

The quantity R_2, the remainder after two terms, is not significant if either:

1. $(x - \mu_x)$ and $(y - \mu_y)$ are small

2. The second partials $\frac{\partial^2 Z}{\partial x^2}$ and $\frac{\partial^2 Z}{\partial y^2}$ are small or zero. These partials are zero for linear functions.

By assuming R_2 to be small or zero, Eq. (B-1) becomes

$$Z \doteq \mu_Z + \frac{\partial Z}{\partial x}(x - \mu_x) + \frac{\partial Z}{\partial y}(y - \mu_y) \tag{B-3}$$

or

$$Z - \mu_Z \doteq \frac{\partial Z}{\partial x}(x - \mu_x) + \frac{\partial Z}{\partial y}(y - \mu_y) \tag{B-4}$$

By defining μ_Z as the average value of the distribution of Z, the difference $(Z - \mu_Z)$ is the difference of Z about its average value. This difference may be approximated by (Eq. (B-4))

$$Z - \mu_Z \approx \frac{\partial Z}{\partial x}(x - \mu_x) + \frac{\partial Z}{\partial y}(y - \mu_y) \tag{B-5}$$

where the partials are evaluated at the point (μ_x, μ_y).

The variation in Z is defined by

$$\sigma_Z^2 \equiv \int (Z - \mu_Z)^2 p_Z dZ$$

where p_Z is the probability density function of Z. Therefore,

$$\sigma_Z^2 \approx \iint \left[\frac{\partial Z}{\partial x}(x - \mu_x) + \frac{\partial Z}{\partial y}(y - \mu_y)\right]^2 p_{xy}\, dxdy \tag{B-6}$$

$$\approx \iint \left[\frac{\partial Z}{\partial x}(x - \mu_x)\right]^2 p_{xy}\, dydx + \iint \left[\frac{\partial Z}{\partial y}(y - \mu_y)\right]^2 p_{xy}\, dxdy + 2\iint \left[\frac{\partial Z}{\partial x}(x - \mu_x)\right]\left[\frac{\partial Z}{\partial y}(y - \mu_y)\right] p_{xy}\, dxdy \tag{B-7}$$

where P_{xy} is the joint distribution function of x and y. Integrating the first term of Eq. (B-7) with respect to y and the second term of Eq (B-7) with respect to x gives

$$\sigma_Z^2 \approx \int \frac{\partial Z^2}{\partial x}(x - \mu_x)^2 p_x dx + \int \frac{\partial Z^2}{\partial y}(y - \mu_y)^2 p_y dy + 2\iint \frac{\partial Z}{\partial x}(x - \mu_x)\frac{\partial Z}{\partial y}(y - \mu_y) p_{xy} dxdy \tag{B-8}$$

If μ_x and μ_y are the means of the distributions of x and y, then define the following:

$$\sigma_x^2 = \int (x - \mu_x)^2 p_x dx \tag{B-9}$$

$$\sigma_y^2 = \int (y - \mu_y)^2 p_y dy \tag{B-10}$$

$$\rho_{xy}\sigma_x\sigma_y = \iint (x - \mu_x)(y - \mu_y) p_{xy}\, dxdy \tag{B-11}$$

where ρ_{xy} is the coefficient of correlation between x and y. Combining the definitions and Eq. (B-8) gives

$$\sigma_Z^2 \approx \left[\frac{\partial Z}{\partial x}^2 \sigma_x^2 + \frac{\partial Z}{\partial y}^2 \sigma_y^2 + 2\frac{\partial Z}{\partial y}\frac{\partial Z}{\partial x}\rho\sigma_x\sigma_y\right] \tag{B-12}$$

If x and y are independent variables, then $\rho = 0$ and

$$\sigma_Z^2 \approx \left(\frac{\partial Z}{\partial x}\right)^2 \sigma_x^2 + \left(\frac{\partial Z}{\partial y}\right)^2 \sigma_y^2 \tag{B-13}$$

THREE INDEPENDENT VARIABLES

If it is assumed that Z is a function of variables x, y, and w, two restrictions must be considered:

1. Z is continuous in a neighborhood of the point (μ_x, μ_y, μ_w)
2. Z has continuous partial derivatives in a neighborhood of (μ_x, μ_y, μ_w)

If these restrictions are satisfied, then the Taylor's series expansion for Z in the vicinity of (μ_x, μ_y, μ_w) is

$$Z = \mu_Z + \frac{\partial Z}{\partial x}(x - \mu_x) + \frac{\partial Z}{\partial y}(y - \mu_y) + \frac{\partial Z}{\partial w}(w - \mu_w) + R_2 \tag{B-14}$$

where $\frac{\partial Z}{\partial x}$, $\frac{\partial Z}{\partial y}$, and $\frac{\partial Z}{\partial w}$ are evaluated at (μ_x, μ_y, μ_w),

$$R_2 \leq \frac{1}{2}\left[\frac{\partial^2 Z}{\partial x^2}(x - \mu_x)^2 + \frac{\partial^2 Z}{\partial y^2}(y - \mu_y)^2 + \frac{\partial^2 Z}{\partial w^2}(w - \mu_w)^2\right] \tag{B-15}$$

These second partials are evaluated at a point $\theta_1, \theta_2, \theta_3$ defined so that θ_1 is between μ_x and x, θ_2 is between μ_y and y, and θ_3 is between μ_w and w. The same restrictions apply to R_2 as defined for two-variable functions.

By assuming R_2 to be small or zero, Eq. (B-14) becomes

$$Z - \mu_Z \doteq \frac{\partial Z}{\partial x}(x - \mu_x) + \frac{\partial Z}{\partial y}(y - \mu_y) + \frac{\partial Z}{\partial w}(w - \mu_w) \tag{B-16}$$

where the partials are evaluated at the point (μ_x, μ_y, μ_w).

The variation in Z is defined by

$$\sigma_Z^2 \equiv \int (Z - \mu_Z)^2 \, p_Z \, dZ \tag{B-17}$$

where p_Z is the probability density function of Z. Therefore,

$$\sigma_Z^2 \approx \iiint \left[\frac{\partial Z}{\partial x}(x - \mu_x) + \frac{\partial Z}{\partial y}(y - \mu_y) + \frac{\partial Z}{\partial w}(w - \mu_w) \right]^2 p_{x,y,w} \, dxdydw \tag{B-18}$$

$$\approx \iiint \left[\frac{\partial Z}{\partial x}(x - \mu_x) \right]^2 p_{x,y,w} \, dwdydx + \ldots$$

$$+ 2 \iiint \frac{\partial Z}{\partial x} \frac{\partial Z}{\partial y}(x - \mu_x)(y - \mu_y) p_{x,y,w} \, dwdxdy + \ldots \tag{B-19}$$

where $p_{x,y,w}$ is the joint distribution function of x, y, and w. Integrating in the proper order produces these results:

$$\sigma_Z^2 \approx \int \left(\frac{\partial Z}{\partial x} \right)^2 (x - \mu_x)^2 p_x \, dx + \ldots + 2 \iint \frac{\partial Z}{\partial x} \frac{\partial Z}{\partial y}(x - \mu_x)(y - \mu_y) \, p_{xy} \, dxdy \tag{B-20}$$

Therefore,

$$\sigma_Z^2 \approx \left(\frac{\partial Z}{\partial x} \right)^2 \sigma_x^2 + \left(\frac{\partial Z}{\partial y} \right)^2 \sigma_y^2 + \left(\frac{\partial Z}{\partial w} \right)^2 \sigma_w^2 + 2 \frac{\partial Z}{\partial x} \frac{\partial Z}{\partial y} \rho_{xy} \sigma_x \sigma_y$$

$$+ 2 \frac{\partial Z}{\partial x} \frac{\partial Z}{\partial w} \rho_{xw} \sigma_x \sigma_w + 2 \frac{\partial Z}{\partial y} \frac{\partial Z}{\partial w} \rho_{yw} \sigma_y \sigma_w \tag{B-21}$$

If x, y, and w are independent variables, then $\rho_{xy} = \rho_{xw} = \rho_{yw} = 0$ and

$$\sigma_Z^2 \approx \left(\frac{\partial Z}{\partial x} \right)^2 \sigma_x^2 + \left(\frac{\partial Z}{\partial y} \right)^2 \sigma_y^2 + \left(\frac{\partial Z}{\partial w} \right)^2 \sigma_w^2 \tag{B-22}$$

MONTE CARLO SIMULATION

To determine the restrictions that must be placed on applications of the method of partial derivatives, a Monte Carlo Simulator was designed to provide simulation checks for the computation of various functions. Comparative results are listed in Tables B-1 and B-2.

Table B-1 contrasts the results of the Monte Carlo simulation of the functions tabulated, column (7), with the estimates using Partial Derivatives, column (6). One thousand functional values were obtained in each simulation. Column (1) identifies the function simulated and column (2) gives the number of the simulation run. Column (3), Theoretical Input, includes the parameters of the populations from which the random

Table B-1 Results of Monte Carlo Simulation for Theoretical Input (σ_x^2, μ_x, σ_y^2, μ_y)

(1) Function	(2) Simulation Run Number	(3) Theoretical Input σ_x^2	μ_x	σ_y^2	μ_y	(4) Method of Partials Estimated Variance (Theoretical)	(5) Method of Partials Estimated Variance (Actual Input)	(6) Input Variance Corrected for Nonindependence (Method of Partials)	(7) Observed Variance (Simulator Results)
x + y	1	1.0	10	4.0	20	5.0	4.9477	4.8496	4.8567
	2	1.0	10	4.0	20	5.0	4.9186	4.8435	4.8506
	3	1.0	10	4.0	20	5.0	5.0786	4.9493	4.9564
	4	1.0	10	4.0	20	5.0	5.1639	5.2444	5.2515
x - y	1	1.0	10	4.0	20	5.0	4.9477	5.0358	5.0410
	2	1.0	10	4.0	20	5.0	4.9186	4.9937	4.9885
	3	1.0	10	4.0	20	5.0	5.0786	5.2079	5.2028
	4	1.0	10	4.0	20	5.0	5.1639	5.0834	5.0782
(x)(y)	1	1.0	10	4.0	20	800.0	792.81	773.27	768.63
	2	1.0	10	4.0	20	800.0	794.33	779.29	797.48
	3	1.0	10	4.0	20	800.0	802.28	776.41	775.78
	4	1.0	10	4.0	20	800.0	867.67	883.85	883.38
x/y	1	1.0	10	4.0	20	0.005	0.0050	0.0051	0.0054
	2	1.0	10	4.0	20	0.005	0.0050	0.0051	0.0054
	3	1.0	10	4.0	20	0.005	0.0050	0.0052	0.0055
	4	1.0	10	4.0	20	0.005	0.0054	0.0053	0.0057

numbers were drawn. Column (4) lists the method of partials estimates of variance for the function based on the theoretical input (column 3). Column (5) lists the estimates of variance for the function calculated using the method of partial derivatives from the observed variation of the variables x and y. Column (6) gives column (5) corrected for the observed correlation between the pairs of x, y input values. The correction factor is:

$$2\rho\sigma_x^2\sigma_y^2\frac{\partial Z}{\partial x}\frac{\partial Z}{\partial y}$$

where ρ is the observed correlation between paired values of x and y, σ_x^2 and σ_y^2 are the observed variances of x and y, and $\frac{\partial Z}{\partial x}$ and $\frac{\partial Z}{\partial y}$ are the partial derivatives of the function Z. Column (7) lists the simulator results for the function (column 1) for 1000 data points.

Table B-2 Results of Monte Carlo Simulation for Theoretical Input μ_{x_i}, $\sigma_{x_i}^2$

(1) Function Z	(2) Number of Simulations	(3) Theoretical Input μ_{x_i}	$\sigma_{x_i}^2$	(4) Estimated Parameters (Method of Partials) μ_Z	σ_Z^2	(5) Simulation Results μ_Z	σ_Z^2
$(x_1x_2)/x_3$	2	20	1.0	20	3.00	20.2 20.6	2.56 3.24
$(x_1x_2)/(x_3x_4x_5)$	1	20	1.0	0.05	3.12×10^{-5}	0.0505	3.6×10^{-5}
$(x_1x_2x_3x_4)/(x_5x_6x_7)$	2	20	1.0	20	7.00	20.04 20.25	8.41 8.41
$(x_1x_2x_3)\Big/\left(\prod_{i=4}^{9} x_i\right)$	1	20	1.0	1.25×10^{-4}	3.52×10^{-10}	1.29×10^{-4}	4.0×10^{-10}
$\left(\prod_{i=1}^{6} x_i\right)\Big/(x_7x_8x_9)$	2	20	1.0	8000	1.44×10^{6}	8150 8300	1.69×10^{6} 1.82×10^{6}

Columns (1) through (3) of Table B-2 present the input to the Monte Carlo Simulator. The theoretical imput column (3) shows the parameters of the population of random numbers that were used to produce the functional values. Column (5) summarizes the results of the simulation. These results may be compared with the estimates from the method of partials, column (4).

Simulation results have shown that the method of partial derivatives is most accurate for functions involving sums and differences of the observed variables. For these functions, if the variables are mutually independent, the Taylor's series is exact for any magnitude of error in the measured parameters. If the variables are not mutually independent, a correction factor can be computed that will ensure exactitude of the method. (The correction factor $(2\rho_{xy}\sigma_x\sigma_y \frac{\partial Z}{\partial x}\frac{\partial Z}{\partial y})$ is the third term in Eq. (B-12). If ρ_{xy} is not zero, this term should be included in estimating $\sigma_Z{}^2$. From data, ρ_{xy} may be estimated with

$$r = \frac{S_{xy}}{S_x S_y} = \frac{\Sigma (x_i - \bar{x})\ (y_i - \bar{y})}{\sqrt{\Sigma (x_i - \bar{x})^2\ \Sigma (y_i - \bar{y})^2}}$$

where n pairs of observations are available and $\bar{x}$ and $\bar{y}$ are the average of the x_i and y_i values, respectively.)

Close approximations can be made for errors that exist in functions involving products and quotients of independently varying observed values if the ratio of measured errors to their respective nominal values is small (less than 0.1). The approximation improves as measured errors decrease in relation to their nominals. For all of the functions examined involving two or more independent variables, the approximation is within 10 percent of the true error. The simulation results are summarized in Tables B-1 and B-2.

Table B-3 shows the Taylor's formula for several functions. In addition, the Taylor's formula for the coefficient of variation is also listed. The coefficient of variation is easily converted to a percentage variation by multiplying by 100.

Table B-3 Error Propagation Formulas

Function	Taylor's Formula	Coefficient of Variation Formula
$w = f(x,y)$	$S_w^2 \approx \left(\frac{\partial w}{\partial x} S_x\right)^2 + \left(\frac{\partial w}{\partial y} S_y\right)^2$	- - - - - - - - - -
$w = Ax + By$	$S_w^2 \approx A^2 S_x^2 + B^2 S_y^2$	$V_w^2 \approx \frac{A^2 x^2 V_x^2 + B^2 y^2 V_y^2}{(Ax + By)^2}$
$w = \frac{1}{y}$	$S_w^2 \approx \frac{S_y^2}{y^4}$	$V_w^2 \approx V_y^2$
$w = \frac{x}{x + y}$	$S_w^2 \approx \left(\frac{y S_x}{(x+y)^2}\right)^2 + \left(\frac{x S_y}{(x+y)^2}\right)^2$	$V_w^2 \approx y^2 (V_x^2 + V_y^2) / (x+y)^2$
$w = \frac{x}{1 + x}$	$S_w^2 \approx \frac{S_x^2}{(1 + x)^4}$	$V_w^2 \approx \frac{V_x^2}{(1+x)^2}$
$w = xy$	$S_w^2 \approx (yS_x)^2 + (xS_y)^2$	$V_w^2 \approx V_x^2 + V_y^2$
$w = x^2$	$S_w^2 \approx 4x^2 S_x^2$	$V_w^2 \approx 4V_x^2$
$w = x^{1/2}$	$S_w^2 \approx \frac{S_x^2}{4x}$	$V_w^2 \approx \frac{V_x^2}{4}$
$w = \ln x$	$S_w^2 \approx \frac{S_x^2}{x^2}$	$V_w^2 \approx \left(\frac{V_x}{\ln x}\right)^2$
$w = kx^a y^b$	$S_w^2 \approx \left(aky^b x^{a-1} S_x\right)^2 + \left(bkx^a y^{b-1} S_y\right)^2$	$V_w^2 \approx (aV_x)^2 + (bV_y)^2$

where:

$$V_x = \frac{S_x}{\bar{x}}$$

$$V_y = \frac{S_y}{\bar{y}}$$

$$V_w = \frac{S_w}{\bar{w}} \; ; \quad \bar{w} = f(\bar{x}, \bar{y})$$

APPENDIX C
ESTIMATES OF THE PRECISION INDEX FROM MULTIPLE MEASUREMENTS

INTRODUCTION

The derivatives, proofs, and examples of this section are presented for measurement schemes using two instruments measuring the same parameter. These instruments are read simultaneously and the difference between the readings is analyzed statistically to estimate instrumentation precision index. The proofs and derivations can easily be extended to instrumentation setups using more than two instruments by considering all independent combinations of instrument pairs. Instrumentation pairs which have a fixed constant locational bias between them can also be analyzed to provide estimates of precision index.

DISCUSSION

In any measurement system, if the parameter which is being measured is a constant, the precision error of the measurement instruments is easy to identify. The variance (S^2) of the measurements (X_i) about the average measurement ($\bar{X}$) provides an unbiased estimate of the variance of the instrument:

$$S^2 = \frac{\Sigma(X_i - \bar{X})^2}{N - 1} \qquad \text{(for N measurements)} \tag{C-1}$$

In the usual case, the measured parameter is not constant. Then the variation of the readings is increased by the variation of the parameter, and any directly computed statistic is subjected to large errors. However, multiple instruments can be analyzed to estimate the precision error in the measurement system.

For example, if two instruments are measuring a parameter X, then an appropriate mathematical model for each reading would be $X_i + \epsilon_{ij}$ where X_i is a typical parameter value and ϵ_{ij} is the corresponding precision error for the jth instrument. (For simplicity, bias error is ignored as it has no effect on these methods.) A series of such readings is illustrated in Table C-1.

Table C-1 Multiple Measurements of a Parameter

True Value	Instrument One	Instrument Two
X_1	$X_1 + \epsilon_{11}$	$X_1 + \epsilon_{12}$
X_2	$X_2 + \epsilon_{21}$	$X_2 + \epsilon_{22}$
X_3	$X_3 + \epsilon_{31}$	$X_3 + \epsilon_{32}$
⋮	⋮	⋮
X_n	$X_n + \epsilon_{n1}$	$X_n + \epsilon_{n2}$

This list is provided by making simultaneous readings of instruments one and two. By subtracting the reading of instrument one from instrument two, a column of differences can be produced which is independent of the variation of the parameter (Table C-2).

Table C-2 Multiple Measurement Difference

Instrument One	Instrument Two	Average	Difference
$X_1 + \epsilon_{11}$	$X_1 + \epsilon_{12}$	$X_1 + \frac{\epsilon_{11} + \epsilon_{12}}{2}$	$\epsilon_{11} - \epsilon_{12} = \Delta_1$
$X_2 + \epsilon_{21}$	$X_2 + \epsilon_{22}$	$X_2 + \frac{\epsilon_{21} + \epsilon_{22}}{2}$	$\epsilon_{21} - \epsilon_{22} = \Delta_2$
$X_3 + \epsilon_{31}$	$X_3 + \epsilon_{32}$	$X_3 + \frac{\epsilon_{31} + \epsilon_{32}}{2}$	$\epsilon_{31} - \epsilon_{32} = \Delta_3$
.	.	.	.
.	.	.	.
.	.	.	.
$X_n + \epsilon_{n1}$	$X_n + \epsilon_{n2}$	$X_n + \frac{\epsilon_{n1} + \epsilon_{n2}}{2}$	$\epsilon_{n1} - \epsilon_{n2} = \Delta_n$

The variation of these differences (S_Δ) provides an unbiased estimate of the precision error of the average reading of the two instruments. That is, S_Δ can be used to estimate $S_{reading}$ based on Eq. (C-1).

$$S_\Delta = \sqrt{\frac{\sum_{i=1}^{n} (\Delta_i - \bar{\Delta})^2}{n - 1}} \tag{C-2}$$

where $\bar{\Delta}$ is the average difference between the meters and n is the number of differences. It can be proved that the estimate of the precision index of the average reading is then

$$S_\Delta/2 = \sqrt{\frac{\sum_{i=1}^{n} (\Delta_i - \bar{\Delta})^2}{4(n - 1)}} \tag{C-3}$$

This is based on the assumption that the two meters have independent precision errors. The formulation is derived from Taylor's Series expansion in Appendix B, for precision errors in calculated values. For example, if a single pair of multiple readings is made, the error is $(\epsilon_{i1} + \epsilon_{i2})/2$ if the average of the two readings is recorded. The precision index of this average value may be estimated using the Taylor's series expansion:

$$S_{\left(\frac{\epsilon_{i1} + \epsilon_{i2}}{2}\right)} \approx \sqrt{\left(\frac{\partial\left(\frac{\epsilon_{i1} + \epsilon_{i2}}{2}\right)}{\partial \epsilon_{i1}} S_{\epsilon_{i1}}\right)^2 + \left(\frac{\partial\left(\frac{\epsilon_{i1} + \epsilon_{i2}}{2}\right)}{\partial \epsilon_{i2}} S_{\epsilon_{i2}}\right)^2} \tag{C-4}$$

Thus

$$S_{\left(\frac{\epsilon_{i1} + \epsilon_{i2}}{2}\right)} \approx \sqrt{\left(\frac{1}{2} S_{\epsilon_{i1}}\right)^2 + \left(\frac{1}{2} S_{\epsilon_{i2}}\right)^2} \tag{C-5}$$

and

$$S_{\left(\frac{\epsilon_{i1} + \epsilon_{i2}}{2}\right)} \approx \sqrt{\frac{1}{4}\left(S^2_{\epsilon_{i1}} + S^2_{\epsilon_{i2}}\right)} = \frac{1}{2}\sqrt{S_{\epsilon_{i1}}{}^2 + S_{\epsilon_{i2}}{}^2} \tag{C-6}$$

In the same manner, the precision index of $\epsilon_{i1} - \epsilon_{i2}$ (Eq. (C-2)) can be shown to be:

$$S_{\left(\epsilon_{i1} - \epsilon_{i2}\right)} \approx \sqrt{\left(\frac{\partial\left(\epsilon_{i1} - \epsilon_{i2}\right)}{\partial \epsilon_{i1}} S_{\epsilon_{i1}}\right)^2 + \left(\frac{\partial\left(\epsilon_{i1} - \epsilon_{i2}\right)}{\partial \epsilon_{i2}} S_{\epsilon_{i2}}\right)^2} \tag{C-7}$$

or

$$S_{\left(\epsilon_{i1} - \epsilon_{i2}\right)} \approx \sqrt{(1)^2 S^2_{\epsilon_{i1}} + (-1)^2 S^2_{\epsilon_{i2}}} \tag{C-8}$$

By combining Eqs. (C-2), (C-6), and (C-8), the precision error estimate for the average reading of Table C-2 is

$$S_{\left(\frac{\epsilon_{i1} + \epsilon_{i2}}{2}\right)} \approx \frac{1}{2}\sqrt{S^2_{\epsilon_{i1}} + S^2_{\epsilon_{i2}}} \approx \frac{1}{2} S_{\left(\epsilon_{i1} - \epsilon_{i2}\right)} = \frac{1}{2} S_{\Delta} = \sqrt{\frac{\sum_{i=1}^{n} (\Delta_i - \bar{\Delta})^2}{4(n-1)}} \tag{C-9}$$

The method described in the preceding discussion does not include long-term drifts, calibration errors, and other precision errors that do not vary from data point-to-data point, from stand-to-stand, and from calibration-to-calibration. A new mathematical model must be developed based on an engineering analysis including these effects.

To illustrate the method, the mathematical model derived for a turbojet engine will be used. Again, X is the parameter being measured; then

$$\text{Reading}_{\ell} = X_{ij\ell} + \alpha_i + \beta_{ij} + \epsilon_{ij\ell}$$

is the mathematical model of reading ℓ of a typical instrument during run j and since calibration i. The model assumes a within test (short-term) component of precision error ($\epsilon_{ij\ell}$), a test-to-test (long-term) component or precision error (β_{ij}) which is constant within a test and a calibration-to-calibration error (a_i) which is constant within each calibration and within test within each calibration.

Table C-3 illustrates a series of readings of a multiple instrumented parameter, assuming this model and the differences of the simultaneous readings of instruments one and two. Notice that, within each run, the run-to-run and calibration-to-calibration components are constant. Between the averages of each run, the within run components are reduced and the calibration-to-calibration components are constant allowing estimates of run-to-run components. Finally, the between two calibrations, the within run, and run-to-run components are reduced allowing an estimate of calibration-to-calibration error. The method of analysis is that of a one-way nested analysis of variance.

The analysis can be completed using the formulas of Table C-4. The last column of this table provides the estimates of the precision index for calibration-to-calibration error, run-to-run error, and within run error. The third column, mean square, is calculated by dividing the value of the sum of squares (column 1) by the proper degrees of freedom (column 2).

The estimate of the total precision index, for a multiple instrumented parameter (average of two measurements) on a particular run and calibration, would be the root-sum-square of the three estimates: within test precision index (S_{wt}), test-to-test precision index (S_{tt}), and calibration-to-calibration precision index (S_{cc}); that is,

$$S_T^2 = S_{wt}^2 + S_{tt}^2 + S_{cc}^2$$

The degrees of freedom for this estimate can be calculated from the degrees of freedom for each estimate using the Welch-Satterthwaite formula.

Table C-3 Differences in Readings of Multiple Instruments

		1ST INSTRUMENT	2ND INSTRUMENT	DIFFERENCES	DELTAS
Cal 1	1st Run	$X_{111} + \alpha_{11} + \beta_{111} + \epsilon_{1111}$	$X_{111} + \alpha_{12} + \beta_{112} + \epsilon_{1112}$	$\alpha_{11} + \beta_{111} + \epsilon_{1111} - \left[\alpha_{12} + \beta_{112} + \epsilon_{1112}\right]$	$= \Delta_{111}$
		$X_{112} + \alpha_{11} + \beta_{111} + \epsilon_{1121}$	$X_{112} + \alpha_{12} + \beta_{112} + \epsilon_{1122}$	$\alpha_{11} + \beta_{111} + \epsilon_{1121} - \left[\alpha_{12} + \beta_{112} + \epsilon_{1122}\right]$	$= \Delta_{112}$
		. . . . .	. . . . .	. . . . .	. . . .
		$X_{11n} + \alpha_{11} + \beta_{111} + \epsilon_{11n1}$	$X_{11n} + \alpha_{12} + \beta_{112} + \epsilon_{11n2}$	$\alpha_{11} + \beta_{111} + \epsilon_{11n1} - \left[\alpha_{12} + \beta_{112} + \epsilon_{11n2}\right]$	$= \Delta_{11n}$
	2nd Run	$X_{121} + \alpha_{11} + \beta_{121} + \epsilon_{2111}$	$X_{121} + \alpha_{12} + \beta_{122} + \epsilon_{2112}$	$\alpha_{11} + \beta_{121} + \epsilon_{2111} - \left[\alpha_{12} + \beta_{122} + \epsilon_{2112}\right]$	$= \Delta_{211}$
		$X_{122} + \alpha_{11} + \beta_{121} + \epsilon_{2121}$	$X_{122} + \alpha_{12} + \beta_{122} + \epsilon_{2122}$	$\alpha_{11} + \beta_{121} + \epsilon_{2121} - \left[\alpha_{12} + \beta_{122} + \epsilon_{2122}\right]$	$= \Delta_{212}$
		. . . . .	. . . . .	. . . . .	. . . .
		$X_{12n} + \alpha_{11} + \beta_{121} + \epsilon_{21n1}$	$X_{12n} + \alpha_{12} + \beta_{122} + \epsilon_{21n2}$	$\alpha_{11} + \beta_{121} + \epsilon_{21n1} - \left[\alpha_{12} + \beta_{122} + \epsilon_{21n2}\right]$	$= \Delta_{21n}$
	Kth Run	$X_{1K1} + \alpha_{11} + \beta_{1K1} + \epsilon_{K111}$	$X_{1K1} + \alpha_{12} + \beta_{1K2} + \epsilon_{K112}$	$\alpha_{11} + \beta_{1K1} + \epsilon_{K111} - \left[\alpha_{12} + \beta_{1K2} + \epsilon_{K112}\right]$	$= \Delta_{K11}$
		$X_{1K2} + \alpha_{11} + \beta_{1K1} + \epsilon_{K121}$	$X_{1K2} + \alpha_{12} + \beta_{1K2} + \epsilon_{K122}$	$\alpha_{11} + \beta_{1K1} + \epsilon_{K121} - \left[\alpha_{12} + \beta_{1K2} + \epsilon_{K122}\right]$	$= \Delta_{K12}$
		. . . . .	. . . . .	. . . . .	. . . .
		$X_{1Kn} + \alpha_{11} + \beta_{1K1} + \epsilon_{K1n1}$	$X_{1Kn} + \alpha_{12} + \beta_{1K2} + \epsilon_{K1n2}$	$\alpha_{11} + \beta_{1K1} + \epsilon_{K1n1} - \left[\alpha_{12} + \beta_{1K2} + \epsilon_{K1n2}\right]$	$= \Delta_{K1n}$
Cal 2	1st Run	$X_{211} + \alpha_{21} + \beta_{211} + \epsilon_{1211}$	$X_{211} + \alpha_{22} + \beta_{212} + \epsilon_{1212}$	$\alpha_{21} + \beta_{211} + \epsilon_{1211} - \left[\alpha_{22} + \beta_{212} + \epsilon_{1212}\right]$	$= \Delta_{121}$
		$X_{212} + \alpha_{21} + \beta_{211} + \epsilon_{1221}$	$X_{212} + \alpha_{22} + \beta_{212} + \epsilon_{1222}$	$\alpha_{21} + \beta_{211} + \epsilon_{1221} - \left[\alpha_{22} + \beta_{212} + \epsilon_{1222}\right]$	$= \Delta_{122}$
		. . . . .	. . . . .	. . . . .	. . . .
		$X_{21n} + \alpha_{21} + \beta_{211} + \epsilon_{12n1}$	$X_{21n} + \alpha_{22} + \beta_{212} + \epsilon_{12n2}$	$\alpha_{21} + \beta_{211} + \epsilon_{12n1} - \left[\alpha_{22} + \beta_{212} + \epsilon_{12n2}\right]$	$= \Delta_{12n}$
	2nd Run	$X_{221} + \alpha_{21} + \beta_{221} + \epsilon_{2211}$	$X_{221} + \alpha_{22} + \beta_{222} + \epsilon_{2212}$	$\alpha_{21} + \beta_{221} + \epsilon_{2211} - \left[\alpha_{22} + \beta_{222} + \epsilon_{2212}\right]$	$= \Delta_{221}$
		$X_{222} + \alpha_{21} + \beta_{221} + \epsilon_{2221}$	$X_{222} + \alpha_{22} + \beta_{222} + \epsilon_{2222}$	$\alpha_{21} + \beta_{221} + \epsilon_{2221} - \left[\alpha_{22} + \beta_{222} + \epsilon_{2222}\right]$	$= \Delta_{222}$
		. . . . .	. . . . .	. . . . .	. . . .
		$X_{22n} + \alpha_{21} + \beta_{221} + \epsilon_{22n1}$	$X_{22n} + \alpha_{22} + \beta_{222} + \epsilon_{22n2}$	$\alpha_{21} + \beta_{221} + \epsilon_{22n1} - \left[\alpha_{22} + \beta_{222} + \epsilon_{22n2}\right]$	$= \Delta_{22n}$
	Kth Run	$X_{2K1} + \alpha_{21} + \beta_{2K1} + \epsilon_{K211}$	$X_{2K1} + \alpha_{22} + \beta_{2K2} + \epsilon_{K212}$	$\alpha_{21} + \beta_{2K1} + \epsilon_{K211} - \left[\alpha_{22} + \beta_{2K2} + \epsilon_{K212}\right]$	$= \Delta_{K21}$
		$X_{2K2} + \alpha_{21} + \beta_{2K1} + \epsilon_{K221}$	$X_{2K2} + \alpha_{22} + \beta_{2K2} + \epsilon_{K222}$	$\alpha_{21} + \beta_{2K1} + \epsilon_{K221} - \left[\alpha_{22} + \beta_{2K2} + \epsilon_{K222}\right]$	$= \Delta_{K22}$
		. . . . .	. . . . .	. . . . .	. . . .
		$X_{2Kn} + \alpha_{21} + \beta_{2K1} + \epsilon_{K2n1}$	$X_{2Kn} + \alpha_{22} + \beta_{2K2} + \epsilon_{K2n2}$	$\alpha_{21} + \beta_{2K1} + \epsilon_{K2n1} - \left[\alpha_{22} + \beta_{2K2} + \epsilon_{K2n2}\right]$	$= \Delta_{K2n}$

Table C-4 Analysis of Precision Error from Multiple Instrument Differences

Source of Variation	Sum of Squares	Degrees of Freedom	Mean Square	Variance Estimates
Between Cals	$\sum_{i=1}^{M} (T_i^2/N_i) - \frac{T^2}{N}$	M-1	$M_2 = \sigma_0^2 + \bar{N}_2\sigma_1^2 + \bar{N}_3\sigma_2^2$	$\sigma^2_{\text{Cal Cal}} = \sigma_2^2 = \frac{M_2 - \sigma_0^2 - \bar{N}_2\sigma_1^2}{\bar{N}_3}$
Between Runs	$\sum_{i=1}^{M}\sum_{j=1}^{K_i} (T_{ij}^2/N_{ij}) - \sum_{i=1}^{M} (T_i^2/N_i)$	R-M	$M_1 = \sigma_0^2 + \bar{N}_1\sigma_1^2$	$\sigma^2_{\text{Run Run}} = \sigma_1^2 = \frac{M_1 - \sigma_0^2}{\bar{N}_1}$
Within Runs	$\sum_{i=1}^{M}\sum_{j=1}^{K_i}\sum_{l=1}^{N_{ij}} \Delta_{ijl}^2 - \sum_{i=1}^{M}\sum_{j=1}^{K_i} (T_{ij}^2/N_{ij})$	N-R	$M_0 = \sigma_0^2$	$\sigma^2_{\text{Within}} = \sigma_0^2$
Total	$\sum_{i=1}^{M}\sum_{j=1}^{K_i}\sum_{l=1}^{N_{ij}} \Delta_{ijl}^2 - \frac{T^2}{N}$	N-1		

$$T = \sum_{i=1}^{M} T_i = \sum_{i=1}^{M}\sum_{j=1}^{K_i} T_{ij} = \sum_{i=1}^{M}\sum_{j=1}^{K_i}\sum_{l=1}^{N_{ij}} \Delta_{ijl}$$

$$N = \sum_{i=1}^{M} N_i = \sum_{i=1}^{M}\sum_{j=1}^{K_i} N_{ij} \qquad R = \sum_{i=1}^{M} K_i$$

$$\bar{N}_1 = \left[N - \sum_{i=1}^{M}\left(\sum_{j=1}^{K_i} N_{ij}^2/N_i\right)\right] / (R-M)$$

$$\bar{N}_2 = \left[\sum_{i=1}^{M}\left(\sum_{j=1}^{K_i} N_{ij}^2/N_i\right) - \sum_{i=1}^{M}\sum_{j=1}^{K_i} N_{ij}^2/N\right] / (M-1)$$

$$\bar{N}_3 = \left(N^2 - \sum_{i=1}^{M} N_i^2\right) \Big/ \left((M-1)N\right)$$

APPENDIX D
OUTLIER DETECTION

GENERAL

All measurement systems may produce wild data points. These points may be caused by temporary or intermittent malfunctions of the measurement system, or they may represent actual variations in the measurement. Errors of this type cannot be estimated as part of the uncertainty of the measurement. The points are out-of-control points for the system and are meaningless as steady-state test data. They should be discarded. Figure D-1 shows two spurious data points (sometimes called outliers).

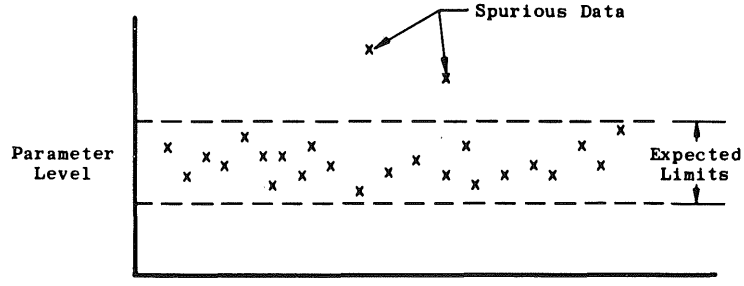

Fig. D-1 Outliers Outside the Range of Acceptable Data

All data should be inspected for wild data points as a continuing quality control check on the measurement process. Identification criteria should be based on engineering analysis of instrumentation, thermodynamics, flow profiles, and past history with similar data. To ease the burden of scanning large masses of data, a computerized routine is available to scan steady-state data and flag suspected outliers. The flagged points should then be subjected to a comprehensive engineering analysis.

This routine is intended to be used in scanning small samples of data from a large number of parameters at many time slices. The work of paging through volumes of data can be reduced to a manageable job with this approach. The computer will scan the data and flag suspect points. The engineer, relieved of the burden of scanning the data, can closely examine each suspected wild point.

ARNOLD ENGINEERING DEVELOPMENT CENTER OUTLIER METHOD

Several general purpose outlier techniques were reviewed and discussed in the ICRPG Handbook CPIA 180. The U.S. Air Force Arnold Engineering Development Center (AEDC) has developed a new technique to flag outliers in small or moderately sized samples of data. This technique was compared with the Thompson's Tau Technique used in ICRPG CPIA 180. The AEDC method as compared with the Thompson's Tau method detects a larger proportion of the outliers in the data, and when no outliers are present, it flags fewer good points. The AEDC method is useful for computer routines since it is fast and requires little core storage. The method discriminates between good data and outliers by examining how far each point lies from the average value.

The first step is to calculate an average value ($\bar{X}$) and a standard deviation (s) from the data.

$$\bar{X} = \sum_{i=1}^{N} \frac{X_i}{N} \qquad s = \pm \sqrt{\frac{\sum_{i=1}^{N} (X_i - \bar{X})^2}{N-1}}$$

Then, from the sample size (N), a test value (C) is calculated from

$$C = \frac{-1.6819236 + 1.6386898N - 0.00721312N^2}{1.0 + 0.59286772N - 0.00355709N^2}$$

when $N < 65$. When $N \geq 65$, $C = 3$ is used. Each data point is tested to determine if it falls in the interval, average value plus or minus the standard deviation times C, i.e.,

$$\bar{X} \pm Cs$$

If a data point falls outside the interval, it is flagged as an outlier.

The formula for calculating C was determined at AEDC and was based on engineering judgment to determine the expected intervals for good data in the range of 10 to 30 samples. Then the curve (C) was fit to the data (Fig. D-2). For sample sizes of 65 or greater, C = 3 should be used.

AN EXAMPLE OF THE AEDC METHOD

The AEDC Fortran Subroutine is used to test the data in Table D-1 for outliers.

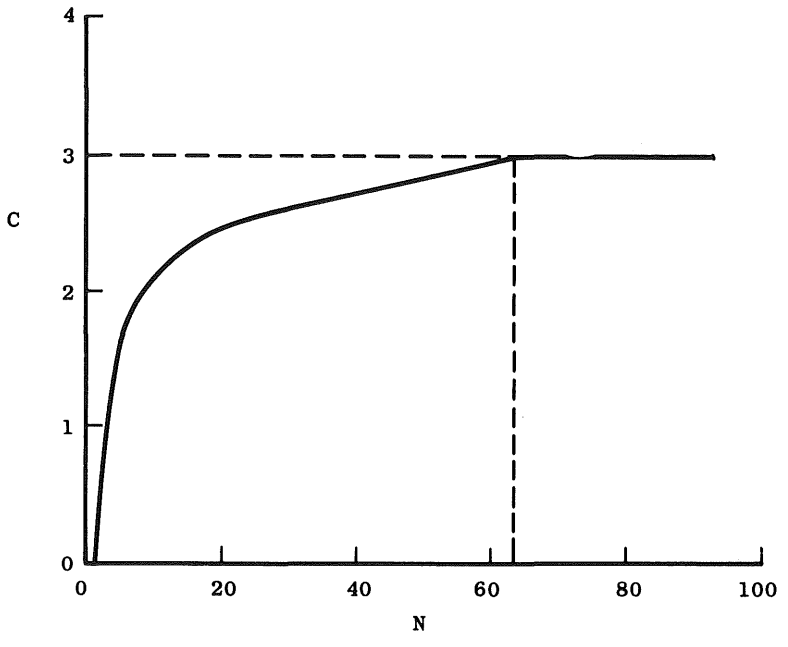

Fig. D-2 Parameter C versus Sample Size

Table D-1 Pressure Data for Outlier Test

Point No.	Pressure, psia
1	12.96
2	13.15
3	13.01
4	13.11
5	13.30
6	13.68
7	13.26
8	13.10
9	12.84
10	13.19
11	13.25
12	13.39
13	13.11
14	13.03
15	12.96

The first step is to calculate the mean ($\bar{X}$) and standard deviation (s) for the data:

$$\bar{X} = \frac{\sum_{i=1}^{15} X_i}{15} = 13.156$$

$$s = \pm\sqrt{\frac{\sum_{i=1}^{15} (X_i - \bar{X})^2}{14}} = \pm 0.2057$$

The test value (C) is calculated based on the sample size (N).

$$C = \frac{-1.6819236 + 1.6386898N - 0.00721312N^2}{1.0 + 0.59286772N - 0.00355709N^2} = 2.3398$$

Each data point is checked to determine if it falls in the interval $\bar{X} \pm Cs$, which in this case is 12.6747 to 13.6373. A convenient method for doing this is to subtract $\bar{X}$ from each data point to determine the deviation ($X_i - \bar{X}$). Then, this is checked against Cs = 2.3398 times 0.2057 = 0.4813.

Table D-2 lists the deviations ($X_i - \bar{X}$) for the data. In this case, point number six has a deviation which is greater than 0.4813. It is flagged as an outlier and printed out by the subroutine.

Table D-2

Point No.	Deviation ($X_i - \bar{X}$)
1	-0.196
2	-0.006
3	-0.146
4	-0.046
5	0.144
6	0.524
7	0.104
8	-0.056
9	-0.316
10	0.034
11	0.094
12	0.234
13	-0.046
14	-0.126
15	-0.196

THE FORTRAN SUBROUTINE

The following is a listing of a subroutine to implement the AEDC outlier rejection method in a computer program. The subroutine is written in American National Standard Fortran IV. The subroutine was compiled and run on an IBM 360, model 75, with a G-level compiler operating under IBM release 20.1.

```
      SUBROUTINE CAVG ( XBAR, SIG , X , N , IELIM )
C
C                AEDC OUTLIER REJECTION SUBROUTINE
C
C
C     XBAR       MEAN CALCULATED AFTER OUTLIERS HAVE BEEN REMOVED FROM
C                DATA
C
C     X          INPUT ARRAY OF SAMPLE DATA
C
C     SIG        STANDARD DEVIATION CALCULATED AFTER OUTLIERS HAVE BEEN
C                REMOVED FROM THE DATA
C
C     N          NUMBER OF DATA POINTS IN DATA SAMPLE, X
C
C     IELIM      NUMBER OF OUTLIERS REJECTED IN SAMPLE OF DATA
C
C
```

```
C      IF A SAMPLE DATA POINT IS FOUND TO BE AN OUTLIER, ITS VALUE IS
C      SET TO 0.0 .
C
C      SAMPLE DATA POINTS EQUAL TO ZERO INPUT TO THE SUBROUTINE ARE
C      DISCARDED FROM THE SAMPLE.
C
C
       DIMENSION X(1) , DEL(100)
       IND = 0
       IELIM = 0
       WRITE(6,102)
  102  FORMAT(/' BEFORE REMOVING OUTLIERS'/)
    1  SUM = 0.
       NN = 0
       DO 3 I=1,N
       IF ( X(I) .EQ. 0. ) GO TO 3
       NN = NN + 1
       SUM = SUM + X(I)
    3  CONTINUE
       IF ( NN .LT. 2 ) RETURN
       XBAR = SUM / NN
       SUM2 = 0.
       DO 4 I = 1,N
       IF ( X(I) .EQ. 0. ) GO TO 4
       DEL(I) = ABS( X(I) - XBAR )
       SUM2 = SUM2 + DEL(I)**2
    4  CONTINUE
       C = 3.
       SIG = SQRT ( SUM2 / ( NN - 1 ))
       WRITE(6,101)XBAR,SIG,NN
  101  FORMAT(/' MEAN=',E20.7,5X,'STD. DEV.=',E20.7,5X,'N=',I5/)
       IF ( IND .EQ. 1 ) RETURN
       IF ( NN .LE. 65 ) C = (-1.6819236D0 + 1.6386898D0 * NN
      1                       -.00721312D0 * NN * NN ) / ( 1.D0
      2                       +.59286772D0 * NN - .00355709D0 * NN * NN )
       CS = C * SIG
       K = NN
       DO 5 I = 1,N
       IF ( X(I) .EQ. 0. .OR. DEL(I) .LE. CS ) GO TO 5
       NN = NN - 1
       WRITE(6,100)I,X(I)
  100  FORMAT(/5X,'POINT NO.',I5,' VALUE=',E20.7,' HAS BEEN REJECTED'/)
       X(I) = 0.
    5  CONTINUE
       IELIM = K - NN
       IND = 1
       IF ( K .EQ. NN) RETURN
       WRITE(6,103)
  103  FORMAT(/' AFTER REMOVING OUTLIERS'/)
       GO TO 1
  999  CONTINUE
       END
```

APPENDIX E
TABLES

This section of the Appendix presents the tables of the Student's "t" distribution, the F table for comparison of precision indices, and the Thompson's Tau table for the outlier test.

STUDENT'S "t" TABLE

The table of Student's "t" distribution (Table E-1) presents the two-tailed 95-percent "t" values for the degrees of freedom from one to 30. Above 30, round the value to 2.0.

Table E-1 Two-Tailed Student's "t" Table

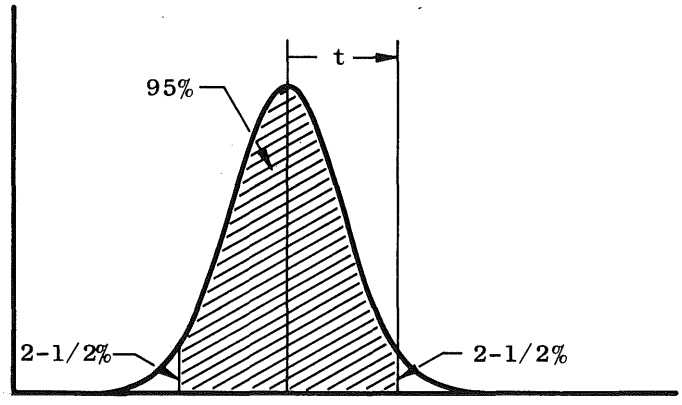

Degrees of Freedom	"t"	Degrees of Freedom	"t"
1	12.706	17	2.110
2	4.303	18	2.101
3	3.182	19	2.093
4	2.776	20	2.086
5	2.571	21	2.080
6	2.447	22	2.074
7	2.365	23	2.069
8	2.306	24	2.064
9	2.262	25	2.060
10	2.228	26	2.056
11	2.201	27	2.052
12	2.179	28	2.048
13	2.160	29	2.045
14	2.145	30	2.042
15	2.131		
16	2.120	31 or more use 2.0	

The table is used to provide an interval estimate of the true value about an observed value. The interval is the measurement plus and minus the standard deviation of the observed value times the "t" value (for the degrees of freedom of that standard deviation):

$$\text{interval} = \text{measurement} \pm t_{95}S$$

The 95-percent Student's "t" value for a standard deviation of 50 lb with 17 deg of freedom is 2.110. The interval is

$$\text{measurement} \pm 2.11 \times 50 = \text{measurement} \pm 105.50 \text{ lb}$$

F TABLE

The table of 95-percent F values (Table E-2) is presented for tests for a significant increase in precision index. The test is performed by dividing the square of the new precision index by the square of the old index:

$$F_{calculated} = \frac{S_{new}^2}{S_{old}^2}$$

This calculated value is compared with the F table value for f_1 and f_2 degrees of freedom; f_1 is the degrees of freedom for S_{new}^2, and f_2 is the degrees of freedom for S_{old}^2.

For example, suppose that the pooled precision index for a force measuring device is 0.05 percent based on four sets of 5 tests each (total of 16 degrees of freedom). A new estimate of precision index is 0.10 percent based on a sample size of 5. The F calculated value is:

$$F_{calculated} = \frac{S_{new}^2}{S_{old}^2} = \frac{(0.1)^2}{(0.05)^2} = \frac{0.0100}{0.0025} = 4.00$$

$f_1 = 4$ and $f_2 = 16$, the table value of F is 3.01. Because 4.00 is greater than 3.01, this indicates the new index is significantly larger than the old index.

THOMPSON'S TAU TABLE

Thompson's Tau Table (Table E-3) is presented to aid in detecting outliers or bad data in a sample. The table is given for several levels of significance (p). If p = 0.05 level is used, this sets the probability of a good point at 5 percent. The procedure for the test is this:

1. From the data (X_j; i = 1,n) containing the suspected outlier X', two statistics are calculated:

$$\bar{X} = \frac{\sum_{i=1}^{N} X_i}{N}$$

Table E-2 5-percent Fractiles of the F Distribution

$$F(f_1, f_2) = \frac{S^2_{new}}{S^2_{old}}$$

Degrees of Freedom for the Numerator (f_1)

Degrees of Freedom for the Denominator (f_2)	1	2	3	4	5	6	7	8	9	10	12	15	17
1	161	200	216	225	230	234	237	239	241	242	244	246	247
2	18.5	19.0	19.2	19.2	19.3	19.3	19.4	19.4	19.4	19.4	19.4	19.4	19.4
3	10.1	9.55	9.28	9.12	9.01	8.94	8.89	8.85	8.81	8.79	8.74	8.70	8.68
4	7.71	6.94	6.59	6.39	6.26	6.16	6.09	6.04	6.00	5.96	5.91	5.86	5.83
5	6.61	5.79	5.41	5.19	5.05	4.95	4.88	4.82	4.77	4.74	4.68	4.62	4.59
6	5.99	5.14	4.76	4.53	4.39	4.28	4.21	4.15	4.10	4.06	4.00	3.94	3.91
7	5.59	4.74	4.35	4.12	3.97	3.87	3.79	3.73	3.68	3.64	3.57	3.51	3.48
8	5.32	4.46	4.07	3.84	3.69	3.58	3.50	3.44	3.39	3.35	3.28	3.22	3.19
9	5.12	4.26	3.86	3.63	3.48	3.37	3.29	3.23	3.18	3.14	3.07	3.01	2.97
10	4.96	4.10	3.71	3.48	3.33	3.22	3.14	3.07	3.02	2.98	2.91	2.85	2.81
11	4.84	3.98	3.59	3.36	3.20	3.09	3.01	2.95	2.90	2.85	2.79	2.72	2.69
12	4.75	3.89	3.49	3.26	3.11	3.00	2.91	2.85	2.80	2.75	2.69	2.62	2.58
13	4.67	3.81	3.41	3.18	3.03	2.92	2.83	2.77	2.71	2.67	2.60	2.53	2.50
14	4.60	3.74	3.34	3.11	2.96	2.85	2.76	2.70	2.65	2.60	2.53	2.46	2.43
15	4.54	3.68	3.29	3.06	2.90	2.79	2.71	2.64	2.59	2.54	2.48	2.40	2.37
16	4.49	3.63	3.24	3.01	2.85	2.74	2.66	2.59	2.54	2.49	2.42	2.35	2.32
17	4.45	3.59	3.20	2.96	2.81	2.70	2.61	2.55	2.49	2.45	2.38	2.31	2.27
18	4.41	3.55	3.16	2.93	2.77	2.66	2.58	2.51	2.46	2.41	2.34	2.27	2.23
19	4.38	3.52	3.13	2.90	2.74	2.63	2.54	2.48	2.42	2.38	2.31	2.23	2.20
20	4.35	3.49	3.10	2.87	2.71	2.60	2.51	2.45	2.39	2.35	2.28	2.20	2.17
21	4.32	3.47	3.07	2.84	2.68	2.57	2.49	2.42	2.37	2.32	2.25	2.18	2.14
22	4.30	3.44	3.05	2.82	2.66	2.55	2.46	2.40	2.34	2.30	2.23	2.15	2.11
23	4.28	3.42	3.03	2.80	2.64	2.53	2.44	2.37	2.32	2.27	2.20	2.13	2.09
24	4.26	3.40	3.01	2.78	2.62	2.51	2.42	2.36	2.30	2.25	2.18	2.11	2.07
25	4.24	3.39	2.99	2.76	2.60	2.49	2.40	2.34	2.28	2.24	2.16	2.09	2.05
26	4.23	3.37	2.98	2.74	2.59	2.47	2.39	2.32	2.27	2.22	2.15	2.07	2.03
28	4.20	3.34	2.95	2.71	2.56	2.45	2.36	2.29	2.24	2.19	2.12	2.04	2.00
30	4.17	3.32	2.92	2.69	2.53	2.42	2.33	2.27	2.21	2.16	2.09	2.01	1.98
34	4.13	3.28	2.88	2.65	2.49	2.38	2.29	2.23	2.17	2.12	2.05	1.97	1.93
38	4.10	3.24	2.85	2.62	2.46	2.35	2.26	2.19	2.14	2.09	2.02	1.94	1.90
40	4.08	3.23	2.84	2.61	2.45	2.34	2.25	2.18	2.12	2.08	2.00	1.92	1.89
44	4.06	3.21	2.82	2.58	2.43	2.31	2.23	2.16	2.10	2.05	1.98	1.90	1.86
48	4.04	3.19	2.80	2.57	2.41	2.29	2.21	2.14	2.08	2.03	1.96	1.88	1.84
50	4.03	3.18	2.79	2.56	2.40	2.29	2.20	2.13	2.07	2.03	1.95	1.87	1.83
55	4.02	3.16	2.77	2.54	2.38	2.27	2.18	2.11	2.06	2.01	1.93	1.85	1.81
60	4.00	3.15	2.76	2.53	2.37	2.25	2.17	2.10	2.04	1.99	1.92	1.84	1.80
65	3.99	3.14	2.75	2.51	2.36	2.24	2.15	2.08	2.03	1.98	1.90	1.82	1.78
80	3.96	3.11	2.72	2.49	2.33	2.21	2.13	2.06	2.00	1.95	1.88	1.79	1.75
100	3.94	3.09	2.70	2.46	2.31	2.19	2.10	2.03	1.97	1.93	1.85	1.77	1.73
150	3.90	3.06	2.66	2.43	2.27	2.16	2.07	2.00	1.94	1.89	1.82	1.73	1.69
200	3.89	3.04	2.65	2.42	2.26	2.14	2.06	1.98	1.93	1.88	1.80	1.72	1.67
1000	3.85	3.00	2.61	2.38	2.22	2.11	2.02	1.95	1.89	1.84	1.76	1.68	1.63
∞	3.84	3.00	2.60	2.37	2.21	2.10	2.01	1.94	1.88	1.83	1.75	1.67	1.62

Table E-2 (Concluded)

$$F(f_1, f_2) = \frac{S^2_{new}}{S^2_{old}}$$

Degrees of Freedom for the Numerator (f_1)

19	20	22	24	26	30	35	40	50	100	500	∞	
248	248	249	249	249	250	251	251	252	253	254	254	1
19.4	19.4	19.5	19.5	19.5	19.5	19.5	19.5	19.5	19.5	19.5	19.5	2
8.67	8.66	8.65	8.64	8.63	8.62	8.60	8.59	8.58	8.55	8.53	8.53	3
5.81	5.80	5.79	5.77	5.76	5.75	5.73	5.72	5.70	5.66	5.64	5.63	4
4.57	4.56	4.54	4.53	4.52	4.50	4.48	4.46	4.44	4.41	4.37	4.37	5
3.88	3.87	3.86	3.84	3.83	3.81	3.79	3.77	3.75	3.71	3.68	3.67	6
3.46	3.44	3.43	3.41	3.40	3.38	3.36	3.34	3.32	3.27	3.24	3.23	7
3.16	3.15	3.13	3.12	3.10	3.08	3.06	3.04	3.02	2.97	2.94	2.93	8
2.95	2.94	2.92	2.90	2.89	2.86	2.84	2.83	2.80	2.76	2.72	2.71	9
2.78	2.77	2.75	2.74	2.72	2.70	2.68	2.66	2.64	2.59	2.55	2.54	10
2.66	2.65	2.63	2.61	2.59	2.57	2.55	2.53	2.51	2.46	2.42	2.40	11
2.56	2.54	2.52	2.51	2.49	2.47	2.44	2.43	2.40	2.35	2.31	2.30	12
2.47	2.46	2.44	2.42	2.41	2.38	2.36	2.34	2.31	2.26	2.22	2.21	13
2.40	2.39	2.37	2.35	2.33	2.31	2.28	2.27	2.24	2.19	2.14	2.13	14
2.34	2.33	2.31	2.29	2.27	2.25	2.22	2.20	2.18	2.12	2.08	2.07	15
2.29	2.28	2.25	2.24	2.22	2.19	2.17	2.15	2.12	2.07	2.02	2.01	16
2.24	2.23	2.21	2.19	2.17	2.15	2.12	2.10	2.08	2.02	1.97	1.96	17
2.20	2.19	2.17	2.15	2.13	2.11	2.08	2.06	2.04	1.98	1.93	1.92	18
2.17	2.16	2.13	2.11	2.10	2.07	2.05	2.03	2.00	1.94	1.89	1.88	19
2.14	2.12	2.10	2.08	2.07	2.04	2.01	1.99	1.97	1.91	1.86	1.84	20
2.11	2.10	2.07	2.05	2.04	2.01	1.98	1.96	1.94	1.88	1.82	1.81	21
2.08	2.07	2.05	2.03	2.01	1.98	1.96	1.94	1.91	1.85	1.80	1.78	22
2.06	2.05	2.02	2.00	1.99	1.96	1.93	1.91	1.88	1.82	1.77	1.76	23
2.04	2.03	2.00	1.98	1.97	1.94	1.91	1.89	1.86	1.80	1.75	1.73	24
2.02	2.01	1.98	1.96	1.95	1.92	1.89	1.87	1.84	1.78	1.73	1.71	25
2.00	1.99	1.97	1.95	1.93	1.90	1.87	1.85	1.82	1.76	1.71	1.69	26
1.97	1.96	1.93	1.91	1.90	1.87	1.84	1.82	1.79	1.73	1.67	1.65	28
1.95	1.93	1.91	1.89	1.87	1.84	1.81	1.79	1.76	1.70	1.64	1.62	30
1.90	1.89	1.86	1.84	1.82	1.80	1.77	1.75	1.71	1.65	1.59	1.57	34
1.87	1.85	1.83	1.81	1.79	1.76	1.73	1.71	1.68	1.61	1.54	1.53	38
1.85	1.84	1.81	1.79	1.77	1.74	1.72	1.69	1.66	1.59	1.53	1.51	40
1.83	1.81	1.79	1.77	1.75	1.72	1.69	1.67	1.63	1.56	1.49	1.48	44
1.81	1.79	1.77	1.75	1.73	1.70	1.67	1.64	1.61	1.54	1.47	1.45	48
1.80	1.78	1.76	1.74	1.72	1.69	1.66	1.63	1.60	1.52	1.46	1.44	50
1.78	1.76	1.74	1.72	1.70	1.67	1.64	1.61	1.58	1.50	1.43	1.41	55
1.76	1.75	1.72	1.70	1.68	1.65	1.62	1.59	1.56	1.48	1.41	1.39	60
1.75	1.73	1.71	1.69	1.67	1.63	1.60	1.58	1.54	1.46	1.39	1.37	65
1.72	1.70	1.68	1.65	1.63	1.60	1.57	1.54	1.51	1.43	1.35	1.32	80
1.69	1.68	1.65	1.63	1.61	1.57	1.54	1.52	1.48	1.39	1.31	1.28	100
1.66	1.64	1.61	1.59	1.57	1.53	1.50	1.48	1.44	1.34	1.25	1.22	150
1.64	1.62	1.60	1.57	1.55	1.52	1.48	1.46	1.41	1.32	1.22	1.19	200
1.60	1.58	1.55	1.53	1.51	1.47	1.44	1.41	1.36	1.26	1.13	1.08	1000
1.59	1.57	1.54	1.52	1.50	1.46	1.42	1.39	1.35	1.24	1.11	1.00	∞

Degrees of Freedom for Denominator (f_2)

Table E-3 Thompson's Tau

Sample Size N	Level of Significance P= .1	.05	.02	.01
3	1.3968	1.4099	1.41352	1.414039
4	1.559	1.6080	1.6974	1.7147
5	1.611	1.757	1.869	1.9175
6	1.631	1.814	1.973	2.0509
7	1.640	1.848	2.040	2.142
8	1.644	1.870	2.087	2.207
9	1.647	1.885	2.121	2.256
10	1.648	1.895	2.146	2.294
11	1.648	1.904	2.166	2.324
12	1.649	1.910	2.183	2.348
13	1.649	1.915	2.196	2.368
14	1.649	1.919	2.207	2.385
15	1.649	1.923	2.216	2.399
16	1.649	1.926	2.224	2.411
17	1.649	1.928	2.231	2.422
18	1.649	1.931	2.237	2.432
19	1.649	1.932	2.242	2.440
20	1.649	1.934	2.247	2.447
21	1.649	1.936	2.251	2.454
22	1.649	1.937	2.255	2.460
23	1.649	1.938	2.259	2.465
24	1.649	1.940	2.262	2.470
25	1.649	1.941	2.264	2.475
26	1.648	1.942	2.267	2.479
27	1.648	1.942	2.269	2.483
28	1.648	1.943	2.272	2.487
29	1.648	1.944	2.274	2.490
30	1.648	1.944	2.275	2.493
31	1.648	1.945	2.277	2.495
32	1.648	1.945	2.279	2.498
∞	1.64485	1.95996	2.32634	2.57582

and

$$SD = \sqrt{\frac{\sum_{i=1}^{N} (X_i - \overline{X})^2}{N}}$$

These are the average value and standard deviation of the sample.

2. Calculate the difference in (absolute value) between the average value $\overline{X}$ and the outlier X′:

$$\delta = \left|\overline{X} - X'\right|$$

3. Entering the table for N and P, (take P = 0.05) read a value of Tau.

4. The comparison is made between δ and the product of SD and Tau. If δ is larger or equal to that product, the data point is declared an outlier. A new mean and standard deviation must be calculated. If δ is smaller, the point is not rejected.

Example:

In the following sample of 15 data points, $\overline{X}$ and S were calculated to be 9.949 and 0.997:

9.558	10.478	9.609	9.582	9.583
11.447	11.485	11.067	9.173	10.303
10.472	10.310	7.416	9.488	9.257
		↑ Suspected outlier		

The test is to compare δ (the absolute difference between the suspected outlier and the average value) with the product Tau value times calculated standard deviation.

$$\delta = \left|\overline{X} - X'\right| = \left|9.949 - 7.416\right| = 2.533$$

$$\text{Tau} \times SD = 1.923 \times 0.997 = 1.917$$

where Tau is the Table E-3 value for P = 0.05 and N =15. Since δ is greater, the point 7.416 is discarded.

UNCLASSIFIED

Security Classification

DOCUMENT CONTROL DATA - R & D

(Security classification of title, body of abstract and indexing annotation must be entered when the overall report is classified)

1. ORIGINATING ACTIVITY (Corporate author)	2a. REPORT SECURITY CLASSIFICATION
Arnold Engineering Development Center, Arnold Air Force Station, Tennessee 37389	UNCLASSIFIED
	2b. GROUP N/A

3. REPORT TITLE

HANDBOOK, UNCERTAINTY IN GAS TURBINE MEASUREMENTS

4. DESCRIPTIVE NOTES (Type of report and inclusive dates)

Final Report

5. AUTHOR(S) (First name, middle initial, last name)

Dr. R. B. Abernethy et al., Pratt & Whitney Aircraft
J. W Thompson, Jr., ARO, Inc.

6. REPORT DATE	7a. TOTAL NO. OF PAGES	7b. NO. OF REFS
Eebruary 1973	182	0

8a. CONTRACT OR GRANT NO.	9a. ORIGINATOR'S REPORT NUMBER(S)
b. PROJECT NO.	AEDC-TR-73-5
c. Program Element 65802F	9b. OTHER REPORT NO(S) (Any other numbers that may be assigned this report)
d.	ARO-ETF-TR-72-60

10. DISTRIBUTION STATEMENT

Approved for public release; distribution unlimited.

11. SUPPLEMENTARY NOTES	12. SPONSORING MILITARY ACTIVITY
Available in DDC	Arnold Engineering Development Center Arnold Air Force Station Tennessee 37389

13. ABSTRACT

The lack of a standard method for estimating the errors associated with gas turbine performance data has made it impossible to compare measurement systems between facilities, and there has been confusion over the interpretation of error analysis. Therefore, a standard uncertainty methodology is proposed in this Handbook. The mathematical uncertainty model presented is based on two components of measurement error: the fixed (bias) error and the random (precision) error. The result of applying the model is an estimate of the error in the measured performance parameter. The uncertainty estimate is the interval about the measurement which is expected to encompass the true value. The propagation of error from basic measurements through calculated performance parameters is presented. Traceability of measurement back to the National Bureau of Standards and associated error sources is reviewed.

DD FORM 1 NOV 65 1473

UNCLASSIFIED

Security Classification

14. KEY WORDS	LINK A		LINK B		LINK C	
	ROLE	WT	ROLE	WT	ROLE	WT
handbook						
gas turbine engines						
measurement						
uncertainty						
error analysis						
mathematical model						

AFSC
Arnold AFS Tenn